

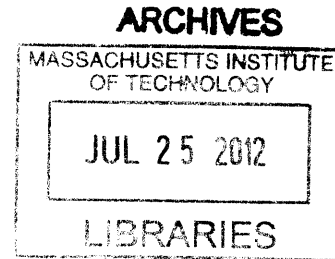
REACTOR PHYSICS CONSIDERATIONS FOR IMPLEMENTING SILICON CARBIDE
CLADDING INTO A PWR ENVIRONMENT

By

Jacob P. Dobisesky

B.S., Systems Engineering (2009)

United States Naval Academy




SUBMITTED TO THE DEPARTMENT OF NUCLEAR SCIENCE AND ENGINEERING IN
PARTIAL FULFILLMENT OF THE REQUIREMENTS FOR THE DEGREE OF

MASTER OF SCIENCE IN NUCLEAR SCIENCE AND ENGINEERING
AT THE
MASSACHUSETTS INSTITUTE OF TECHNOLOGY

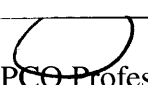
JUNE 2011

© 2011 Massachusetts Institute of Technology
All rights reserved

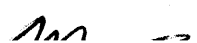
Signature of Author: _____


Jacob P. Dobisesky
Department of Nuclear Science and Engineering
May 6, 2011


Certified By: _____


Mujid S. Kazimi, Ph. D.
TEPCO Professor of Nuclear Engineering
Thesis Supervisor

Certified By: _____


Edward E. Pilat, Ph.D.
Research Scientist
Thesis Reader

Accepted By: _____


Mujid S. Kazimi, Ph.D.
TEPCO Professor of Nuclear Engineering
Chairman, Committee on Graduate Students

Reactor Physics Considerations for Implementing Silicon Carbide Cladding into a PWR Environment

By
Jacob Dobisesky

Submitted to the Department of Nuclear Science and Engineering on May 6, 2011, in partial fulfillment of the requirements for the Degrees of Bachelor of Science and Master of Science in Nuclear Science and Engineering

Abstract

Silicon carbide (SiC) offers several advantages over zirconium (Zr)-based alloys as a potential cladding material for Pressurized Water Reactors: very slow corrosion rate, ability to withstand much higher temperature with little reaction with steam, and more favorable neutron absorption. To evaluate the feasibility of longer fuel cycles and higher power density in SiC clad fuel, a core design study was completed with uranium dioxide fuel and SiC cladding in a standard, Westinghouse 4-loop PWR. NRC-limited values for hot channel and hot spot values were taken into account as well as acceptable values for the reactivity feedback and control mechanisms and shutdown margin. The Studsvik Core Management System, which consisted of CASMO-4E, CMS-Link, and SIMULATE-3, provided an accurate tool to design the new core loading patterns that would satisfy current nuclear industry standards.

Libraries of Westinghouse robust fuel assemblies (RFAs) were modeled in CASMO-4E with varying enrichments, burnable poison layouts, and power conditions. Using these assemblies, full core, three-dimensional analyses were performed in SIMULATE-3 for operating conditions similar to the Seabrook Nuclear Power Station. In this study, SiC-clad fuel rods held 10% less heavy metal to allow for central holes in the UO₂ pellets, limiting peak fuel temperature during anticipated operational transients but raising the average enrichment per fuel batch. The cladding dimensions remained similar to the current Zircaloy 4 cladding. Three approaches were followed in creating the PWR core designs: 1) constant core power density (or total reactor power) and cycle length, but fewer fresh assemblies loaded, 2) constant cycle length, but increased core power density to the maximum feasible level, staying within the capability of the reactor etc., and 3) constant power density, but extended fuel cycle length from 18 to 24 months.

Sixteen core designs were completed with three different types of burnable poison (IFBA, WABA, and gadolinium) that achieved the desired operating cycle lengths and target values for reactor physics parameters limited by the NRC. Batch average discharge burnups ranged from ~41 to ~80 MWd/kgU, reinforcing SiC's advantage and potential appeal to power utilities. Additionally, a power uprate of 10% was found to be feasible, but beyond this value would require a redesign of the control rod material and/or layout to allow for an acceptable shutdown margin by end of cycle (EOC). Nevertheless, all other reactivity coefficients and safety margins were met, confirming the feasibility of operating to higher burnups beyond the current limits of Zr cladding.

Thesis Supervisor: Mujid S. Kazimi

Title: TEPCO Professor of Nuclear Science and Engineering

ACKNOWLEDGEMENTS

I would like to thank the Electric Power Research Institute (EPRI) for partially funding this research and the team of researchers and engineers from across the country that provided me with priceless insight into the advantages of SiC cladding.

Professor Kazimi was a truly wonderful advisor to work with for the past two years. He was patient, understanding, and extremely knowledgeable in the area, but never over-demanding. He believed that I could complete this thesis even when I thought I did not have the experience. As a result, he helped me learn one vital lesson in life as described by Publilius Syrus, “No one knows what he can do until he tries.”

I am also very grateful to Dr. Pilat for his amazing patience and guidance through designing each of these cores. I have never learned so much from one person without opening a book. His personal insights can be found throughout this thesis and without them, it would have probably been one quarter of the size.

Dr. Shwageraus was also instrumental in helping me decipher code inputs and outputs. Without his expertise, I may still have a high “f-delta-h.”

To the team of SiC research scientists in NW-14, Dr. Kohse, Dr. Ostrovsky, Dr. Kim, and Dr. Carpenter, thank you for providing me with the hands-on experience in the reactor and labs during the irradiation experiments. My experiences moving lead blocks, taking logs, and measuring the SiC specimens gave me an even greater appreciation for experimental work.

To the United States Navy, I am grateful for the opportunity I was given to delay my commitment after graduation to earn a Master’s degree at MIT. After two years in Boston, I am looking forward to rejoining the fleet as a more experienced, knowledgeable naval officer.

To my beautiful and sweet girlfriend, Rosemary Sugrue, thank you for your support and cookies while I researched by your side on movie nights - you mean the world to me. And to my fellow graduate students, Bo Feng, Bryan Herman, Koroush Shirvan, Brittany Guyer, and Jake DeWitte, thank you for your technical insights into my thesis and emotional support while I wrote it.

Finally, I would like to thank my family for providing me with the guidance and love I needed to reach this point in my life. It has been a wild 23 years.

TABLE OF CONTENTS

Abstract	2
Acknowledgements	3
Table of Contents	4
List of Figures	6
List of Tables	9
Nomenclature	11
1. Objectives of the Study	13
1.1 Background.....	13
1.2 Scope	17
1.3 Thesis Organization	17
2. Pressurized Water Reactor Design.....	20
2.1 Fuel Dimensions & Cladding Material.....	20
2.2 Assembly & Burnable Poison Design	22
2.3.a. Integral Fuel Burnable Absorber (IFBA).....	26
2.3.b. Gadolinium (Gd).....	28
2.3.c. Erbium (Er).....	28
2.3.d. Wet Annular Burnable Absorber (WABA)	28
2.3 Core Design & Operating Conditions.....	30
3. Design Implementation	37
3.1 Computer Simulation Tools.....	37
3.1.a. CASMO-4e	37
3.1.b. CMS-Link	38
3.1.c. SIMULATE-3	38
3.2 Evaluation of Key Reactor Physics Parameters.....	40
3.2.a. Coolant Enthalpy Rise Hot Channel Factor, $F_{\Delta h}$	40
3.2.b. Local Pin Power F_q	41
3.2.c. Soluble Boron Concentration.....	41
3.2.d. Moderator Temperature Coefficient (MTC).....	42
3.2.e. Burnup	42
4. 18-Month Cycle Core Designs.....	44

4.1	52-reload SiC Core	47
4.2	64-Reload SiC Core.....	51
4.3	84-Reload Zr Core	54
4.4	84-Reload SiC Core.....	57
4.5	84-Reload Uprated SiC Cores	59
5.	24-Month Cycle Core Designs.....	63
5.1	96-Reload SiC Core.....	65
5.2	112-Reload SiC Core.....	69
5.3	136-Reload SiC Core.....	72
6.	Reactivity Control and Coefficient Analysis	77
6.1	Moderator Temperature Coefficient (MTC).....	77
6.2	Isothermal Temperature Coefficient (ITC).....	79
6.3	Uniform Doppler Coefficient (UDC)	80
6.4	Boron Coefficient	80
6.5	Power Coefficient.....	81
6.6	Shutdown Margin	82
7.	Diverse Burnable Poison Core Designs	86
7.1	Gadolinium Core	86
7.2	Gadolinium-IFBA Core	90
7.3	IFBA-WABA Core.....	92
7.4	Safety Coefficients of Diverse Burnable Poisons.....	96
8.	Transition Cycle Core Design.....	100
8.1	Reactor Physics Considerations.....	100
8.2	Safety Parameters of Transition Cycle	103
9.	Summary and Recommendations for Future Work	107
9.1	Summary of Core Design	107
9.2	Summary of Safety Parameter Analysis	108
9.3	Future work.....	108
	References.....	110
	Appendix A: Burnable Poison Layouts.....	113
	Appendix B: Computer-Based Modeling Input Files & Flowcharts.....	117
	Appendix C: Transition Cycle Fuel Reloading Summaries	123

LIST OF FIGURES

Figure 1.1 Triplex SiC cladding design	15
Figure 2.1 (To left) Zr-clad fuel rod with solid UO ₂ Fuel pellet. (To right) SiC-clad fuel rod with cored (10% voided) fuel pellet.....	22
Figure 2.2 Standard PWR assembly layout with no burnable poison. The white circles indicate fuel rod locations and the black circles represent guide tubes where water may flow. The center black dot is also considered a guide tube but is commonly used as an “instrumentation thimble.”	23
Figure 2.3 A quick comparison of five dimensionally-identical assemblies with varying amounts of different BP rods. The magnitude of these curves can change based on the amount of absorbing isotope loaded, but the general shape remains the same.	24
Figure 2.4 An assembly with axial blankets (on left). An assembly with axial blankets removed (on right).	26
Figure 2.5 Cross-section view of IFBA.	27
Figure 2.6 Comparison of IFBA loading in the core. “L” refers to 1X IFBA and “H” refers to 1.5X IFBA.....	27
Figure 2.7 WABA rod dimensions, including guide tube cladding.....	29
Figure 2.8 Comparison of assemblies with identical enrichments and different combinations of WABA and other burnable poisons. The amount of WABA in each assembly was kept constant. The alpha-numeric designator after “WABA” in the legend indicates first the type of BP (“G” for Gd or “I” for IFBA), the number of BP rods per assembly (12, 16 or 156), and the concentration of BP (“L” for low, “M” for medium, “H” for high). A low or high concentration of BP for Gd meant 4.0% or 10%, respectively, and a low or high concentration of BP for IFBA meant 1X or 1.5X, respectively.	30
Figure 2.9 A blank core reloading map consisting of 193 potential locations for assemblies in the core.....	32
Figure 2.10 LHGR curves for nominal and uprated cases for both SiC and Zr core designs.....	35
Figure 2.11 Shutdown and control bank location map for control rods in PWR model.....	36
Figure 3.1 Flow diagram of computer-based modeling approach.	39
Figure 4.1 $F_{\Delta h}$ for all 18-month core designs.....	45
Figure 4.2 Boron concentration (ppm) for all 18-month core designs.	46
Figure 4.3 F_q for all 18-month core designs.....	46
Figure 4.4 52-reload core loading map.	48
Figure 4.5 $F_{\Delta h}$ for 52-reload core design.	49
Figure 4.6 Boron concentration (ppm) for 52-reload core design.	50
Figure 4.7 F_q for 52-reload core design.	50
Figure 4.8 64-reload core loading map.....	51
Figure 4.9 $F_{\Delta h}$ for 64-reload core design.	52
Figure 4.10 Boron concentration (ppm) for 64-reload core design.	53

Figure 4.11 F_q for 64-reload core design.	53
Figure 4.12 84-reload core loading map for the Zr, SiC, and uprated cases.	54
Figure 4.13 $F_{\Delta h}$ for 84-reload Zr core design.	55
Figure 4.14 Boron concentration (ppm) for 84-reload Zr core design.	56
Figure 4.15 F_q for the 84-reload Zr core design.	56
Figure 4.16 $F_{\Delta h}$ for 84-reload SiC core design.	58
Figure 4.17 Boron concentration (ppm) for 84-reload SiC core design.	58
Figure 4.18 F_q for 84-reload SiC core design.	59
Figure 4.19 $F_{\Delta h}$ for 84-reload uprated core designs.	61
Figure 4.20 Boron concentration (ppm) for 84-reload uprated core designs.	61
Figure 4.21 F_q for 84-reload uprated core designs.	62
Figure 5.1 $F_{\Delta h}$ for all 24-month core designs.	64
Figure 5.2 Boron concentration (ppm) for all 24-month core designs.	64
Figure 5.3 F_q for all 24-month core designs.	65
Figure 5.4 96-reload core loading map.	66
Figure 5.5 $F_{\Delta h}$ for 96-reload core design.	67
Figure 5.6 Boron concentration (ppm) for 96-reload core design.	68
Figure 5.7 F_q for 96-reload core design.	68
Figure 5.8 112-reload core loading map.	70
Figure 5.9 $F_{\Delta h}$ for 112-reload core design.	71
Figure 5.10 Boron concentration (ppm) for 112-reload core design.	71
Figure 5.11 F_q for 112-reload SiC core design.	72
Figure 5.12 Leakage rates for all core designs.	73
Figure 5.13 136-reload core loading map.	74
Figure 5.14 $F_{\Delta h}$ for 136-reload core design.	75
Figure 5.15 Boron concentration (ppm) for 136-reload core.	76
Figure 5.16 F_q for 136-reload core design.	76
Figure 6.1 Moderator temperature coefficients for all 18- and 24-month core designs.	78
Figure 6.2 Isothermal temperature coefficient for all 18- and 24-month core designs.	79
Figure 6.3 Uniform doppler coefficient for all 18- and 24-month core designs.	80
Figure 6.4 Boron coefficient for all 18- and 24-month core designs.	81
Figure 6.5 Power coefficient for all core designs.	82
Figure 6.6 Labels that start with “S” refer to <i>shutdown</i> banks and are either completely inserted or withdrawn during operation. Labels that start with “C” refer to <i>control</i> banks and have variable insertion/withdrawal levels.	83
Figure 6.7 Graphic representation of reactivity gains and losses from steps during a shutdown margin calculation.	84
Figure 7.1 Burnable poisons hold down reactivity in varying ways As a result of different isotopic abundances.	86
Figure 7.2 84-reload (with Gd) core loading map.	87

Figure 7.3 $F_{\Delta h}$ for 84-reload core (with Gd).	88
Figure 7.4 Boron concentration (ppm) for 84-reload core (with Gd).	89
Figure 7.5 F_q for 84-reload core (with Gd).	89
Figure 7.6 $F_{\Delta h}$ for 84-reload core with Gd & IFBA.	91
Figure 7.7 Boron concentration for 84-reload core with Gd & IFBA.	91
Figure 7.8 F_q for 84-reload core with Gd & IFBA.	92
Figure 7.9 84-reload core reloading map for WABA. An “X” over an assembly location demarcates a shutdown or control bank location.	93
Figure 7.10 $F_{\Delta h}$ throughout cycle length of 84-reload design with WABA.	94
Figure 7.11 Boron Concentration throughout cycle length of 84-reload design with WABA.	95
Figure 7.12 F_q throughout cycle length of 84-reload design with WABA.	95
Figure 7.13 Boron coefficient for all cores with additional burnable poison.	96
Figure 7.14 MTC for all cores with additional burnable poison.	97
Figure 7.15 ITC for all cores with additional burnable poison.	97
Figure 7.16 Power coefficient for all cores with additional burnable poison.	98
Figure 7.17 UDC for all cores with additional burnable poison.	98
Figure 8.1 Transition Cycles from Initial Core (Cycle 1) with all Zr assemblies (white) to final core (Cycle 4) with all SiC assemblies (gray).	100
Figure 8.2 $F_{\Delta h}$ for all transition cycles.	102
Figure 8.3 Boron concentration (ppm) for all transition cycles.	102
Figure 8.4 F_q for all transition cycles.	103
Figure 8.5 Boron coefficients for all transition cycles.	104
Figure 8.6 ITC for all transition cycles.	104
Figure 8.7 MTC for all transition cycles.	105
Figure 8.8 Power Coefficient for all transition cycles.	105
Figure 8.9 Uniform doppler coefficient for all transition cycles	106

LIST OF TABLES

Table 2.1 Cold dimensions for SiC and Zr-clad fuel rods	22
Table 2.2 Fuel assembly dimensions for SiC and Zr clad cases	23
Table 2.3 A list of the various isotopes and their absorption cross-sections. All the isotopes are utilized in BP rods, but their total concentration may vary for increasing or decreasing neutron absorption.....	25
Table 2.4 Physical parameters of core design.....	31
Table 2.5 Estimated cycle burnups for SiC- and Zr-clad fuel at selected power uprates.	33
Table 2.6 Coolant temperatures for PWR model at full power.	34
Table 2.7 Average fuel temperatures for PWR model at full power.	34
Table 3.1 Steady-state design target values for key reactor physics parameters.	40
Table 4.1 18-month cycle core designs.....	44
Table 4.2 52-reload core design summary of reactor physics parameters.	48
Table 4.3 52-reload batch summary.....	49
Table 4.4 64-reload core design summary of reactor physics parameters.	51
Table 4.5 64-reload fuel batch summary.	52
Table 4.6 84-reload Zr core design summary of reactor physics parameters.	54
Table 4.7 84-reload Zr fuel batch summary.....	55
Table 4.8 84-reload core design summary of reactor physics parameters.	57
Table 4.9 84-reload SiC core design fuel batch summary.	57
Table 4.10 84-reload uprated core design summary of reactor physics parameters.	59
Table 4.11 84-reload 10% uprated core design fuel batch summary.....	60
Table 4.12 84-reload 20% uprated core design fuel batch summary.....	60
Table 5.1 Summary of 24-month core designs.	63
Table 5.2 96-reload core design summary of reactor physics parameters.	66
Table 5.3 96-reload core design fuel batch summary.	67
Table 5.4 112-reload core design summary of reactor physics parameters.	69
Table 5.5 112-reload core design fuel batch summary.	70
Table 5.6 136-reload core design summary of reactor physics parameters.	73
Table 5.7 136-reload core design (with IFBA) fuel batch summary.	74
Table 5.8 136-reload core design (with Er) fuel batch summary.	75
Table 6.1 Core designs evaluated for transient analysis	77
Table 6.2 Shutdown margin for all cores.....	83
Table 6.3 Step-by-step description of shutdown margin calculation.....	84
Table 6.4 Shutdown and control rod bank worth for the nominal 84-reload SiC case.....	85
Table 6.5 Reactivity balance for nominal 84-reload SiC case.....	85
Table 7.1 84-reload core design (with Gd) summary of reactor physics parameters.	87
Table 7.2 84-reload core design (with Gd) fuel batch summary.	88
Table 7.3 Target core parameters for 84-reload SiC case with Gd & IFBA BP.....	90

Table 7.4 Fuel Loading for 84-reload SiC case with Gd & IFBA BP.	90
Table 7.5 84-reload core physics parameters with WABA as additional burnable poison.	93
Table 7.6 84-reload refueling summary with WABA as additional burnable poison.	94
Table 7.7 Shutdown margin for all cores with additional burnable poison.	99
Table 8.1 Reactor Physics parameters for the transition cycles.....	101
Table 8.2 Shutdown margin for all transition cycles.	103

NOMENCLATURE

°C	degrees Celsius	gm	gram
°F	degrees Fahrenheit	HFIR	High Flux Isotope Reactor
Ag	silver	hr	hour
AOO	Anticipated Operational Occurrence	IFBA	integral fuel burnable absorber
ASSY	assembly	IFEL	Irradiated Fuels Examination Laboratory
B	boron	in	inch
B _c	cycle burnup	In	Indium
B _d	average discharge burnup	INL	Idaho National Laboratory
BOC	beginning of cycle	ITC	isothermal temperature coefficient
BOL	beginning of life	k-eff	“k effective”
BP	burnable poison	kg	kilogram
Cd	Cadmium	kgU	kilogram of Uranium
cm	centimeter	k-inf	“k infinity” (k _∞)
CMC	Ceramic Matrix Composites	kW	kilo-watt
CTP	Ceramic Tubular Products	L	liter
DOE	Department of Energy	LHGR	linear heat generation rate
EOC	end of cycle	LOCA	Loss Of Coolant Accident
EOL	End of life	LWR	light water reactor
EPRI	Electric Power Research Institute	LWRS	Light Water Reactor Sustainability
Er	erbium	m	meter
F _q	local power fraction	mg	milligram
F _{ΔH}	relative power fraction	min	minute
Gd	gadolinium		

MIT	Massachusetts Institute of Technology	ppm	parts per million
MITR	MIT Reactor	PWR	pressurized water reactor
MT	metric ton	RCCA	Rod Cluster Control Assembly
MTC	moderator temperature coefficient	SDM	shutdown margin
MW	mega-watt	sec	second
MWd	Mega-Watt day	SiC	SiC
MWe	Mega-Watt electric	UDC	uniform Doppler coefficient
MWth	Mega-Watt thermal	VHTR	Very High Temperature Reactor
NASA	National Aeronautics and Space Administration	w/o	235U enrichment
NE	Nuclear Engineering	WABA	wet annular burnable absorber
NRC	Nuclear Regulatory Commission	Zr	Zr
ORNL	Oak Ridge National Laboratory	ρ	reactivity
PIE	Post-Irradiation Examination		
PNNL	Pacific Northwest National Laboratory		

1. OBJECTIVES OF THE STUDY

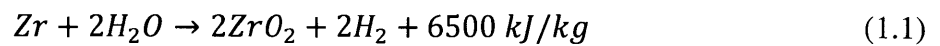
With promising results from ongoing irradiation tests of silicon carbide (SiC) cladding, this work evaluates the potential to utilize a unique composite material to extract more energy per unit volume of fuel in a pressurized water reactor (PWR) environment. Loading patterns of various batch sizes and discharge burnups were created to demonstrate SiC's ability to operate at longer cycle lengths and higher power levels. In addition, a range of different burnable poisons were considered in an effort to study the most effective and efficient means to reduce power peaking and control residual reactivity with SiC-clad fuel. As expected by the nuclear industry, the core designs in this research sought to achieve the same level of safety margins already established with zirconium (Zr)-clad fuel. A transition cycle analysis was also completed to ensure that reactor physics parameters did not complicate the realistic transition from Zr to SiC cladding in the core.

1.1 BACKGROUND

Utilized in naval reactors since the 1940s, Zircaloy, a Zr-based alloy, emerged onto the nuclear industry as an improvement over the traditional stainless steel cladding [Thomas, 1974]. Compared to SiC, Zircaloy offered a few of the same advantages over its predecessor, such as less parasitic neutron absorption and activation and a lower susceptibility to stress corrosion cracking in boiling water reactors (BWRs) [Snead, 2007][Locke, 1975]. Even though Zircaloy was more expensive to manufacture at the time, the nuclear industry began replacing its cladding material in the 1960s. Since then, utilities have witnessed fuel failures go from 1 in 100, to 1 in 10,000 for over 5 million rods currently operating in the United State's 104 nuclear reactors [Rusch, 2008].

As we move forward in the 21st Century, however, fuel failures have begun to rise again. Several factors may be the cause: 1) more aggressive operating conditions, 2) higher power levels, 3) longer cycle lengths, and 4) chemistry changes to reduce corrosion in other areas of the primary system [Yang, 2006]. As will be discussed throughout this work, SiC, promises to withstand all of these additional demands.

On March 11th, 2011, a 9.0 Richter earthquake occurred off the coast of Japan, rattling nearby nuclear power plants and generating a tsunami which destroyed the power grid and back up diesel generators, rendering three of the six Fukushima nuclear power plants with a Loss Of Off-site Power (LOOP) accident. This prevented the circulation of coolant to the cores. Similarly, the spent fuel pools water was heated and boiled away. The old Zircaloy cladding, within the pool of a 40-year old BWR, began to reach temperatures it could no longer withstand, around 1200°C [10 CFR § 50.46]. As the cladding began to react quickly with oxygen and steam, fission products were released, and what eventually became more apparent, an oxidation reaction unique to Zr occurred with the steam, shown in Equation 1.1.



As the heat inside the core accumulated, the pressure rose and threatened the integrity of the containment, and required manual venting. Due to other subsequent errors, the hydrogen within the vented steam or from the spent fuel pool led to an explosion outside of the containment but inside the reactor buildings of Unit 1 and 3, catching the eye of national news agencies and leading to widespread panic about a possible full-core meltdown.

While the situation was not good for these nuclear power plants, public worry spawning from the hydrogen explosions could have been avoided if SiC were the current cladding material. Besides being able to withstand higher temperatures before melting, around 2200°C [Snead, 2007], SiC also does not interact with steam until higher temperatures (1700°C) and the reaction does not lead to hydrogen production in severe accident scenarios. While it may take a few years to fully understand the nuclear accident at Fukushima, weaknesses of current designs were revealed, and fortunately, SiC already promises solutions to many of the concerns.

In addition to an inert response to high temperature steam, fuel cladding made of SiC also promises to lead to lower defect rates and thus, less release of radioactive materials into the primary coolant system. These effects provide the industry with a more robust fuel that could withstand efforts to move to higher efficiencies and power outputs. In fact, despite the nuclear regulatory commission (NRC) limiting the average peak rod burnup to 62 MWd/kgU [NRC, 1997], others have suggested that there may be potential to further enhance the productivity and efficiency of LWRs by allowing even higher burnup [Olander, 2001].

As a result, over the past eight years, a team of researchers in the United States has taken on a new initiative to investigate SiC, a robust ceramic clad, as a potential improvement over the traditional Zr alloy. This team includes researchers from around the country, at the Westinghouse Electric Company, Idaho National Laboratory (INL), Oak Ridge National Laboratory (ORNL), Electric Power Research Institute, Ceramic Tubular Products (CTP), and Massachusetts Institute of Technology (MIT). [Yueh, 2010b]

Initial irradiation experiments with SiC cladding began at the MIT Reactor in May 2006, with 39 specimens prepared by CTP. Since then, three advanced cladding irradiation (ACI) runs have been completed, leading to about 70 specimens, representing 14 different manufacturing approaches, exposed to over 2205 MWd of accumulated power, or about 580 effective days of operation under PWR conditions. The major conclusion was that the manufacturing method and material purity of each specimen greatly affected its ability to withstand radiation. In the end, the right triplex cladding, as shown below in Figure 1.1, demonstrated the ability to withstand irradiation with minimal material degradation. Additionally, SiC showed significantly lower neutron activation compared to the reference Zr samples. A month after exposure, the SiC specimens were measured at less than 10 mR/hr at 10 cm, about 1000 times lower than the zircaloy specimens. [Carpenter, 2010]

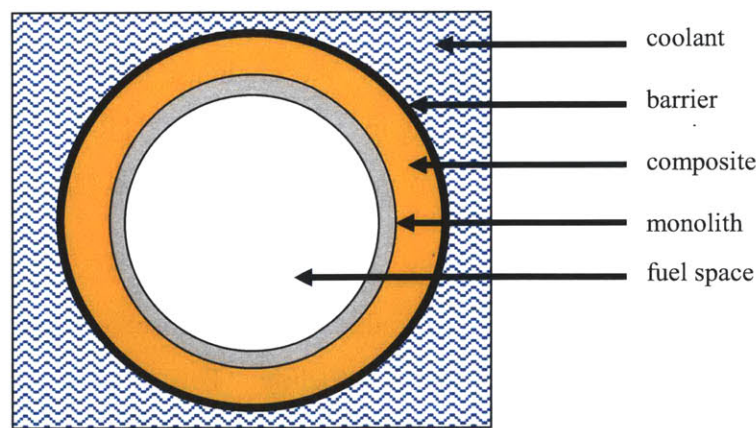


Figure 1.1 Triplex SiC cladding design

At Oak Ridge National Laboratory, as part of the Department of Energy (DOE)/Nuclear Engineering (NE) Gen-IV Very High Temperature Reactor (VHTR) Ceramics program, the irradiation effects of SiC are being tested extensively in their High Flux Isotope Reactor (HFIR).

In December 2010, the first fuel rods with triplex SiC cladding, provided by CTP, and uranium dioxide and uranium nitride fuel, provided by Westinghouse, were placed into the HFIR. The irradiation is expected to conclude in August 2010, with post-irradiation examination (PIE) to be conducted at ORNL's Irradiated Fuels Examination Laboratory (IFEL). [Ott, 2010]

SiC has also peaked interest for other applications in the reactor core. At INL and MIT, through their Light Water Reactor Sustainability (LWRS) program, researchers are currently evaluating SiC and other ceramic matrix composites (CMCs) to replace Zr in BWR channel boxes. This includes working with EPRI to fabricate Hi-Nicalon Type-S SiC fiber that will later be manufactured into a prototype channel box for further testing. [Griffith, 2010][Yueh, 2010a]

A few challenges still exist, however, for the SiC researchers. The most pressing issue has been how to weld or bond a ceramic composite material, like SiC to itself. Researchers at the National Aeronautics and Space Administration (NASA) and Pacific Northwest National Laboratory (PNNL) have been trying to accomplish this task for years for other applications and have so far been unsuccessful. The primary concern has been with the end plugs, which are composed of SiC and must be joined to the cylindrical section of the cladding to provide a vacuum sealed container for the fuel. Without a reliable and certifiable weld that can also prove resistant to irradiation, the NRC could never license a SiC-clad fuel rod. That is why engineers at EWI have been investigating laser welding and ultrasonic brazing processes that show promise for achieving this goal [Cooper, 2010]. In addition, Westinghouse produced "bond specimens" that passed shear and autoclave tests before being inserted into the MITR-II at MIT, but after PIE have still not conclusively shown a solution to the bonding dilemma. [Johnson, 2010][Kohse, 2010]

Regardless, while the manufacturing difficulties are being resolved, a tremendous amount of ground may be covered with computer-based modeling. This process began in 2006 with Carpenter's work with FRAPCON [Carpenter, 2006], a steady-state thermo-mechanical fuel rod modeling code that revealed SiC's potential to reach 100 GWd/MTU and a follow up investigation conducted by Yagnik with EPRI's own fuel performance code called FALCON. Yagnik's results indicated that gap closure may occur sooner than later, around 1000 days, but a conclusion has yet to be reached [Yagnik, 2010]. While the gap closure model may be more

difficult to determine than previously thought, it does reveal the importance of initial assumptions and thermo-mechanical models in accurately predicting how certain materials will perform in a pressurized water reactor environment. As will be seen in this thesis, extra effort was put forth to address each assumption and modeling approximation.

1.2 SCOPE

In order for power utilities to accept fuel with a SiC clad, the material must first satisfy core physics parameters. In this effort, the changes in boron concentration, $f_{\Delta H}$ (peak relative power fraction), and pin and assembly burnups were studied. While initial core layout maps needed to be slightly adjusted to lower power peaking, the introduction of SiC cladding into the core required no paradigm shift in the refueling strategy of a nuclear power plant.

In addition, efforts were made to study the realistic implementation and operation of each of these cores. This meant calculating the shutdown margin and other reactivity feedback and control coefficients that are required during the licensing process. While licensing a reactor is an extremely time-consuming and calculation intensive process, a primary goal of this work was to develop cores that showed promise in possibly being licensable one day. This also involved studying the effect of cycles with both Zr and SiC cladding in the core. If a true transition of cladding material occurred, this situation could not be avoided.

By the end of the study, 16 licensable core layouts were created, including two, three, and four-batch refueling strategies. This variety in batch size, and coincidentally average discharge burnup and enrichment, give the utilities a more realistic expectation for fuel costs and operating cycle lengths possible with SiC cladding. In addition, the variety of burnable poisons utilized, such as integral fuel burnable absorber (IFBA), wet annular burnable absorbers (WABA), erbium, and gadolinium, demonstrated the possibility of SiC being widely implemented in the fleet of PWRs.

1.3 THESIS ORGANIZATION

Consisting of nine chapters, this thesis explores the past studies, current research, and future implementation of SiC cladding into the PWR fleet.

In Chapter 1, the main objectives and scope of the research conducted are discussed. In addition, a brief description of the background informs the reader of the most current research related to SiC cladding and the primary advantages, limitations, and concerns known-to-date.

In Chapter 2, the technical aspects and operating conditions of the pressurized water reactor, which become critical input parameters in the computer software, are described. These include specific dimensions and material compositions of the fuel, assembly, and core along with operating temperatures and pressures. In addition, an overview of the different types of burnable absorbers utilized in a PWR is given.

In Chapter 3, the computer software is addressed. For the most part, this involves the description of the Studsvik Core Management Software package. The second half of this section introduces and thoroughly characterizes the key “reactor physics core parameters.”

In Chapter 4 and 5, the challenges and triumphs of designing the 18 and 24-month core designs are explained on a case-by-case basis. A conversation follows, describing the strengths and weaknesses of each core design.

In Chapter 6, the safety of each core design is addressed. This involves the calculation of several important indicators of reactivity feedback and control, including the moderator temperature coefficient (MTC), isothermal temperature coefficient (ITC), uniform Doppler coefficient (UDC), boron coefficient, power coefficient, and shutdown margin (SDM).

In Chapter 7, standard operating procedures are set aside as unique combinations of burnable poisons are investigated, such as IFBA with gadolinium and IFBA with WABA. Subsequent safety analyses follow to provide additional support for their possible implementation.

In Chapter 8, a transition cycle and follow-up safety analysis shows how each reactor physics parameter and safety margin reacts with both SiC and Zr cladding in the same core.

In Chapter 9, the results are summarized and conclusions drawn for the work outlined above. A discussion also follows illuminating future research required for the implementation of SiC cladding in nuclear reactors.

In general, as a thesis involved with the computer-based modeling of a nuclear reactor core, efforts were put into describing only the essential elements of the input and output files generated during simulation runs. For completeness, an example input and output file for each program utilized was placed in the Appendix, along with figures and illustrations of different assemblies modeled in this work. Unfortunately, the size of the appendix was limited and not every variation in code and subroutines could be included. Regardless, the major assumptions and details necessary to understand the larger context of these files will be addressed in the following chapters.

2. PRESSURIZED WATER REACTOR DESIGN

The first step to evaluating the suitability of SiC cladding in the current fleet of American PWRs involved developing a core model with appropriate fuel, assembly, and core dimensions in addition to operating conditions, such as temperatures and pressures. As will be seen, many of these variables are highly interconnected, where a modification to one variable produced a change in the other, leading to a noticeable difference in the reactor physics parameters and cycle length of the core. Fortunately, as will be discussed in the next chapter, these computer-based programs automatically calculated these extrapolations and approximations at a very high rate. In this chapter, the physical characteristics of a typical four-loop Westinghouse PWR with robust fuel assemblies (RFA) was described. Additionally, selected operating conditions found at the Seabrook Nuclear Power Station were utilized as input variables in the computer modeling phase of this project. By assuming fuel management, dimensions, and operating conditions similar to those found in a licensed, PWR, a more accurate evaluation of SiC's benefits to the current fleet of PWRs was possible.

2.1 FUEL DIMENSIONS & CLADDING MATERIAL

Enriched uranium with approximately three to five percent ^{235}U provided the basis for nuclear fission events found in a PWR. Therefore, it was appropriate to begin our discussion where the fission originated, inside the fuel pin, and then move outward, describing the modeling done on the assembly level, followed by a full-core, three-dimensional analysis. While many options existed for reactor fuel dimensions, special care was taken in choosing a fuel pellet design that satisfied accident scenarios and the Nuclear Regulatory Commission (NRC) guidelines. In particular, a SiC-clad fuel rod had to maintain its integrity under both steady-state and anticipated transient conditions. While fuel behavior during a transient was beyond the scope of this work, it was desired to have a fuel rod capable of surviving an Anticipated Operational Occurrence (AOO), in other words, reduced melting from high temperatures during modest mismatch between power and flow, which in this case is exacerbated by SiC's low thermal conductivity [Kazimi, 2011].

Fortunately, this investigation was completed by Carpenter utilizing FRAPCON, a steady-state fuel rod modeling code developed by the Pacific Northwest National Laboratory and INL for the U.S. Nuclear Regulatory Commission and can be used in evaluation of LWR fuel rod behavior up to 65 MWd/kgU. The code calculates the thermal, mechanical, and material evolution of the fuel and cladding of a single fuel rod over time, based on given initial core conditions and power history [Berna, 1997]. The work by various researchers at the Center for Advanced Nuclear Energy Systems at MIT modified this code to a version called FRAPCON-SiCv2 which addressed high-burnup fission gas release, around 100 MWd/kgU, and additional property models for SiC cladding [Long, 2002][Carpenter, 2010].

There were two main conclusions of this research: 1) the thermal conductivity of irradiated SiC dropped to about one third that of irradiated Zircaloy and 2) the gap closure between the fuel and SiC cladding occurred at a much slower rate, primarily from SiC's resistance to creep, compared to Zircaloy-clad fuel. As a result, higher fuel temperatures, fission gas release, and fuel swelling were anticipated, especially during AOOs and power uprates. To mollify these concerns, in this study the fuel pellet was modeled with a 10% central void, leading to a significant reduction of the maximum fuel temperature experienced at the centerline. In addition, as will be discussed later on, the 10% void led to a 10% reduction of uranium mass loaded into the core, saving money on the amount of fuel required, but slightly increasing the average enrichment needed to achieve the same operating cycle length, thus requiring a larger amount of mined uranium.

The solid Zr clad fuel and the cored SiC fuel, shown below in Figure 2.1 illustrate the two different fuel rod designs utilized in this research. Where applicable, the fuel pellet dimensions were matched with the fuel found in the Westinghouse Robust Fuel Assembly (RFA) to be discussed in the next section. Table 2.1 provides additional information that was required for the PWR modeling. It should be noted that the free volume was not changed between the Zr and SiC-clad fuel rods.

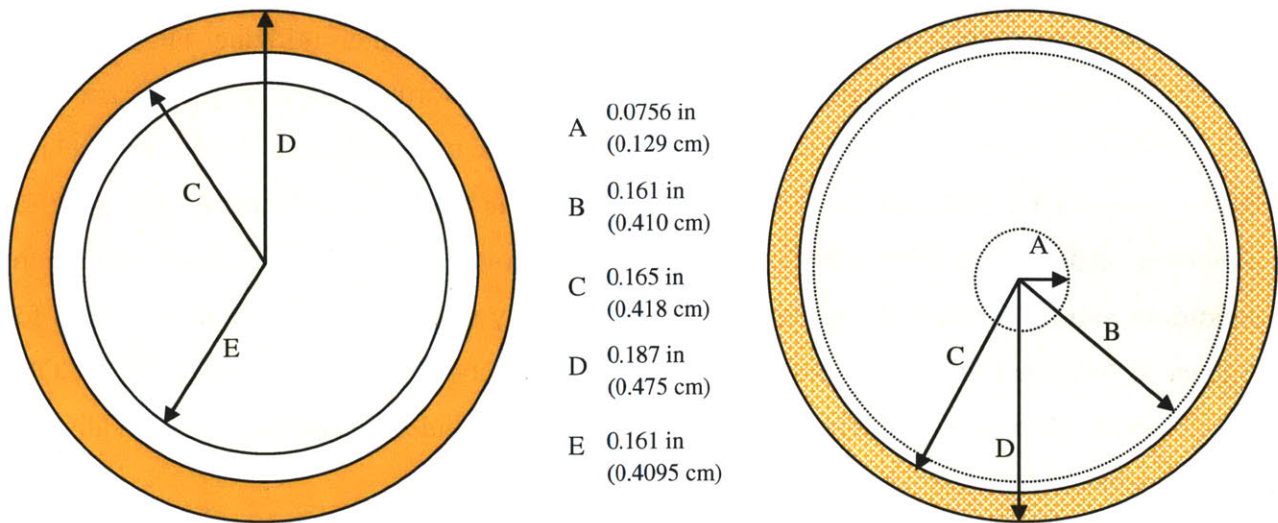


Figure 2.1 (To left) Zr-clad fuel rod with solid UO₂ Fuel pellet. (To right) SiC-clad fuel rod with cored (10% voided) fuel pellet.

Table 2.1 Cold dimensions for SiC and Zr-clad fuel rods

Fuel Parameter	SiC-Clad Fuel	Zr-Clad Fuel
Total Fuel Rod Length (cm)	406	406
Cold Active Fuel Stack Height (cm)	365.8	365.8
Clad Outer Diameter (cm)	0.950	0.950
Fuel Pellet Outer Diameter (cm)	0.820	0.820
Fuel Pellet Inner Diameter (cm)	0.258	0
Cladding Thickness (cm)	0.057	0.057
Stack Density (%)	95.5	95.5
Axial Blanket Region Height, if used (cm)	15.24	15.24
Mass of Uranium Per Fuel Rod UO ₂ (kg)	1.606	1.784

2.2 ASSEMBLY & BURNABLE POISON DESIGN

The next level of design involved the modeling of the Westinghouse Robust Fuel Assembly (RFA). As will be described in Chapter 3, CASMO-4E was the primary program utilized to input the dimensions and material composition of the entire fuel assembly. Figure 2.2 illustrates a cross-section view of a basic, square fuel assembly with no burnable poisons. Table 2.2 summarizes the assembly dimensions, which are identical for both cores with SiC and Zr-clad fuel, except for the amount of uranium loaded per assembly.

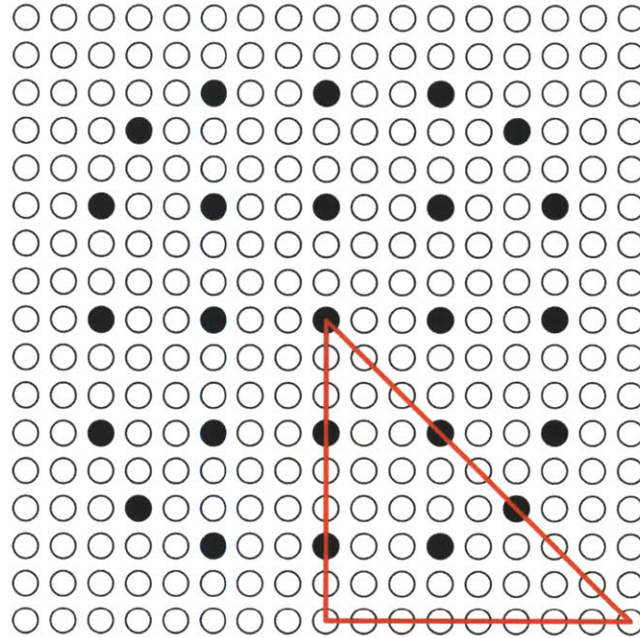


Figure 2.2 Standard PWR assembly layout with no burnable poison. The white circles indicate fuel rod locations and the black circles represent guide tubes where water may flow. The center black dot is also considered a guide tube but is commonly used as an “instrumentation thimble.”

Table 2.2 Fuel assembly dimensions for SiC and Zr clad cases.

Assembly Parameter	SiC-Clad Fuel	Zr-Clad Fuel
Fuel assembly rod array	17x17	17x17
Cold active fuel stack height (cm)	365.8	365.8
Axial blanket region height, if used (cm)	15.24	15.24
Number of guide thimbles	24	24
Number of instrumentation thimbles	1	1
Number of grids per assembly	7	7
Pin-to-pin pitch (mm)	12.6	12.6
Assembly pitch (mm)	215	215
Number of fuel rods per assembly	264	264
Mass of uranium per assembly (kg)	424	471

With the critical dimensions of the assembly now fixed, the next step was to insert burnable poison (BP) into each individual assembly. This was done in a variety of ways utilizing four different burnable poisons – integral fuel burnable absorber (IFBA), wet annular burnable absorber (WABA), erbium (Er), and gadolinium (Gd) rods.

These BP were essential to creating a licensable PWR core that achieved desired cycle lengths and provided effective reactivity control throughout the entire lifetime of the assembly.

Their greatest advantage was the ability to “hold down” or reduce the core’s excess reactivity, especially at BOC. As can be seen in Figure 2.3, without burnable poison, the reactivity reaches a level that would likely cause key reactor physics parameters, described in Chapter 3, to exceed their established limits. The “burnable” aspect in the name refers to the BP’s ability to absorb neutrons at a high rate over the lifetime of the assembly, thus getting consumed in the fuel cycle.

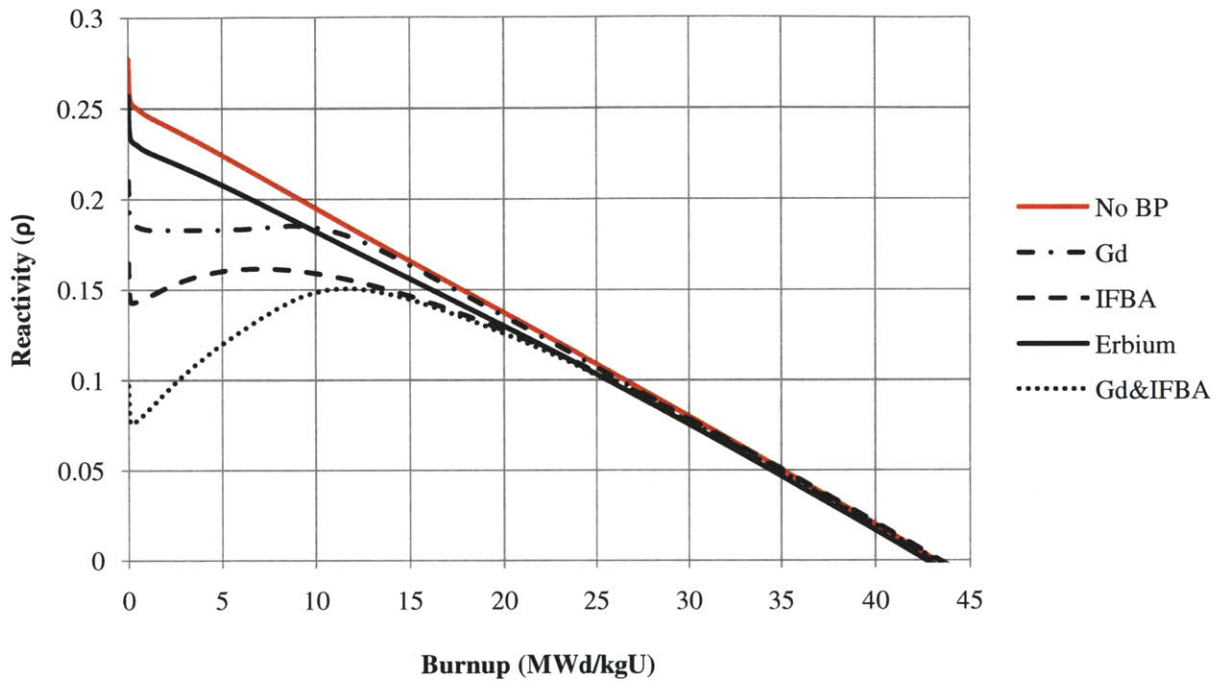


Figure 2.3 A quick comparison of five dimensionally-identical assemblies with varying amounts of different BP rods. The magnitude of these curves can change based on the amount of absorbing isotope loaded, but the general shape remains the same.

As can be seen in Table 2.3, different burnable poisons contain isotopes with varying abilities to absorb neutrons. The average absorption cross-section is a good indicator of each isotope’s ability to absorb neutrons. This characteristic may also be observed in the implementation of different BP in the core. A general observation may be concluded that fewer burnable poison rods are needed if it possesses isotopes with a higher neutron absorption cross section.

Table 2.3 A list of the various isotopes and their absorption cross-sections. All the isotopes are utilized in BP rods, but their total concentration may vary for increasing or decreasing neutron absorption.

Burnable Poison Abbreviation	Element	Chemical Form	Isotopes	Natural Abundance (%) ¹	Thermal Absorption Cross-section, σ_a (barns) ²	Avg. # Rods/ASSY in this Study
Gd	Gadolinium	Gd ₂ O ₃	Gd-152	0.20	300.592	12 - 24
			Gd-154	2.18	85.189	
			Gd-155	14.80	60,886.6	
			Gd-156	20.47	1.7946	
			Gd-157	15.65	254,159	
			Gd-158	24.84	2.20200	
			Gd-160	21.86	1.40990	
Er	Erbium	Er ₂ O ₃	Er-162	0.14	18.908	40 - 84
			Er-164	1.61	12.952	
			Er-166	33.6	16.872	
			Er-167	22.95	649	
			Er-168	26.8	2.741	
			Er-170	14.9	5.776	
			IFBA & WABA	Boron	ZrB ₂	
B-11	80.1	0.0055				16 (WABA)

As will be seen in the following sections, these neutron-absorbing materials can be inserted into the core through a variety of mechanisms, such as fuel rods doped with neutron-absorbing isotope (Gd and Er), fuel pellet coatings (IFBA), and annular rods placed in guide tubes (WABA). Additionally, each PWR core design relied on a constant supply of soluble boron diluted directly into the coolant to provide additional neutron absorption and moderation.

The final characteristic of the assembly modeling was the implementation of axial blankets. In practice, “axial blankets” refer to the assembly region with no burnable poison. Today, axial blankets provide a way to optimize power peaking and its distribution, thus leading to greater power production and increased revenue. As will be seen in Chapters 4 and 5, axial blanket regions significantly alter the peaking factors and, depending upon the circumstances and cycle requirements of the core, have either a helpful or deleterious effect. Figure 2.4 depicts the fashion in which axial zones were implemented in each assembly. If axial blankets were “removed,” it meant that both six inch blanket regions at the top and bottom of the assembly were replaced with the “poisoned” section of the assembly. A keen eye may also spot top and bottom reflectors in Figure 2.4. These were modeled as depleted uranium in CASMO-4E.

¹ Available 16 February 2011 at <http://atom.kaeri.kr/ton/index.html>

² Available 16 February 2011 at <http://www.nndc.bnl.gov/exfor/endl00.jsp>

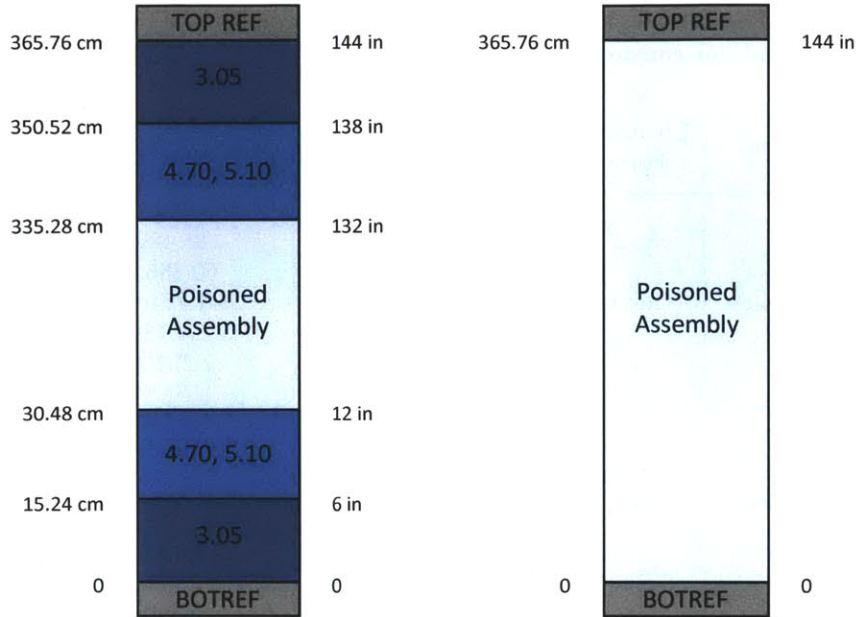


Figure 2.4 An assembly with axial blankets (on left). An assembly with axial blankets removed (on right).

The following sections describe each burnable poison and its specific implementation into the general assembly design.

2.3.a. INTEGRAL FUEL BURNABLE ABSORBER (IFBA)

The primary burnable poison utilized in this research was the Integral Fuel Burnable Absorber (IFBA) rods. This type of burnable absorber was originally developed by Westinghouse for use with its VANTAGE-5 fuel [Cochran, 1990]. In order to manufacture IFBA rods, thin layers of zirconium diboride (ZrB_2), the primary absorber material, was applied directly to the surface of individual UO_2 fuel pellets. Since the application was topical, its surface thickness could be accurately controlled and thus, if certain areas were more susceptible to power peaking, additional ZrB_2 could be applied. In this modeling, however, that level of detail was not necessary. For simulation, the thickness of the coating was considered to be about 3.35 mils (0.0085 centimeters), which can be seen in Figure 2.5. The inner radius of the cladding was kept the same, however, so the very thin application of ZrB_2 only slightly reduced the gap between the fuel and cladding in both the SiC and Zr cases.

Historically, commercial PWRs have loaded between 32 and 156 ZrB_2 -coated fuel rods per assembly. As can be seen in Figure 2.6, as the number of IFBA rods increases, the initial

reactivity hold-down becomes greater, helping to reduce power peaking especially in fresh fuel assemblies. In this study, 64-, 80-, 104-, 128-, 156-, and 180-IFBA rod layouts were considered and can be seen in Appendix A. Westinghouse also introduced a 1.5X IFBA rod which contained, intuitively, one and half times the boron concentration (2.355 mg ¹⁰B/in) [Westinghouse, 2006]. For longer operating periods, like the 24 month cycle length, the 1.5X IFBA rods had to be used. In fact, as will be discussed later, 2X IFBA rods were even considered in the 96-reload case in Chapter 5.1.

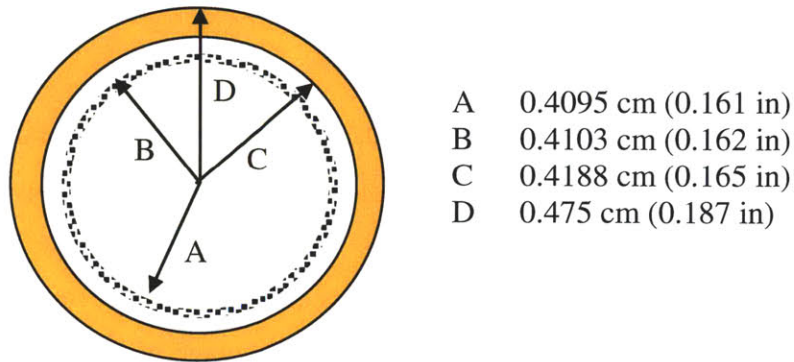


Figure 2.5 Cross-section view of IFBA.

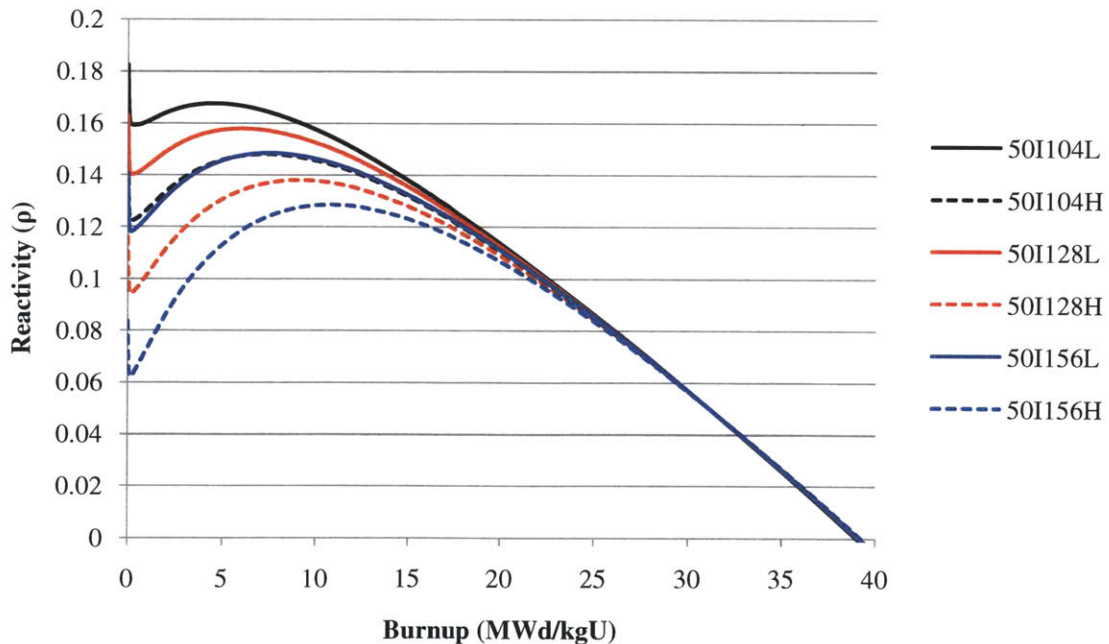


Figure 2.6 Comparison of IFBA loading in the core. “L” refers to 1X IFBA and “H” refers to 1.5X IFBA.

2.3.b. GADOLINIUM (GD)

Gadolinium (III) Oxide, or Gd_2O_3 , has been utilized in both BWRs and PWRs as a very powerful neutron absorbing material. Unlike IFBA, gadolinium was not simply applied as a coating. Instead, the burnable absorber, primarily the ^{155}Gd and ^{157}Gd isotopes, were mixed into uranium dioxide until a predetermined percentage of gadolinium was reached. As a result, a fuel pellet was created with a slightly lower density than non-poisoned UO_2 but with the same fuel and cladding dimensions as described earlier. Consequently, this type of burnable poison led to a reduced linear heat rate and lower average enrichment when compared to older burnable absorbers like $B_4C-Al_2O_3$ [Cochran, 1990].

Unlike the 8,000 to 11,000 IFBA rods required in some cases, only about 400-600 gadolinium rods were required per reload. As a result, less effort was required to manufacture a batch of gadolinium assemblies versus IFBA. This did not automatically imply an economic incentive over IFBA, however, since most vendors already included free IFBA rods as part of a “package deal” for nuclear fuel. Additionally, the percentage of burnable absorber in each rod could be modified as well. Low, medium, and high variants were created that had gadolinium weight percents of 4%, 7%, and 10%, respectively. The specific rod layouts utilized in this research may be viewed in Appendix A.

2.3.c. ERBIUM (ER)

Implemented similarly to gadolinium (III) oxide, erbium (III) oxide was added in similar concentrations to uranium dioxide and then placed into individual fuel rods within the assembly. Since the cross-section for erbium was significantly less than the main absorbing isotopes of gadolinium, more rods of erbium were required per assembly. This led to a more gradual suppression of reactivity, as can be seen in Figure 2.3, improving erbium’s appeal for reducing power peaking and operating at longer cycle lengths.

2.3.d. WET ANNULAR BURNABLE ABSORBER (WABA)

Originally developed by Westinghouse as an improvement over their older burnable poison design known as Pyrex, WABA refers to solid rods of borosilicate glass enclosed in stainless-steel tubing. Like Pyrex, WABA is inserted into the guide tubes, and with an annular

design, utilizes the moderating liquid, in this case water, to enhance its effects. As the water flows through its central annular void, it moderates some of the neutrons which have initially escaped the neutron absorbing tendencies of the aluminum oxide and boron carbide ($\text{Al}_2\text{O}_3\text{-B}_4\text{C}$). This extra moderation in the center of the rod enhances the boron depletion, leading to a significant reduction of the residual reactivity at the cycle's completion [Cochran, 1990]. In practice, the WABA rods were removed after only one cycle in the core. Figure 2.7 describes a WABA rod's physical dimensions while Figure 2.8 illustrates the reactivity hold-down of various assemblies at identical enrichments but varying combinations of WABA and other burnable poisons. In this work, WABA was utilized only in conjunction with other BP, but it could also be implemented as the only BP in a core design.

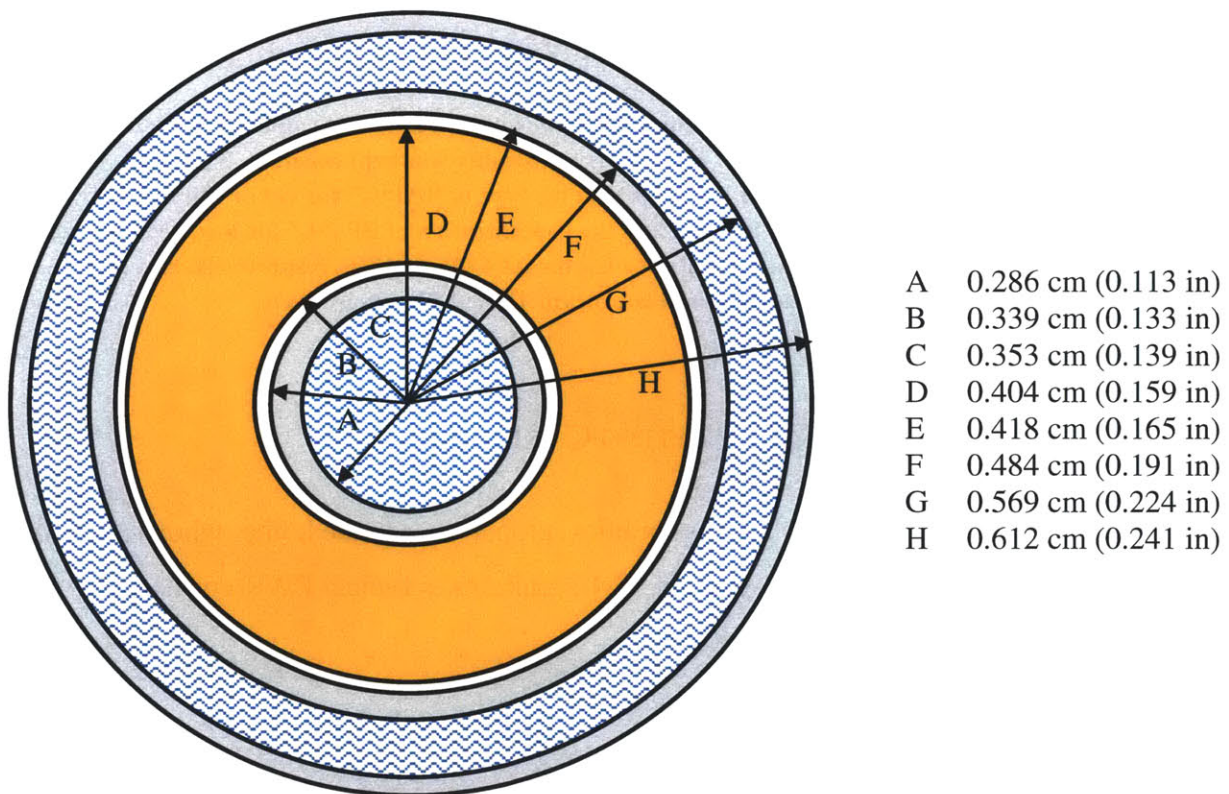


Figure 2.7 WABA rod dimensions, including guide tube cladding.

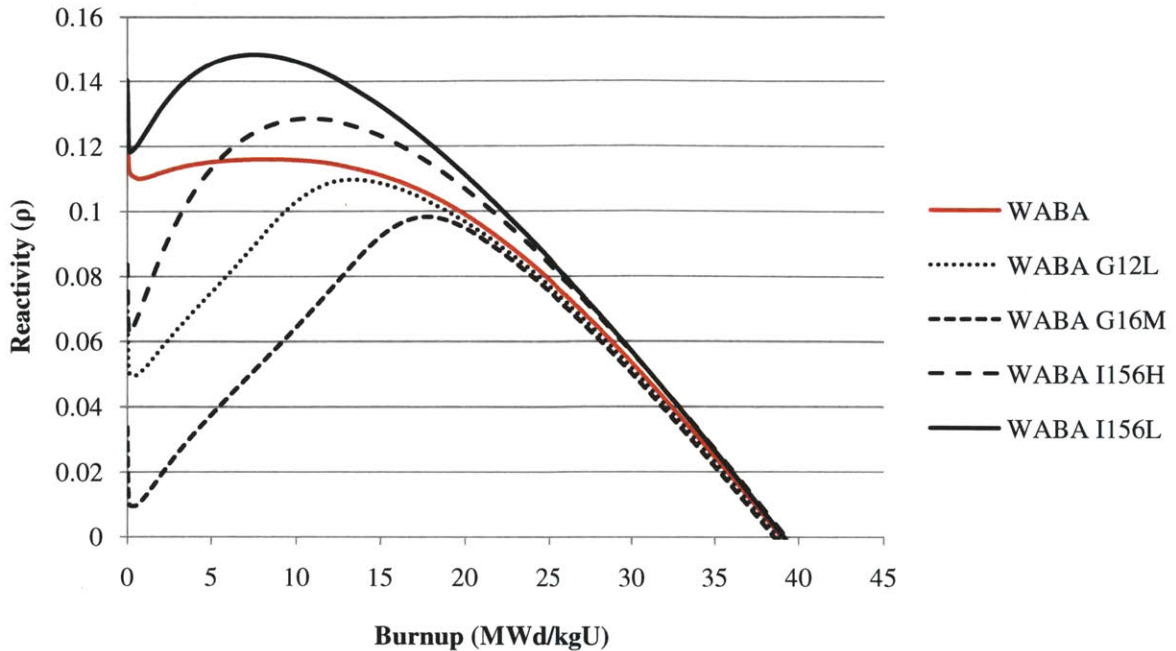


Figure 2.8 Comparison of assemblies with identical enrichments and different combinations of WABA and other burnable poisons. The amount of WABA in each assembly was kept constant. The alpha-numeric designator after “WABA” in the legend indicates first the type of BP (“G” for Gd or “I” for IFBA), the number of BP rods per assembly (12, 16 or 156), and the concentration of BP (“L” for low, “M” for medium, “H” for high). A low or high concentration of BP for Gd meant 4.0% or 10%, respectively, and a low or high concentration of BP for IFBA meant 1X or 1.5X, respectively.

2.3 CORE DESIGN & OPERATING CONDITIONS

Now, with the fuel rods and assemblies properly described, the whole-core, three-dimensional analysis will proceed. As Table 2.4 highlights, a typical PWR consisted of 50,952 fuel rods, organized into 193 assemblies.

Table 2.4 Physical Parameters of Core Design

Operating Parameter	Value
<i>Plant</i>	
Number of primary loops	4
Total heat output of the core (MW _{th}) ³	3587
<i>Core</i>	
Mass of fuel UO ₂ (MT)	101.0
Mass of fuel as U (MTU)	88.2
Rated power density (kW/liter-core)	104.5
Specific power (kW/kgU)	38.7
Core volume (m ³)	32.6
<i>Primary Coolant</i>	
System pressure (MPa)	15.51
Rated coolant mass flux (kg/cm ² ·hr)	751.53
Core inlet temperature (°F)	558.9
<i>Structure</i>	
Number of assemblies	193
Number of fuel rods per assembly	264
Number of fuel rods in core	50,952
Number of grids per assembly	7
Pin-to-pin pitch (mm)	12.6
Assembly pitch (mm)	215
Active fuel height (m)	3.66
<i>Rod Cluster Control Assemblies (RCCA)</i>	
Neutron absorbing material	Ag(80)-In(15)-Cd(5)
Cladding material	Stainless Steel (SS) 304
Cladding thickness (mm)	0.47
Number of RCCA clusters	57

For our work, the 193 assemblies are organized on a chart, referred to from this point forward as a “core loading map,” shown in Figure 2.9.

³ Power level obtained from a Seabrook Cycle Report [Seabrook, 2004].

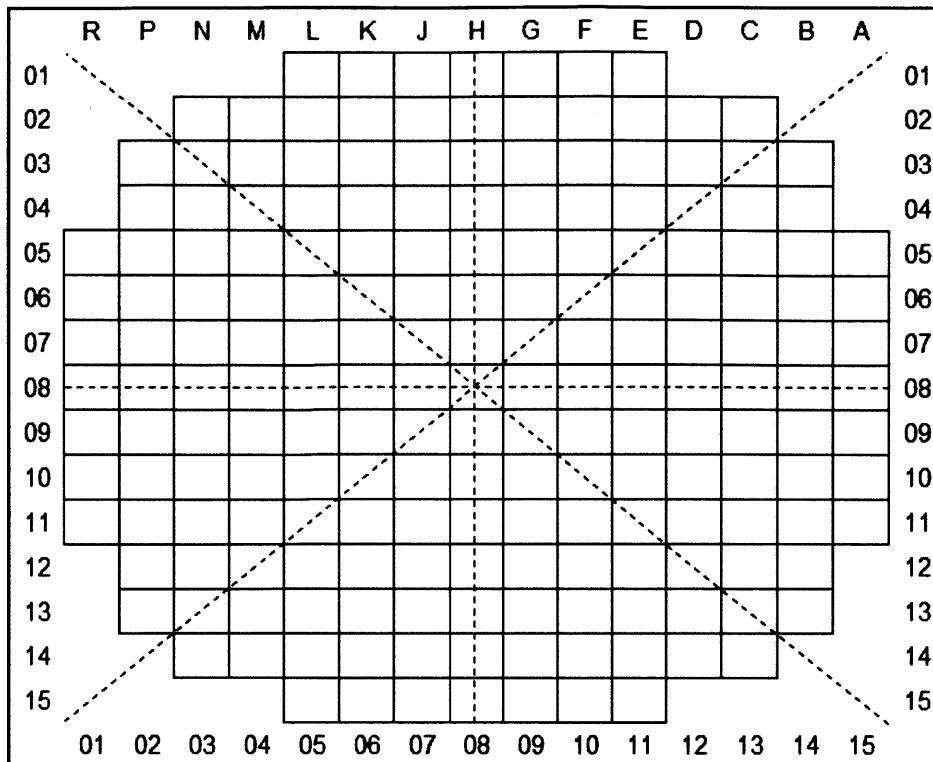


Figure 2.9 A blank core reloading map consisting of 193 potential locations for assemblies in the core.

To better reflect the PWR’s operation, the 193 assemblies were further divided into “batches,” or groups of assemblies that were inserted, shuffled, and removed from the core during refueling outages. This standard approach to fuel management is what has allowed reactors to lower the fuel enrichment needed and utilize older (“more burned”) assemblies to limit the relative power peaking in fresh (“unburned”) assemblies. In the current fleet of PWRs, a three-batch refueling map is the most common; however, the number of batches has ranged from two to six in the fleet. This research has shown though that four batches may be the maximum, usually leading to discharge burnups just below the maximum allowable burnup for SiC.

By estimating the duration of a refueling outage, and assuming a typical operating capacity of a PWR, the cycle burnups discussed earlier may be calculated as follows in Equations 1 through 6. For this research, an optimistic refueling outage of only 28 days was assumed, along with a capacity factor of 95%. Equations 1 and 2 were utilized to calculate the total amount of uranium loaded into the core while Equations 3 through 5 described how the target cycle lengths for both the 18 and 24-month cycles were calculated. Described in Chapter

4, the operating power level was also increased for “uprated” cases to 10% (3946 MW_{th}) and 20% (4304 MW_{th}) above the nominal value. In these cases, the higher power level was simply substituted in Equation 6 and the new cycle burnup was estimated.

$$193 \text{ assemblies} \cdot 264 \text{ pins} \cdot \pi \cdot (.41^2 - .129^2) \cdot 144 \text{ in} \cdot 2.54 \text{ cm} \cdot 10.47 \frac{\text{g}}{\text{cm}^3} \cdot 0.8815 \quad (2.1)$$

$$= 8.1841E7 \text{ g} = 81841 \text{ kg} = 81.8 \text{ MT}$$

$$193 \text{ assemblies} \cdot 264 \text{ pins} \cdot \pi \cdot (.4095^2) \cdot 144 \text{ in} \cdot 2.54 \text{ cm} \cdot 10.47 \frac{\text{g}}{\text{cm}^3} \cdot 0.8815 \quad (2.2)$$

$$= 9.0612E7 \text{ g} = 90612 \text{ kg} = 90.6 \text{ MT}$$

$$CF = \int_0^T \frac{P(t)}{P_o T} dt = 0.95 \quad (2.3)$$

$$\text{Effective Full Power Days (EFPD)} = \int_0^T CF(t) dt = CF \times T(\text{days}) \quad (2.4)$$

$$\text{Target Cycle Length} = \text{EFPD} - \text{Refueling Outage Days} \quad (2.5)$$

$$BU \left(\frac{\text{MWD}}{\text{kgU}} \right) = \frac{P_o [MW(t)] \cdot CF \cdot T(\text{days})}{\text{kgU}} \quad (2.6)$$

As Table 2.5 indicates, higher cycle burnups were expected with SiC-clad fuel, since 10% less fuel was loaded into the core but still expected to reach the same number of EFPDs as the Zr-clad fuel.

Table 2.5 Estimated Cycle burnups for SiC- and Zr-clad fuel at selected power uprates.

	Nominal	10% Uprate	20% Uprate
Power (MW _t)	3587	3946	4304
Specific Power: SiC (kW _t /kgU)	43.83	48.21	52.59
Specific Power: Zr (kW _t /kgU)	39.59	43.55	47.50
18 Month Cycle Burnup: SiC (MWd/kgU)	21652	23816	25980
24 Month Cycle Burnup: SiC (MWd/kgU)	28856	31739	34623
18 Month Cycle Burnup: Zr (MWd/kgU)	19558	21514	23465
24 Month Cycle Burnup: Zr (MWd/kgU)	26064	28671	31272

From an industry point of view, power uprates present utilities with an economic advantage. By increasing the amount of power produced by a nuclear power plant without causing major changes to the structure or design, a tremendous gain in revenue would be achieved with little cost for new construction and parts. In general, most PWRs in operation

today can increase their power levels by at least 10% and still fall within the NRC’s regulations [Kazimi, 2010b].

Differences in power levels also lead to differences in fuel and moderator temperatures which had to be captured in the computer-modeling phase of this project. Table 2.6 and Table 2.7 summarize the assumed average moderator and fuel temperatures, respectively, for the nominal and uprated cases.

Table 2.6 Coolant temperatures for PWR model at full power.

Power Level	Inlet Temperature (°F)	Average Temperature (°F)
Nominal	557	589
10% Uprated	550	589
20% Uprated	541	589

As can be seen in the table above, the moderator temperature was decreased for the 10% uprate case and then again for the 20% uprate case in an attempt to ensure that all heat was removed in the steady-state analysis.

Table 2.7 Average fuel temperatures for PWR model at full power.

Power Level	Fuel Cladding	Core Average Fuel Temperature (°F)
Nominal	Zr	1173
Nominal	SiC	1369
10% Uprated	SiC	1438
20% Uprated	SiC	1506

The fuel temperature values greatly influenced the neutronic calculations performed during the computer-based modeling, primarily as a result of Doppler feedback which led to a flattening of the power distribution and more reactivity, which needed to be controlled during a SCRAM event. In SIMULATE-3, as will be described in the next chapter, a node-averaged fuel pellet temperature versus local linear heat generation rate (LHGR) curve had to be supplied. This average value was found from a Seabrook Operating Note [Seabrook, 2007] that recorded an average LHGR of 5.87 kilowatts (kW) per foot (ft) for a PWR operating at 3587 MW_{th}. Once this piece of information was obtained, a fuel rod temperature history was obtained from one of Carpenter’s FRAPCON results which operated at the same power level and average LHGR.

This was the origin of the temperatures found above in Table 2.7. Finally, by taking the moderator temperatures and LHGR data, the equations required for SIMULATE-3 could be obtained, shown below in Figure 2.10.

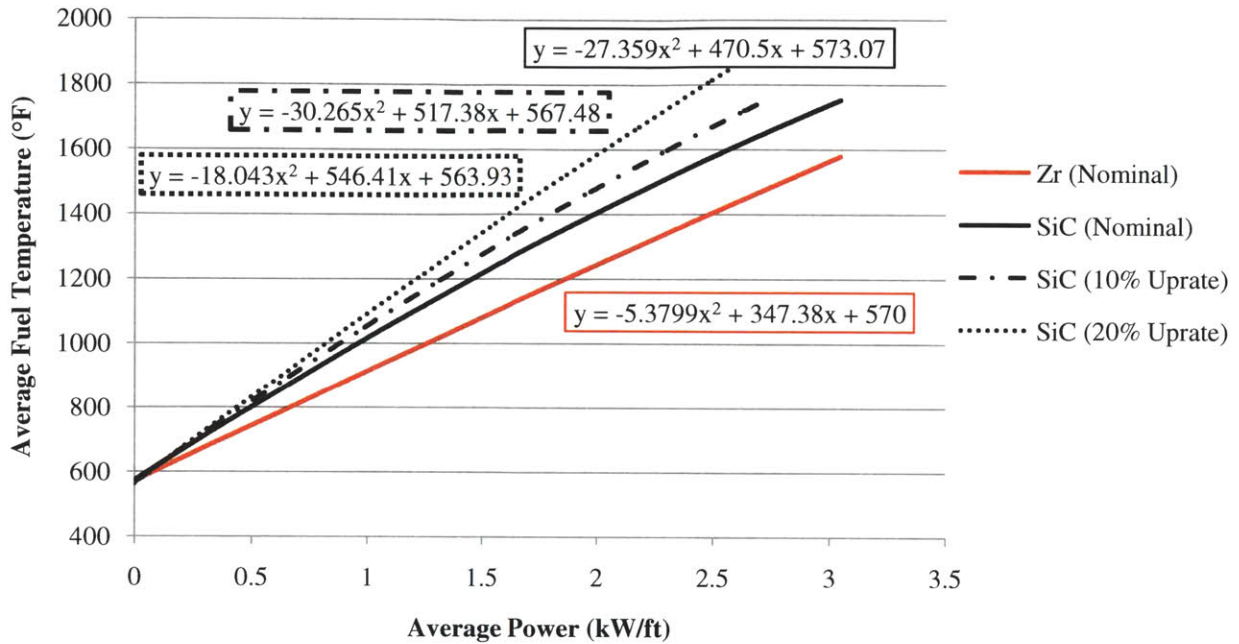
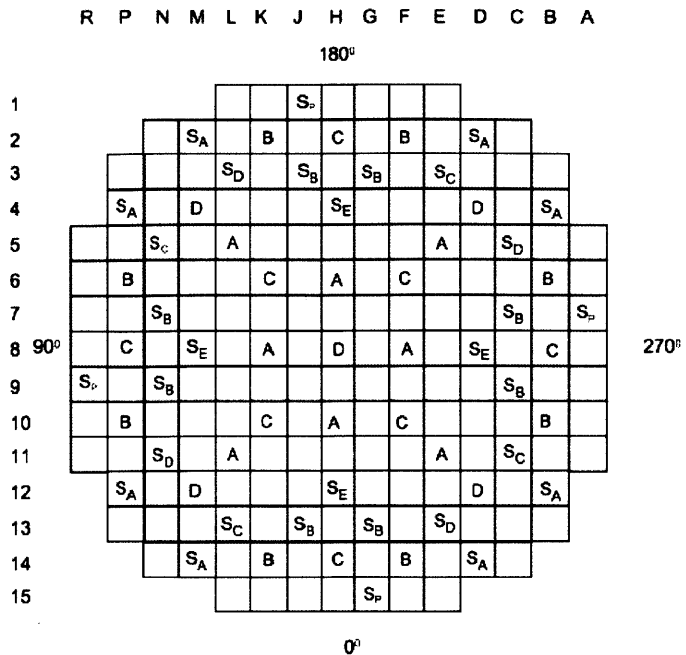


Figure 2.10 LHGR curves for nominal and uprated cases for both SiC and Zr core designs.

It should be noted that in this research, SiC cladding was evaluated only under normal operating conditions. No power transients, accident scenarios, or SCRAM events were simulated. As will be discussed in Chapter 6, each core’s safety was evaluated from a reactivity feedback and control stance, but only involved the calculation of control rod worth for partial and full insertion/withdrawal. As for control rods, as described earlier in Table 2.3 the “rod cluster control assemblies (RCCAs) were assumed to be of the $^{80}\text{Ag}^{15}\text{In}^5\text{Cd}$ type with stainless steel clad found in most Westinghouse PWRs. Dashpots, startup sources, and thimble plugs were not modeled in this work. Figure 2.11 shows the location of the control rod banks modeled in each core design.



<u>Control Bank</u>	<u>Number of Rods</u>		<u>Shutdown Bank</u>	<u>Number of Rods</u>
A	8		SA	8
B	8		SB	8
C	8	S _p - Spare Locations	SC	4
D	5		SD	4
<u>Total</u>	<u>29</u>		SE	4
			<u>Total</u>	<u>28</u>

Figure 2.11 Shutdown and control bank location map for control rods in PWR model

3. DESIGN IMPLEMENTATION

With all the core materials, dimensions, and operating temperatures specified, the next step was to input this data correctly into the appropriate software. This chapter explains the computer-based core modeling approach and the significant reactor physics parameters found in the code's output files.

3.1 COMPUTER SIMULATION TOOLS

In order to accurately investigate SiC's implementation into the current fleet of PWRs, various core designs were simulated via the Studsvik core management system, consisting of CASMO-4e, CMS-Link, and SIMULATE-3. Widely used by industry and regulatory bodies, it is a highly reliable and accurate analysis of steady-state, light water reactor operation. This software provided a licensing-level computer suite that was utilized by more than 200 nuclear reactors around the world [Beccherle, 2007].

3.1.a. CASMO-4E

The first step in designing PWRs was to simulate the assembly-level neutronics (i.e. the neutronics of a square assembly). In the Studsvik core management system, this meant utilizing CASMO-4e, a multi-group two-dimensional transport theory code for burnup calculations, to complete this neutronic analysis. As can be seen in an example CASMO-4e input file found in Appendix B, the code was written in FORTRAN 77 and involved the use of "cards," or three-letter acronyms signaling additional sub-routines in the assembly depletion calculation. Fortunately, this research required no unique geometries or operating conditions so many of the standard cards for a PWR could be utilized. Studsvik's close relationship to industry could also be seen in the newer version of CASMO where cards, like the BPx card, do not need dimensions and materials explicitly stated. Instead, the program automatically assumes default dimensions and material characteristics commonly found in burnable poisons, like IFBA and WABA. For this study, the default values were used where applicable, but in some cases, like defining the SiC cladding, values and materials were defined explicitly.

In addition to modeling geometry and material compositions effectively, CASMO-4e also calculates the reactor physics parameters very accurately with a library containing 40 and 70 energy groups, with neutron energies ranging from 0 to 10 MeV. Effective resonance cross sections and microscopic depletion were calculated individually for each fuel and absorber pin. By utilizing a predictor-corrector approach, the depletion calculation required less burnup steps and greatly simplified the calculations required with burnable poison rods. Despite being programmed in FORTRAN 77, the input file was straight forward and produced an output file that was very informative, giving few-group cross sections and reaction rates for any region of the assembly [Edenius, 1995]. A flow diagram of CASMO-4e can also be found in Appendix B.

3.1.b. CMS-LINK

As TABLES's more advanced and concise successor, CMS-Link functions as a vital linking code that takes CASMO-4e Card Image files, organizes two-group macroscopic cross sections, two-group discontinuity factors, fission product data and other critical depletion information, and then formats them into a binary library utilized by SIMULATE-3. As can be seen in Appendix B, CMS-Link also enables a substantial amount of coding to be removed through the use of the S3C card in the CASMO depletion cases. Without CMS-Link, it would have been much harder to implement and study the various burnable poisons presented in this research, along with modeling the control rods for reactivity feedback and control analysis. As can be seen in Appendix B with an example input file for CMS-Link, only the CASMO-4e card image file name was required to generate a library - no additional user-defined input was required.

3.1.c. SIMULATE-3

Based on the QPANDA neutronics model which employs fourth-order polynomial representations of the intranodal flux distributions in both the fast and thermal groups, SIMULATE-3 provides an advanced two-group nodal code for the analysis of both PWRs and BWRs. Written in FORTRAN 77, the program reconstructs pin power, requires no normalization against higher order calculations, automatically expands geometry, explicitly represents the reflector region, and possesses expanded cross-section modeling among other

capabilities [DiGiovine, 1995]. Most importantly, SIMULATE-3 facilitates fuel management to be studied extensively by allowing core follow and reload physics calculations.

In SIMULATE-3, depletions may be conducted in two or three dimensions with one-eighth, quarter, half, or full core. The core shuffling interface can be easily manipulated along with control rod insertion and withdrawal. As a result, it was also convenient to calculate reactivity coefficients and shutdown margin. The entire core modeling process followed the flow diagram below, in Figure 3.1.

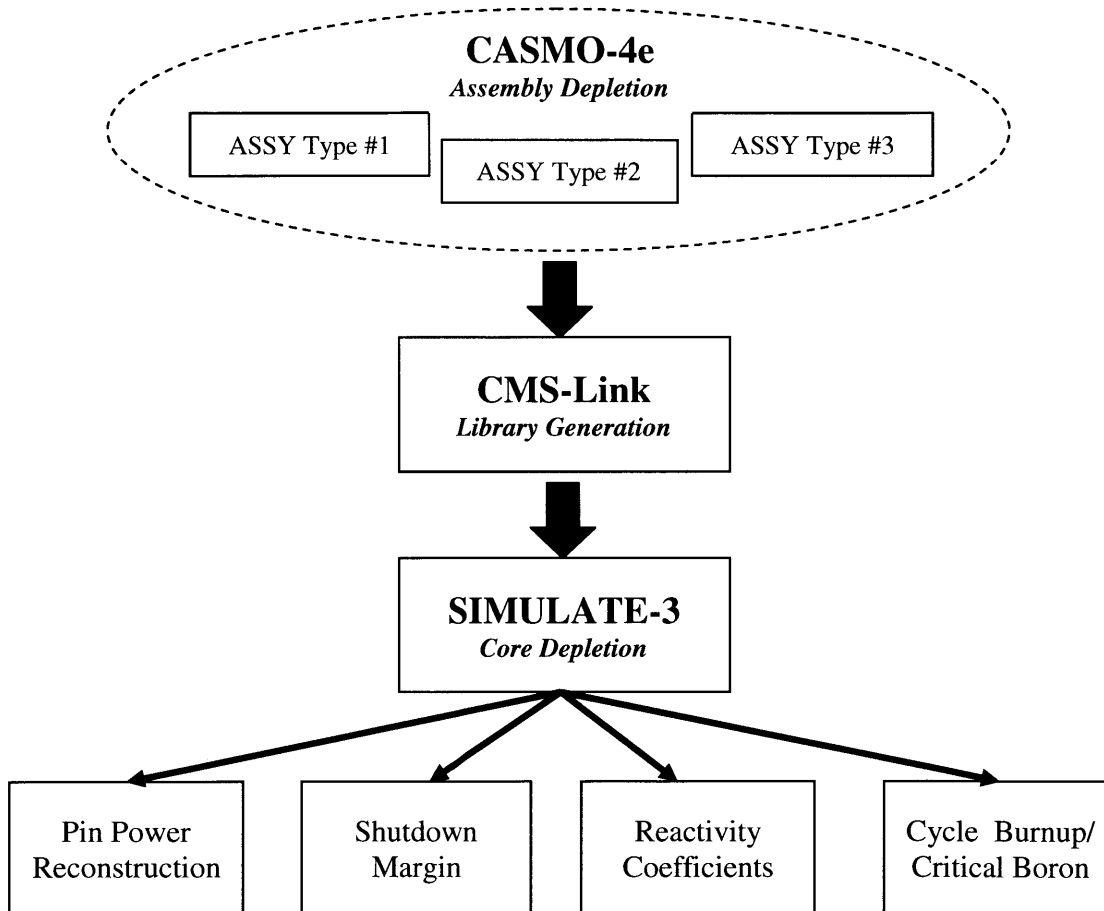


Figure 3.1 Flow diagram of computer-based modeling approach.

3.2 EVALUATION OF KEY REACTOR PHYSICS PARAMETERS

Assessing a reactor core’s worthiness to produce commercial power legally depends on its ability to meet required NRC guidelines and safety margins. For this computer-based modeling study, existing NRC guidelines and industry experience were utilized to establish target values for several major “reactor physics parameters.” Based on these values, slight adjustments were made to the loading pattern and location of burnable poison in order to achieve desired cycle lengths and reduce power peaking, peak burnup, and enrichment. Table 3.1 summarizes the target values for each major reactor physics parameter.

Table 3.1 Steady-state design target values for key reactor physics parameters.

Design Criterion	Target Value
$F_{\Delta h}$	<1.55
F_q	<2.0
Maximum boron concentration (ppm)	<1700
MTC (pcm/°F)	< 0.0
Peak pin burnup (SiC)	< 100 MWd/KgU
Peak pin burnup (Zircaloy)	< 62 MWd/KgU
Shutdown margin	> 1.3%

3.2.a. COOLANT ENTHALPY RISE HOT CHANNEL FACTOR, $F_{\Delta h}$

Thermal design of a PWR required first the nominal performance of the reactor with each primary design variable at its nominal value. Then, given a hypothetical perturbation, each primary design variable was moved away from its nominal value, leading to a new system performance. Hot spot or “hot channel factors” were developed to express the extent to which the new system state departed from its nominal performance as a result of the cumulative effect of variations in all of the primary design variables. The coolant enthalpy rise hot channel factor, $F_{\Delta h}$, was defined as the ratio of the maximum specific enthalpy increase of the coolant (which could possibly occur in any fuel assembly) to the average specific enthalpy increase [Todreas, 1990]. Another similar term used in other thermo-hydraulic analyses was the coolant temperature rise hot channel factor, $F_{\Delta T}$. Both related to the onset of the critical heat flux condition in LWRs, and even more importantly, $F_{\Delta h}$ is required by the NRC to remain under 1.55. As a result, the $F_{\Delta h}$ value was the first variable collected from SIMULATE-3, leading to

changes in the loading pattern, enrichment, and burnable poison location. According to the SIMULATE manual, the $F_{\Delta h}$ is calculated as the maximum, axially-integrated pin-power peaking factor. For brevity, from this point forward, the $F_{\Delta h}$ will be referred to as the “enthalpy rise peaking factor.”

3.2.b. LOCAL PIN POWER F_q

One of the major conveniences of SIMULATE-3 is its ability to perform pin power reconstruction calculations for each fuel rod in the PWR model. Additionally, pin powers were given for each axial node. In this case, 24 axial nodes were specified along the entire length of the fuel pin, about every six inches. All of the nodal powers were then summarized by SIMULATE and the highest value recorded, usually as a core-wide peak-to-average power ratio. Detailed comparisons with critical assembly measurements have demonstrated that PWR pin-by-pin power distributions have root mean square (rms) differences of about 1.0% relative to measured data. Peak pin powers were predicted with rms differences of less than 0.5% relative to measured data [Edenius, 1995]. It should also be noted that the maximum, steady-state F_q value was kept (very conservatively) below 2.0. This was lowered from the typical value of 2.5 in an attempt to account for power maneuvering, xenon transients, and control rod insertions that may lead to local power overshoots of up to 20% from a lack of delays in the SCRAM system [Kazimi, 2010a].

3.2.c. SOLUBLE BORON CONCENTRATION

In addition to PWR cores requiring burnable rods, soluble boron is also used in long-term reactivity control. Also referred to as “chemical shim,” soluble boron is dissolved in PWR coolant to minimize the need for control-rod insertion while allowing spatially uniform neutron absorption. Ideally, the poison would burn out at a rate that matches the depletion of the core’s excess positive reactivity. In our simulations, SIMULATE calculated the amount of soluble boron initially required at BOC and then depleted the core until approximately 0 ppm of boron remained. Realistically the soluble boron in the core is never fully utilized, but this approximation provides the maximum possible cycle length expected with a given core design. For this research, a BOC upper limit on boron concentration was 1700 ppm. This is based primarily on the limits imposed for Zr-clad fuel, since little information exists on the effects of

soluble boron with SiC cladding. In actuality, however, it may be that SiC cladding can withstand a much higher concentration of soluble boron. If this value was slightly eclipsed with one of the core designs to be discussed in Chapter 4 or 5, it was not considered an unacceptable design.

3.2.d. MODERATOR TEMPERATURE COEFFICIENT (MTC)

Like shutdown margin, the MTC exists as both a key reactor physics parameter and an important indicator of design safety. Referred to commonly as a reactivity coefficient or “defect,” the MTC describes the amount of reactivity change resulting from an increase in moderator temperature. As a result, it is desired that this value always be negative throughout the cycle length of the core. This value will be described in more detail and calculated for each core design in Chapter 6.

3.2.e. BURNUP

As one of the most widespread terms in fuel cycle studies, “burnup,” refers to the amount of energy generated by a specific quantity of nuclear fuel, usually expressed in MWd/kgU (or as found in SIMULATE output files, GWd/MTU). When a fuel was said to have been “burned,” this nuclear engineering colloquialism refers to the idea that as the chain reaction occurs, fissionable material within the nuclear fuel rod is removed either by fission or other reactions, and a certain amount of energy is generated. Theoretically, if the fuel were to “burn completely down” this would mean that fissionable material was no longer present and the fission chain reaction would eventually come to a halt. Consequently, this represents a major quantity to understand throughout the entire fuel cycle, since it dictates the amount of energy that could be withdrawn from the core. In this study, three variations of the burnup concept were addressed: 1) cycle burnup, B_c 2) batch average discharge burnup, B_d and 3) maximum (or peak) lead rod burnup. The relationship between the cycle burnup and batch average discharge burnup is given below in Equation 3.1.

$$B_d = B_c \cdot \frac{193}{\# \text{ reload ASSY}} \quad (3.1)$$

Ideally, a PWR should operate to the maximum burnup achievable. According to the NRC, the lead rod burnup in a Zr-clad fuel rod is to be limited to 62 MWd/kgU, but as can be

seen in Table 3.1 and has been mentioned in Chapters 1 and 2, previous research has shown that SiC could withstand burnups as high as 100 MWd/kgU. This was one major advantage to SiC cladding. With the ability to provide 60% greater fuel burnup, SiC promises power utilities with tremendous additional profit. As a result, the core designs in this study were intentionally driven to high burnups, above the current legal limits, in an attempt to develop accurate models of PWR cores with SiC cladding. The assumption was made that eventually the NRC would recognize the higher burnup threshold to SiC and raise their burnup limits accordingly.

4. 18-MONTH CYCLE CORE DESIGNS

Assessing SiC-clad fuel in the core involved designing reload-patterns capable of achieving current operating cycle lengths as well as satisfying the core physics parameters described in the previous section. In order to do this effectively, three approaches were decided upon, listed below:

- Maintain a constant core power density and cycle length, but load fewer fresh assemblies (the first four cases in Table 4.1).
- Maintain a constant cycle length, but increase the core power density (or total reactor power) to the maximum feasible level, staying within the capability of conventional structural materials while utilizing a small increase in pump power and a small decrease in core inlet temperature to remove additional energy (the last two cases in Table 4.1).
- Maintain a constant power density (total reactor power), but extend the fuel cycle length from 18 to 24 months (Chapter 5).

For this chapter, the 18-month cycle with a refueling outage of 28 days was chosen as an appropriate cycle length. Integral Fuel Burnable Absorber (IFBA) was also utilized as the primary burnable poison in all the basic core designs. The significant difference in each case was the reload batch size, which directly affected the average reload enrichment. Table 4.1 summarizes all the 18-month core designs. In the following sections, each core design is specifically discussed, highlighting the advantages and disadvantages to each, along with any other pertinent observations.

Table 4.1 18-month cycle core designs

Batch Size (# Reload)	Uprate	Avg. w/o	B_c	Avg. B_D	EFPD	#IFBA Rods	Boron (ppm)	$F_{\Delta h}$	F_q	Max Pin Burnup
52 SiC (4 bat.)	0%	6.84	21.61	80.2	493	8112 (1.5X)	1465	1.55	1.78	96.0
64 SiC (3 bat.)	0%	5.74	21.70	65.5	495	6656 (1.5X)	1654	1.55	1.81	81.3
84 Zr (3 bat.)	0%	4.52	19.45	44.7	492	12208 (1X)	1477	1.53	1.80	66.8
84 SiC (3 bat.)	0%	4.79	21.56	49.6	492	12208 (1X)	1509	1.50	1.76	74.7
84 SiC (3 bat.)	10%	5.30	23.74	54.5	492	12208 (1X)	1773	1.54	1.80	83.2
84 SiC (3 bat.)	20%	5.78	25.97	59.7	494	12208 (1.5X)	1647	1.50	1.82	88.8

In the proceeding sections, along with summarizing the maximum and average values of various core parameters, graphs are also described for each core, demonstrating the variation of these parameters over the entire cycle length. In most cases, the variation of these parameters was not as important as the maximum value achieved. Given the conservative nature of the nuclear industry, as long as the limits and margins described earlier were not exceeded, it can be assumed that the nuclear reactor would operate safely and effectively. For sake of uniformity, the boron, $F_{\Delta h}$, and F_q parameters were plotted over the cycle length for each core. Below are summary graphs for all the reload cores. As can be seen, the uprated core designs have longer cycle lengths as a result of the greater amount of power produced per kilogram of uranium.

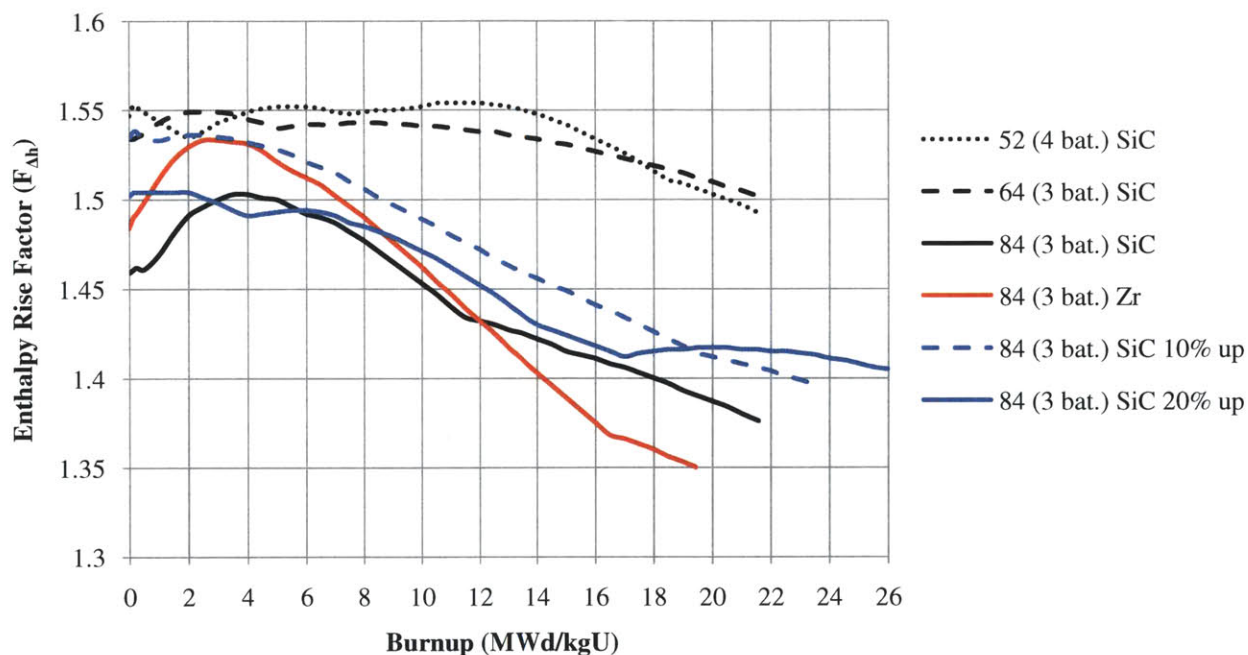


Figure 4.1 $F_{\Delta h}$ for all 18-month core designs.

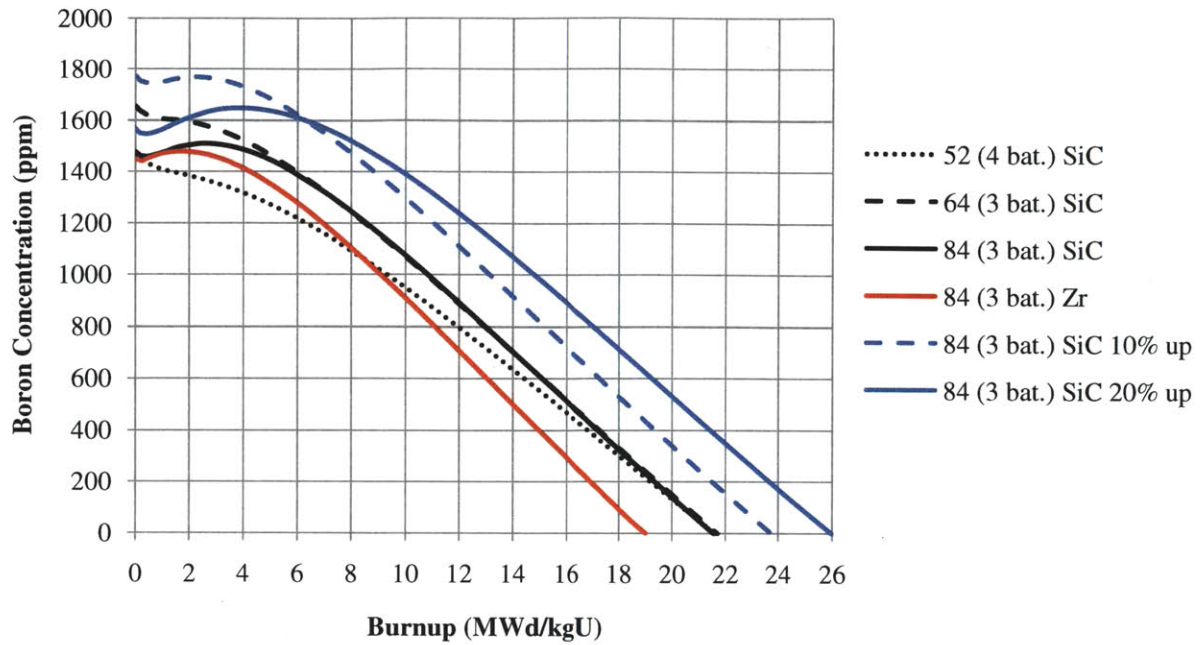


Figure 4.2 Boron concentration (ppm) for all 18-month core designs.

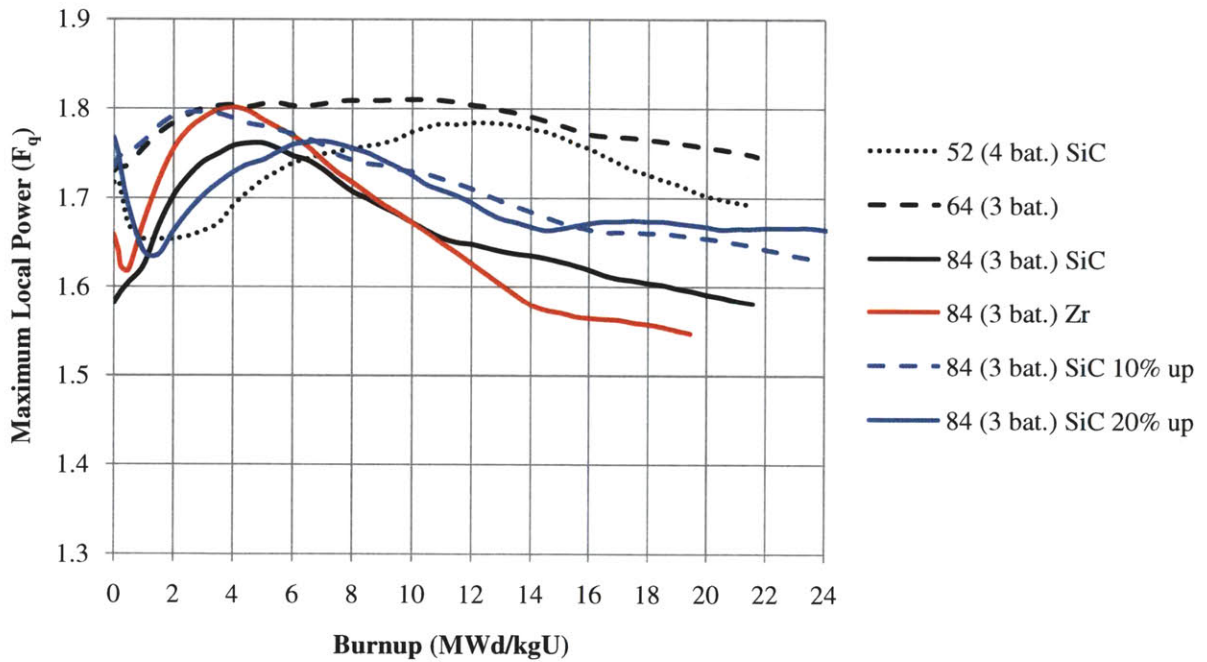


Figure 4.3 F_q for all 18-month core designs.

4.1 52-RELOAD SiC CORE

With only 52 assemblies per reload, the 52-reload pattern was the only four-batch core design investigated in this work. The goal was to implement SiC clad-fuel in a small-batch design. One major drawback, however, was the increased enrichment required to achieve desired cycle length of 493 effective full power days. This design would only be economically desirable if the cost of additional enrichment was higher than the total fabrication costs saved by reloading fewer assemblies. As previous economic analyses have shown, batch size is simply a matter of taste. The additional cost to raise the average enrichment per batch is about the same as the money saved by manufacturing fewer assemblies. If enrichment processes became less expensive, however, decreasing batch size might become a more economically favorable option [Kazimi, 2010a].

Special care was also taken in placing highly burned, older fuel in the proximity of fresh fuel assemblies. In some circumstances, very high peaking factors were created as a result of extreme neutron suppression regions being adjacent to very high neutron generation regions. With the greatest enrichment per reload, the highest average discharge burnup was experienced in the core. In fact, the burnups experienced with this reload pattern (around 100 MWd/kgU), would only be possible with SiC cladding. Figure 4.4 shows the reloading pattern. Unlike the other designs, the fresh fuel was more separated, with half of the assemblies toward the center and the rest in a concentric ring around the twice-burned fuel. As will be seen with all the 3-batch designs, the majority of once-burned assemblies were also placed on the periphery.

Unlike other core designs, the 52-reload pattern also relied on changes in blanket enrichments to lower $F_{\Delta h}$ to an acceptable level. Of course, the nuclear industry has proprietary codes that can optimize these blanket and axial enrichments to achieve the lowest possible $F_{\Delta h}$. Unfortunately, in this research such codes were not available, and as a result, a tremendous amount of effort was put into reducing these factors through trial-and-error. In the end, all these results achieved the target values, but were not the optimal fuel management figures for the given operating conditions.

Table 4.2 52-reload core design summary of reactor physics parameters.

Batch Size (# Reload)	Uprate	Avg. w/o	B_C	Avg. B_D	EFPD	#IFBA Rods	Boron (ppm)	$F_{\Delta h}$	F_q	Max Pin Burnup
52 SiC (4 bat.)	0%	6.84	21.61	80.2	493	8112 (1.5X)	1465	1.55	1.78	96.0

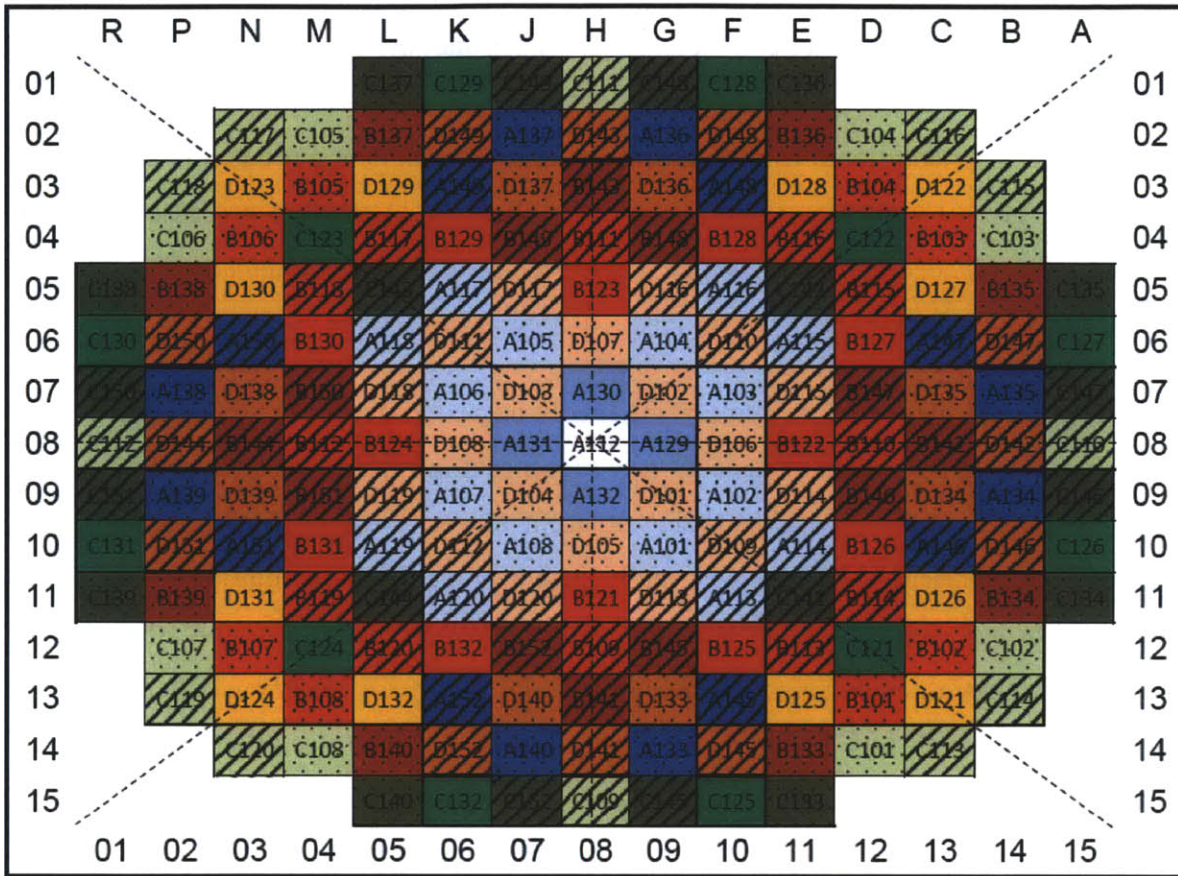


Figure 4.4 52-reload core loading map.

Table 4.3 52-reload batch summary

Fuel	Fuel Batch ID	# ASSYs	ASSY w/o	Blanket w/o	BP Rods per ASSY	IFBA Loading (mg ¹⁰ B/in)
Thrice	67I156H	8	6.7	5.5	156	2.355
Thrice	67I156H	8	6.7	5.0	156	2.355
Thrice	70I156H	4	7.0	5.0	156	2.355
Thrice	67I156H	8	6.7	4.5	156	2.355
Thrice	77I156H	8	7.7	5.5	156	2.355
Twice	67I156H	8	6.7	5.5	156	2.355
Twice	67I156H	12	6.7	5.0	156	2.355
Twice	70I156H	12	7.0	5.0	156	2.355
Twice	67I156H	8	6.7	4.5	156	2.355
Twice	77I156H	12	7.7	5.5	156	2.355
Once	67I156H	8	6.7	5.5	156	2.355
Once	67I156H	12	6.7	5.0	156	2.355
Once	70I156H	12	7.0	5.0	156	2.355
Once	67I156H	8	6.7	4.5	156	2.355
Once	77I156H	12	7.7	5.5	156	2.355
Fresh	67I156H	8	6.7	5.5	156	2.355
Fresh	67I156H	12	6.7	5.0	156	2.355
Fresh	70I156H	12	7.0	5.0	156	2.355
Fresh	67I156H	8	6.7	4.5	156	2.355
Fresh	77I156H	12	7.7	5.5	156	2.355

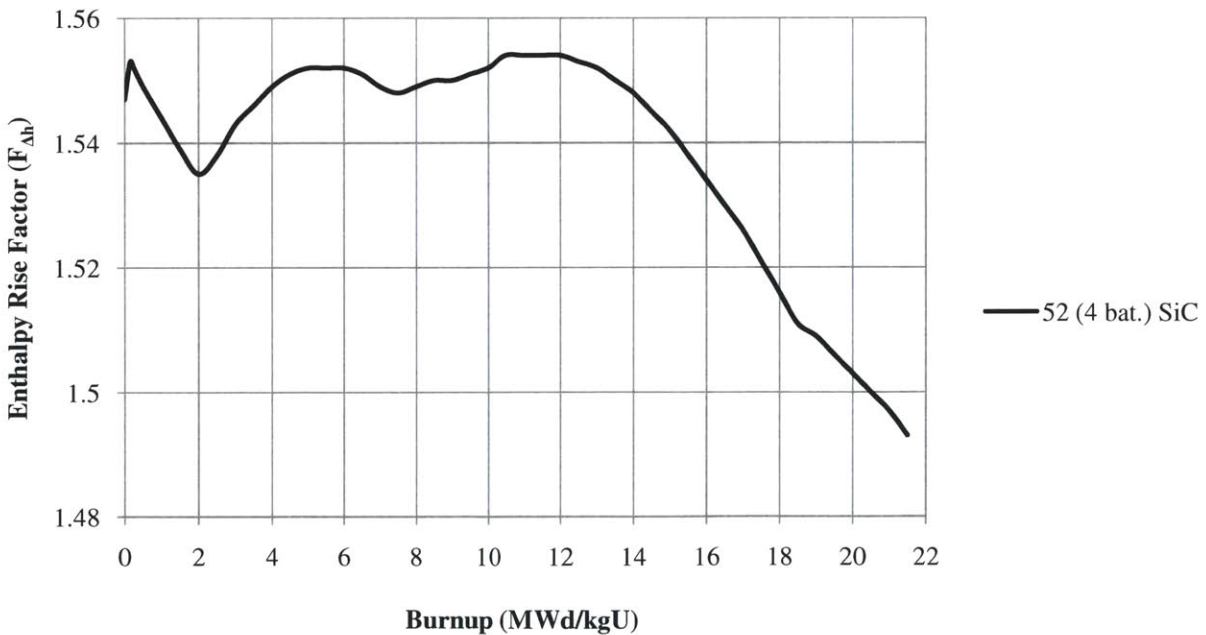


Figure 4.5 F_{Ah} for 52-reload core design.

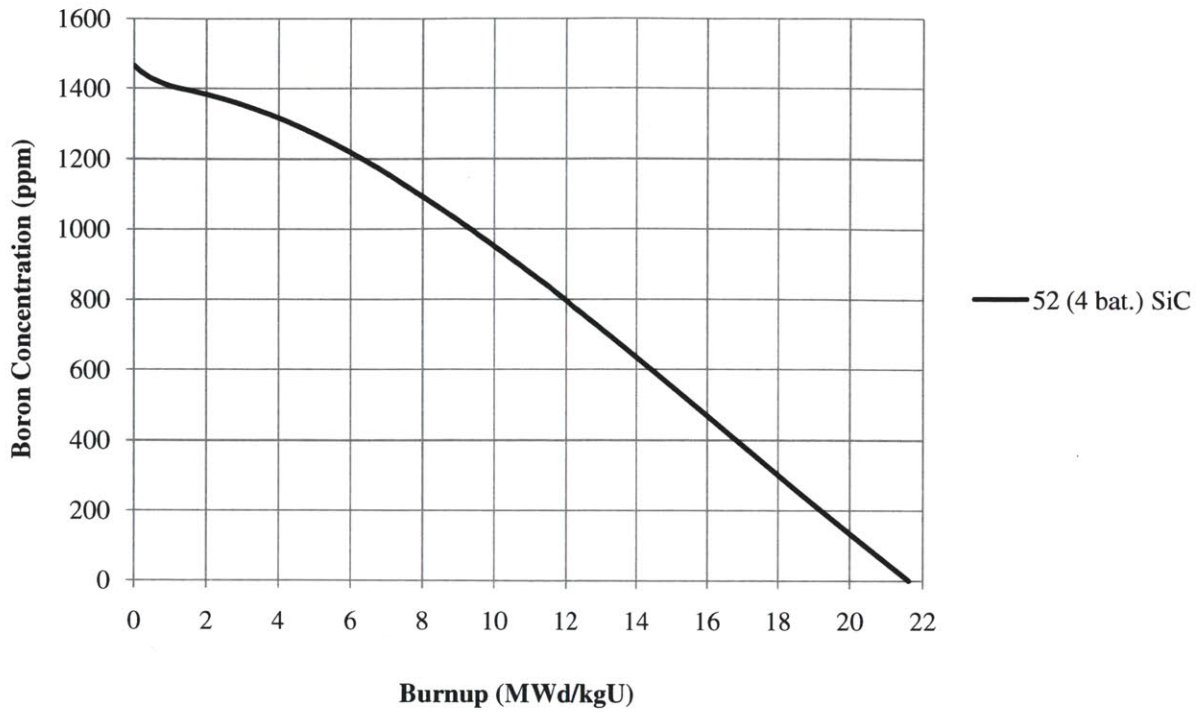


Figure 4.6 Boron concentration (ppm) for 52-reload core design.

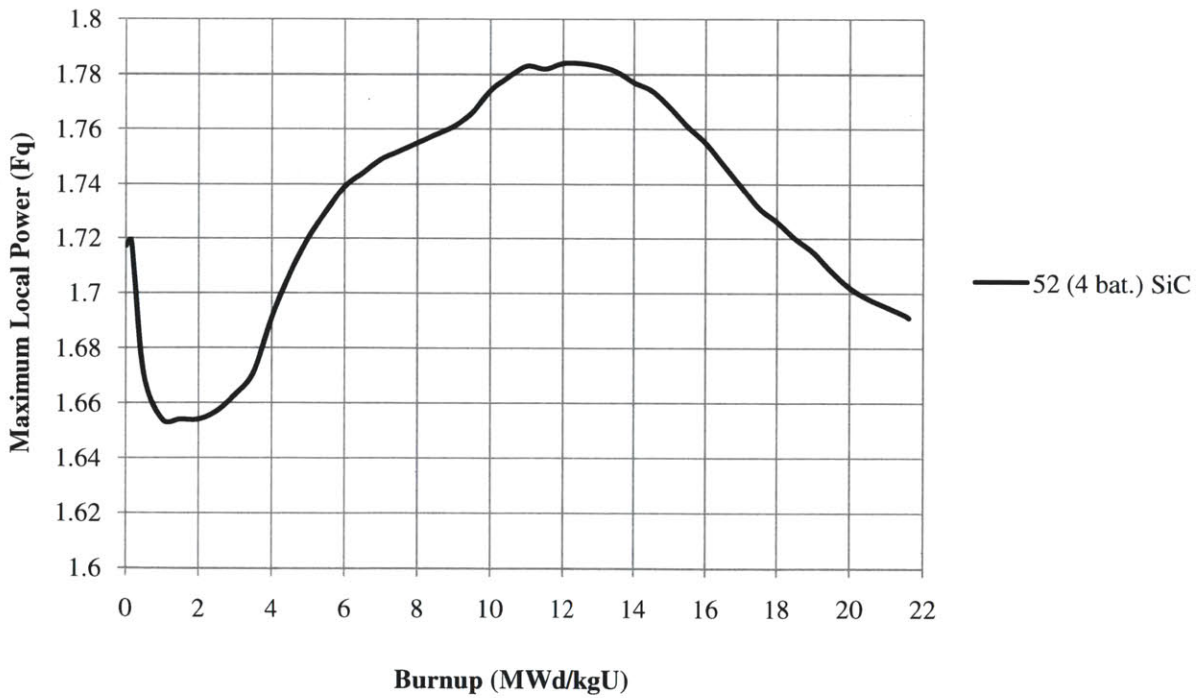


Figure 4.7 F_q for 52-reload core design.

4.2 64-RELOAD SIC CORE

The 64-reload core design was the first in a series of 3-batch designs. The significant difference with this design, however, was the utilization of a thrice-burned assembly in the core's center. Since there were only 193 possible assembly locations, 3 batches of 64 assemblies required an additional assembly in the center to fill all possible locations. As a result, most of the maximum core parameter values occurred in this lead center assembly.

Table 4.4 64-reload core design summary of reactor physics parameters.

Reload #	Uprate	Avg. w/o	B _C	Avg. B _D	EFPD	#IFBA Rods	Boron (ppm)	F _{Δh}	F _q	Max Pin Burnup
64 SiC (3 bat.)	0%	5.74	21.70	65.5	495	6656 (1.5X)	1654	1.55	1.81	81.3

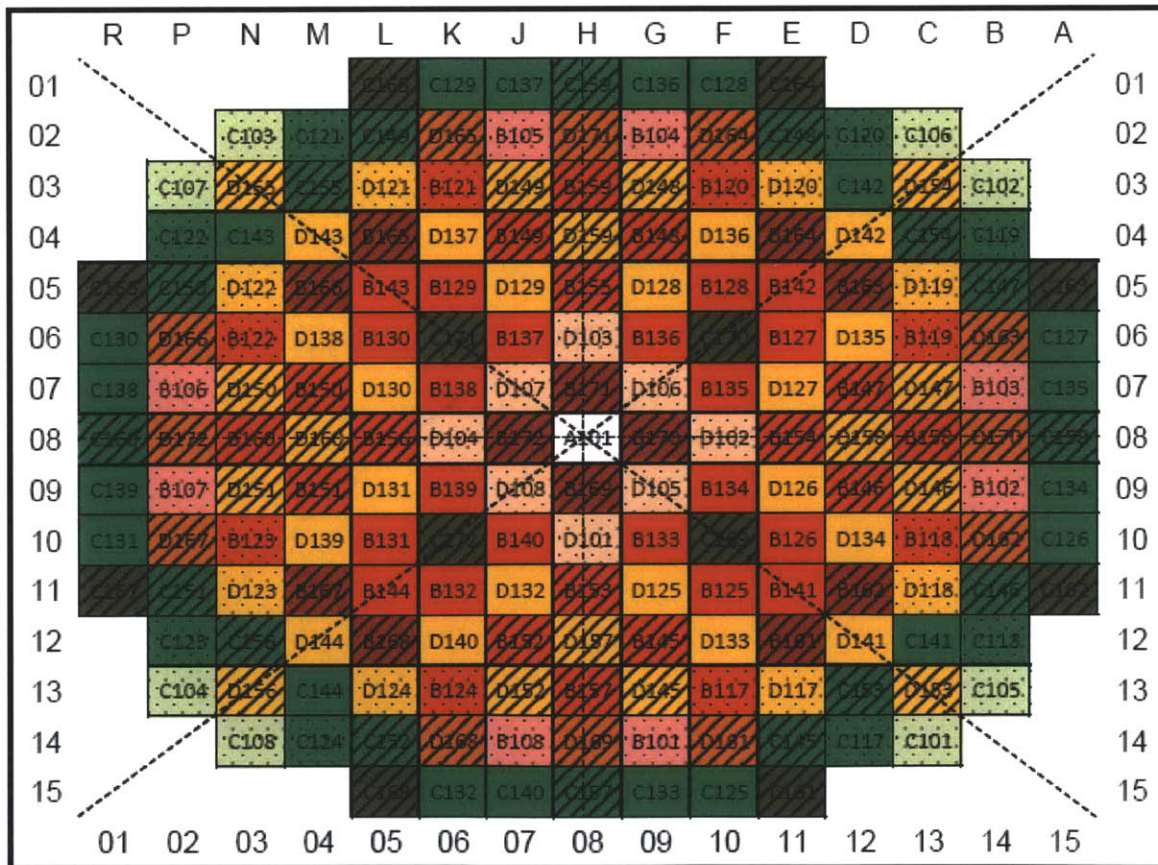


Figure 4.8 64-reload core loading map

Table 4.5 64-reload fuel batch summary.

Fuel	Fuel Batch ID	# ASSYs	ASSY w/o	Blanket w/o	BP Rods per ASSY	IFBA Loading (mg ¹⁰ B/in)
Thrice	60I104H	1	6.0	3.2	104	2.355
Twice	60I104H	8	6.0	3.2	104	2.355
Twice	55I104H	8	5.5	3.2	104	2.355
Twice	55I104H	20	5.5	3.2	104	2.355
Twice	55I104H	16	5.5	3.2	104	2.355
Twice	77I104H	12	7.7	3.2	104	2.355
Once	60I104H	8	6.0	3.2	104	2.355
Once	55I104H	8	5.5	3.2	104	2.355
Once	55I104H	20	5.5	3.2	104	2.355
Once	55I104H	16	5.5	3.2	104	2.355
Once	77I104H	12	7.7	3.2	104	2.355
Fresh	60I104H	8	6.0	3.2	104	2.355
Fresh	55I104H	8	5.5	3.2	104	2.355
Fresh	55I104H	20	5.5	3.2	104	2.355
Fresh	55I104H	16	5.5	3.2	104	2.355
Fresh	77I104H	12	7.7	3.2	104	2.355

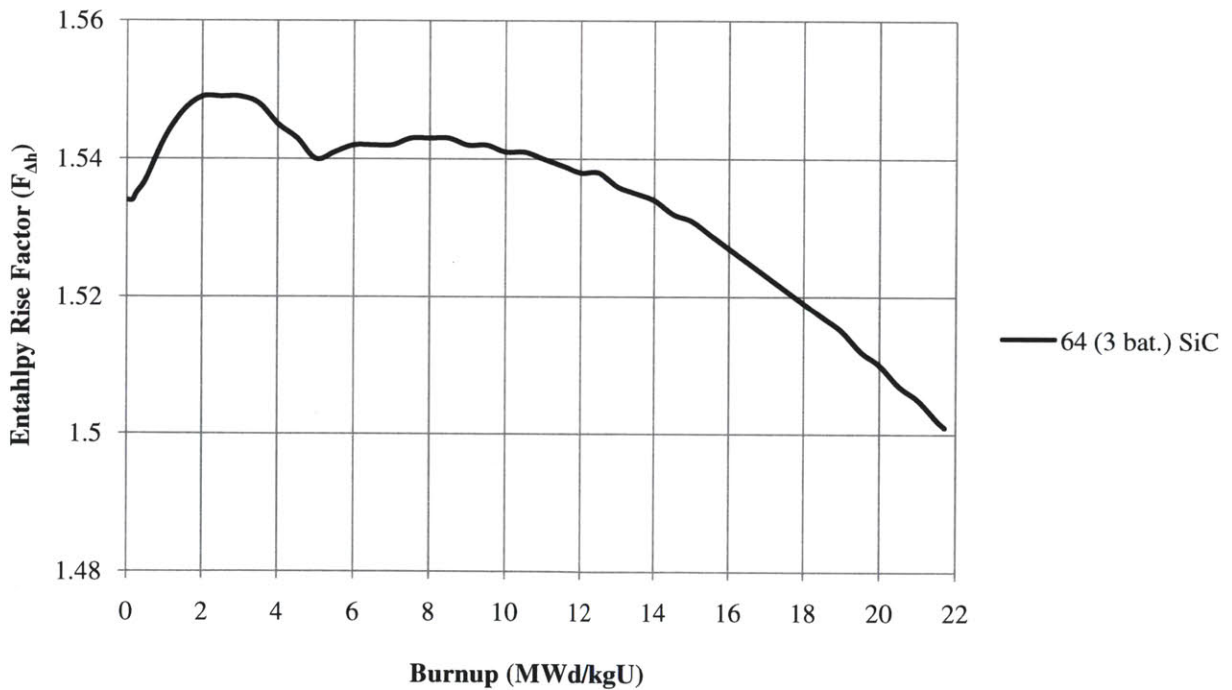


Figure 4.9 F_{Ah} for 64-reload core design.

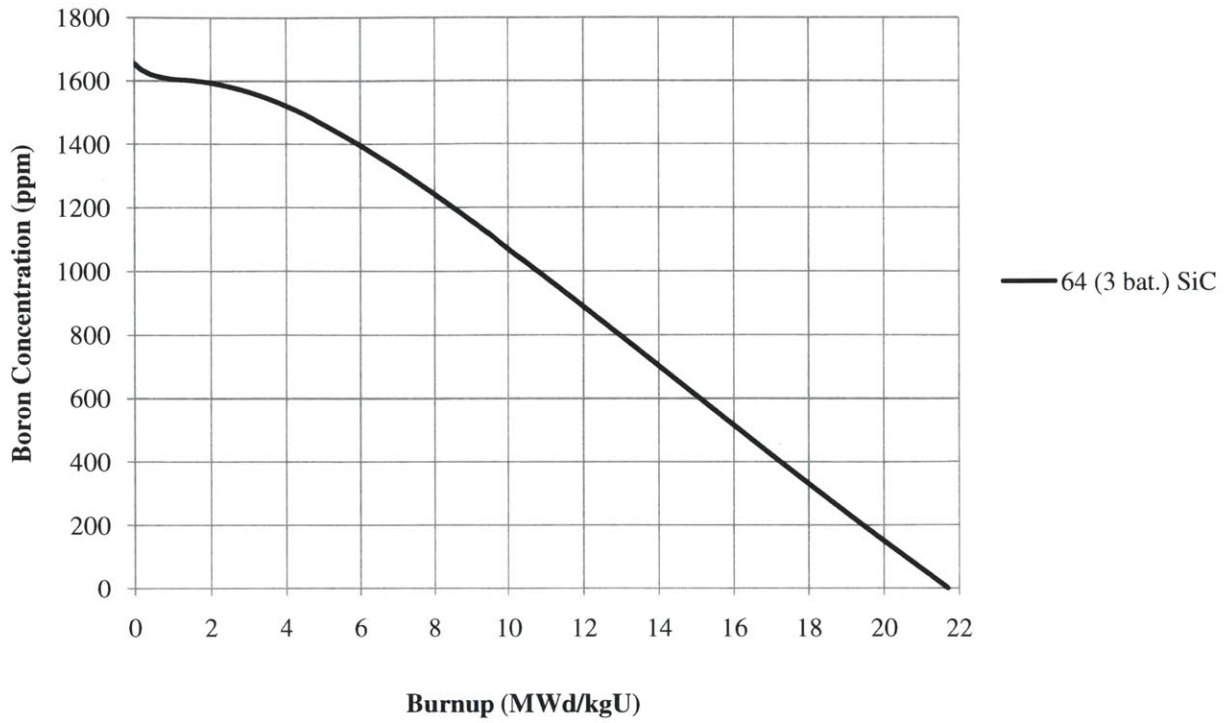


Figure 4.10 Boron concentration (ppm) for 64-reload core design.

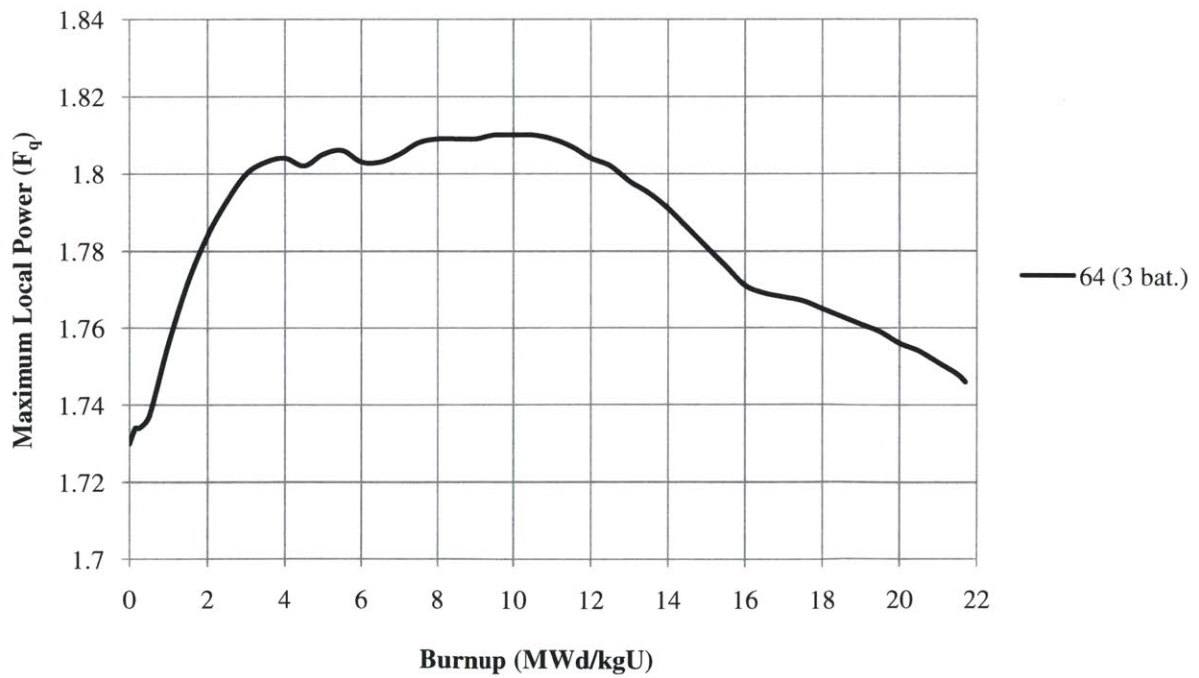


Figure 4.11 F_q for 64-reload core design.

4.3 84-RELOAD ZR CORE

In order to show the advantages and disadvantages of SiC cladding more directly, a reference case with Zr clad was created. Special care was taken in designing a loading pattern that kept the peak burnup limit of zirconium below 75 MWd/kgU. The same reloading pattern was utilized for the reference case as well as the 84-reload nominal and uprated cases. Figure 4.12 represents the loading pattern for all four cases.

Table 4.6 84-reload Zr core design summary of reactor physics parameters.

Reload #	Uprate	Avg. w/o	B _C	Avg. B _D	EFPD	#IFBA Rods	Boron (ppm)	F _{Δh}	F _q	Max Pin Burnup
84 Zr (3 bat.)	0%	4.52	19.45	44.7	492	12208 (1X)	1477	1.53	1.80	66.8

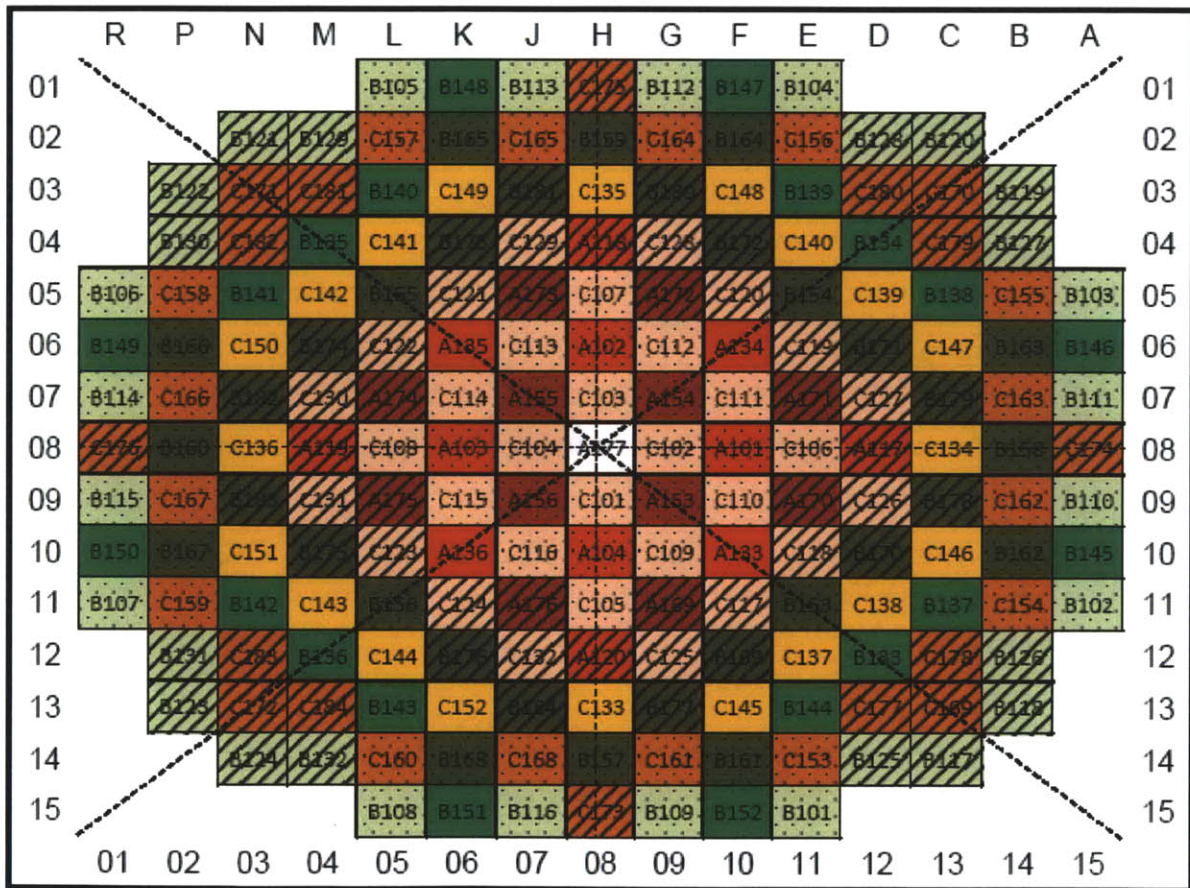


Figure 4.12 84-reload core loading map for the Zr, SiC, and uprated cases.

Table 4.7 84-reload Zr fuel batch summary

Fuel	Fuel Batch ID	# ASSYs	ASSY w/o	Blanket w/o	BP Rods per ASSY	IFBA Loading (mg ¹⁰ B/in)
Twice	50I156L	4	5.0	3.2	156	1.57
	43I156L	4	4.3	3.2	156	1.57
	43I156L	4	4.3	3.2	156	1.57
	47I128L	4	4.7	3.2	128	1.57
	50I128L	9	5.0	3.2	128	1.57
Once	50I156L	16	5.0	3.2	156	1.57
	43I156L	16	4.3	3.2	156	1.57
	43I156L	20	4.3	3.2	156	1.57
	47I128L	16	4.7	3.2	128	1.57
	50I128L	16	5.0	3.2	128	1.57
Fresh	50I156L	16	5.0	3.2	156	1.57
	43I156L	16	4.3	3.2	156	1.57
	43I156L	20	4.3	3.2	156	1.57
	47I128L	16	4.7	3.2	128	1.57
	50I128L	16	5.0	3.2	128	1.57

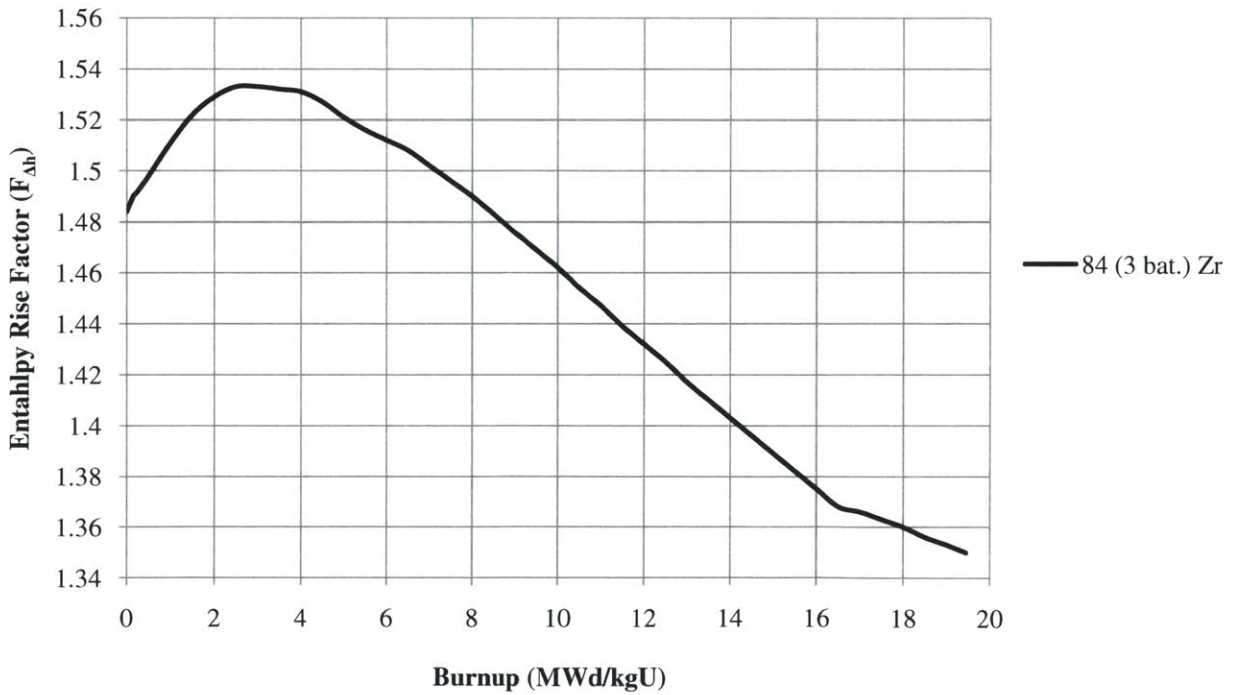


Figure 4.13 F_{Ah} for 84-reload Zr core design.

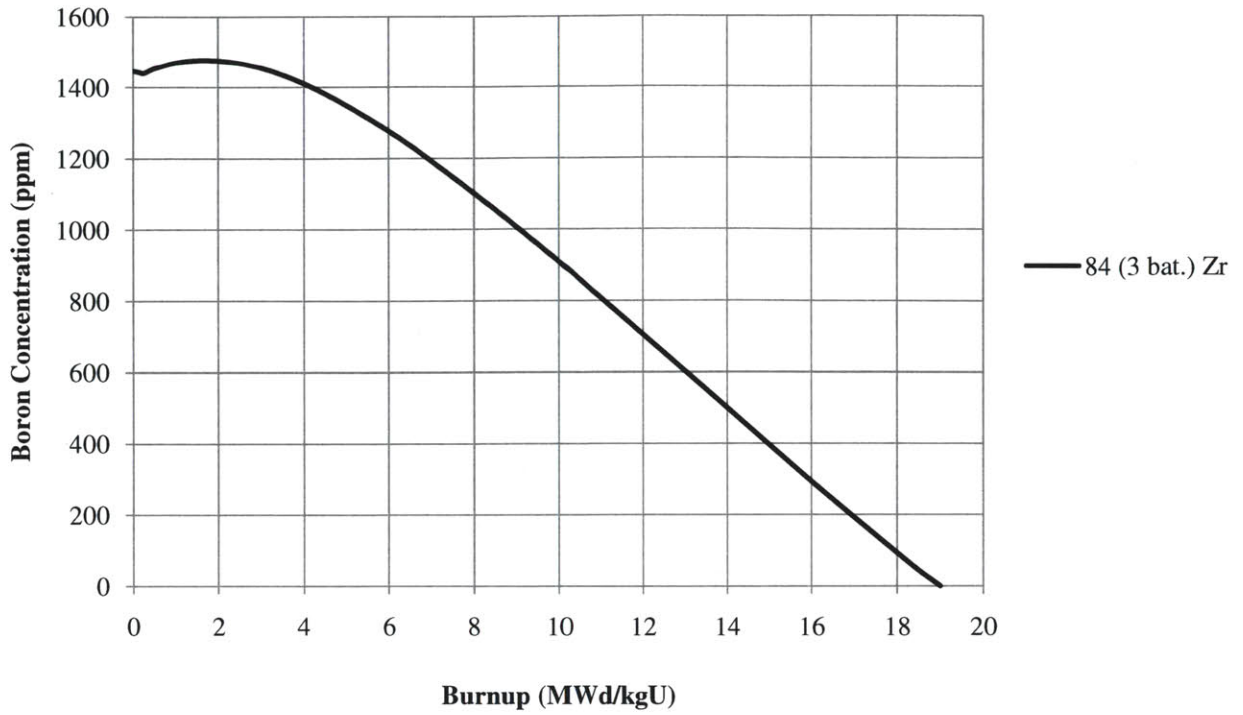


Figure 4.14 Boron concentration (ppm) for 84-reload Zr core design.

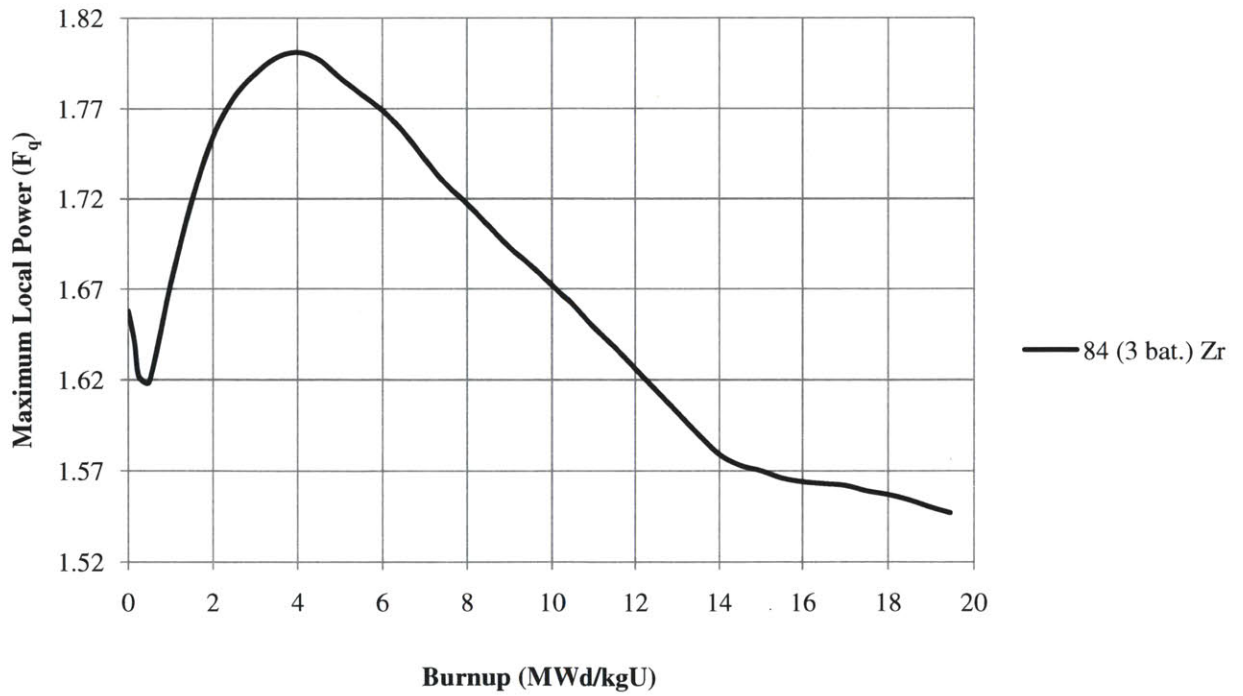


Figure 4.15 F_q for the 84-reload Zr core design.
















4.4 84-RELOAD SiC CORE

Utilizing the same reloading pattern from section 4.3, the 84-reload SiC case was created by changing the cladding material from Zr to SiC and adding a 10% void to each fuel pellet, including the blanket regions. These differences in fuel structure led to higher cycle burnups and greater average enrichments per reload.

Table 4.8 84-reload core design summary of reactor physics parameters.

Reload #	Uprate	Avg. w/o	B _C	Avg. B _D	EFPD	#IFBA Rods	Boron (ppm)	F _{ΔH}	F _q	Max Pin Burnup
84 SiC (3 bat.)	0%	4.79	21.56	49.6	492	12208 (1X)	1509	1.50	1.76	74.7

Table 4.9 84-reload SiC core design fuel batch summary.

Fuel	Fuel Batch ID	# ASSYs	ASSY w/o	Blanket w/o	BP Rods per ASSY	IFBA Loading (mg ¹⁰ B/in)
 Twice	55I156L	4	5.5	3.2	156	1.57
 Twice	44I156L	4	4.4	3.2	156	1.57
 Twice	44I156L	4	4.4	3.2	156	1.57
 Twice	50I128L	4	5.0	3.2	128	1.57
 Twice	55I128L	9	5.5	3.2	128	1.57
 Once	55I156L	16	5.5	3.2	156	1.57
 Once	44I156L	16	4.4	3.2	156	1.57
 Once	44I156L	20	4.4	3.2	156	1.57
 Once	50I128L	16	5.0	3.2	128	1.57
 Once	55I128L	16	5.5	3.2	128	1.57
 Fresh	55I156L	16	5.5	3.2	156	1.57
 Fresh	44I156L	16	4.4	3.2	156	1.57
 Fresh	44I156L	20	4.4	3.2	156	1.57
 Fresh	50I128L	16	5.0	3.2	128	1.57
 Fresh	55I128L	16	5.5	3.2	128	1.57

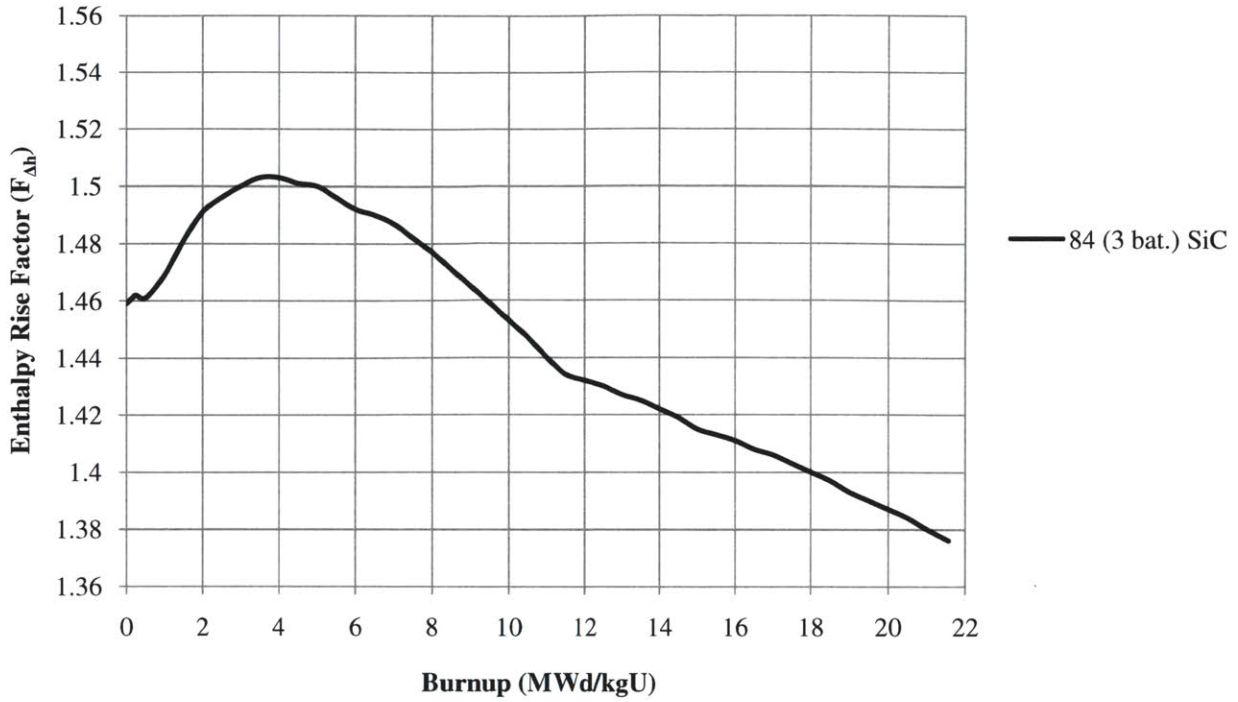


Figure 4.16 F_{Ah} for 84-reload SiC core design.

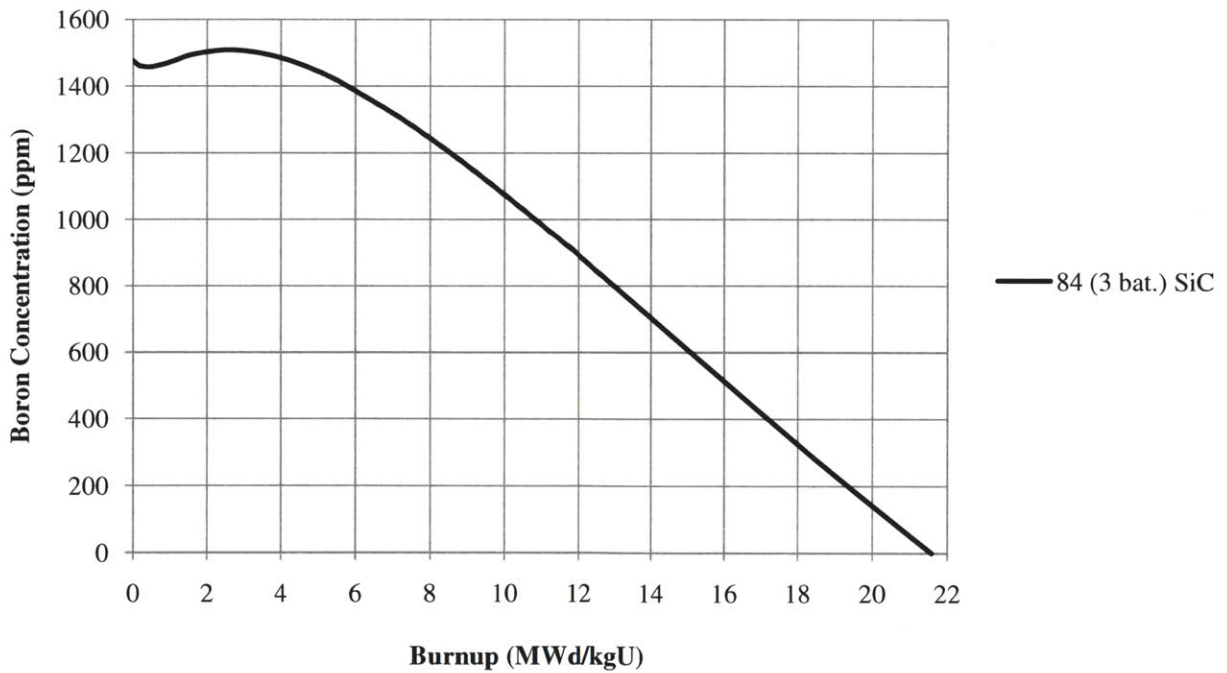


Figure 4.17 Boron concentration (ppm) for 84-reload SiC core design.

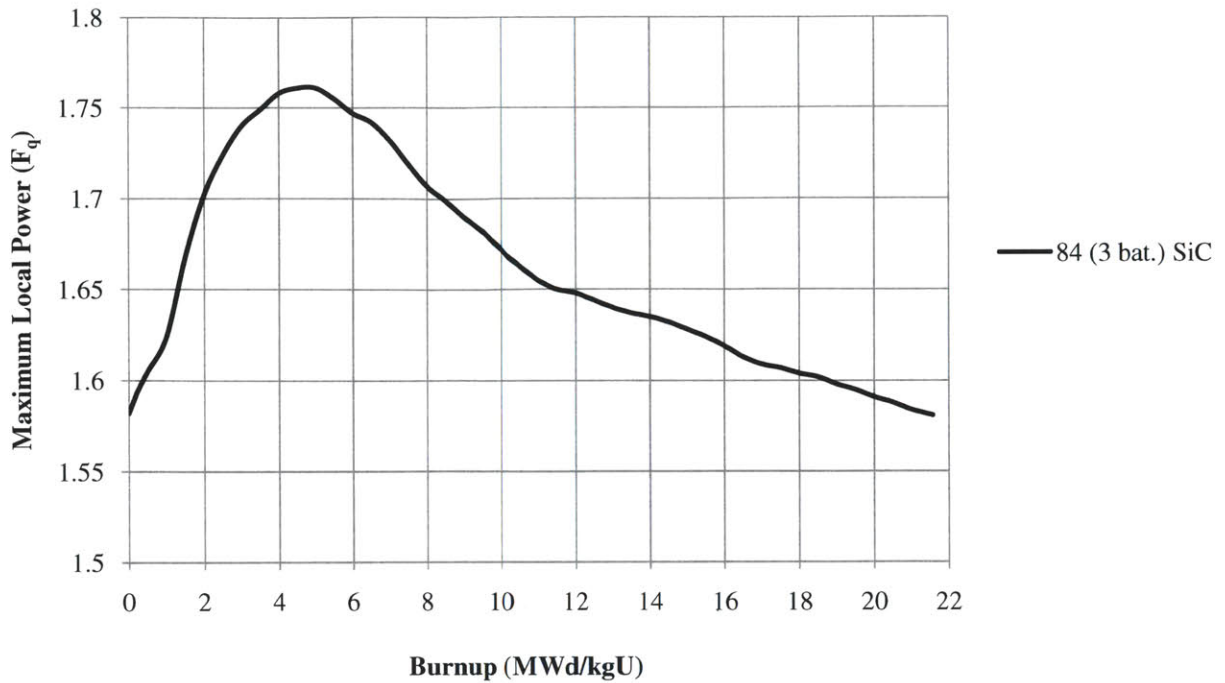


Figure 4.18 F_q for 84-reload SiC core design.

4.5 84-RELOAD UPDATED SiC CORES

Since Section 4.1, all the cores had a nominal power level of 3587 MW_{th}. Now, the cores discussed below were simulated to operate at a higher power density or “uprate.” The tables and graphs below summarize the core parameters over the cycle length for a 10% (3946 MW_{th}) and 20% (4304 MW_{th}) power uprate of the 84-reload core.

Table 4.10 84-reload uprated core design summary of reactor physics parameters.

Reload #	Uprate	Avg. w/o	B_C	Avg. B_D	EFPD	#IFBA Rods	Boron (ppm)	$F_{\Delta h}$	F_q	Max Pin Burnup
84 SiC (3 bat.)	10%	5.30	23.74	54.5	492	12208 (1X)	1773	1.54	1.80	83.2
84 SiC (3 bat.)	20%	5.78	25.97	59.7	494	12208 (1.5X)	1647	1.50	1.82	88.8

Table 4.11 84-reload 10% uprated core design fuel batch summary.







Fuel	Fuel Batch ID	# ASSYs	ASSY w/o	Blanket w/o	BP Rods per ASSY	IFBA Loading (mg ¹⁰ B/in)	
	Twice	63I156L	4	6.3	3.2	156	1.57
	Twice	51I156L	4	5.1	3.2	156	1.57
	Twice	48I156L	4	4.8	3.2	156	1.57
	Twice	51I128L	4	5.1	3.2	128	1.57
	Twice	63I128L	9	6.3	3.2	128	1.57
	Once	63I156L	16	6.3	3.2	156	1.57
	Once	51I156L	16	5.1	3.2	156	1.57
	Once	48I156L	20	4.8	3.2	156	1.57
	Once	51I128L	16	5.1	3.2	128	1.57
	Once	63I128L	16	6.3	3.2	128	1.57
	Fresh	63I156L	16	6.3	3.2	156	1.57
	Fresh	51I156L	16	5.1	3.2	156	1.57
	Fresh	48I156L	20	4.8	3.2	156	1.57
	Fresh	51I128L	16	5.1	3.2	128	1.57
	Fresh	63I128L	16	6.3	3.2	128	1.57

Table 4.12 84-reload 20% uprated core design fuel batch summary.

Fuel	Fuel Batch ID	# ASSYs	ASSY w/o	Blanket w/o	BP Rods per ASSY	IFBA Loading (mg ¹⁰ B/in)	
	Twice	67I156H	4	6.7	3.2	156	2.355
	Twice	52I156H	4	5.2	3.2	156	2.355
	Twice	52I156H	4	5.2	3.2	156	2.355
	Twice	65I128H	4	6.5	3.2	128	2.355
	Twice	67I128H	9	6.7	3.2	128	2.355
	Once	67I156H	16	6.7	3.2	156	2.355
	Once	52I156H	16	5.2	3.2	156	2.355
	Once	52I156H	20	5.2	3.2	156	2.355
	Once	65I128H	16	6.5	3.2	128	2.355
	Once	67I128H	16	6.7	3.2	128	2.355
	Fresh	67I156H	16	6.7	3.2	156	2.355
	Fresh	52I156H	16	5.2	3.2	156	2.355
	Fresh	52I156H	20	5.2	3.2	156	2.355
	Fresh	65I128H	16	6.5	3.2	128	2.355
	Fresh	67I128H	16	6.7	3.2	128	2.355

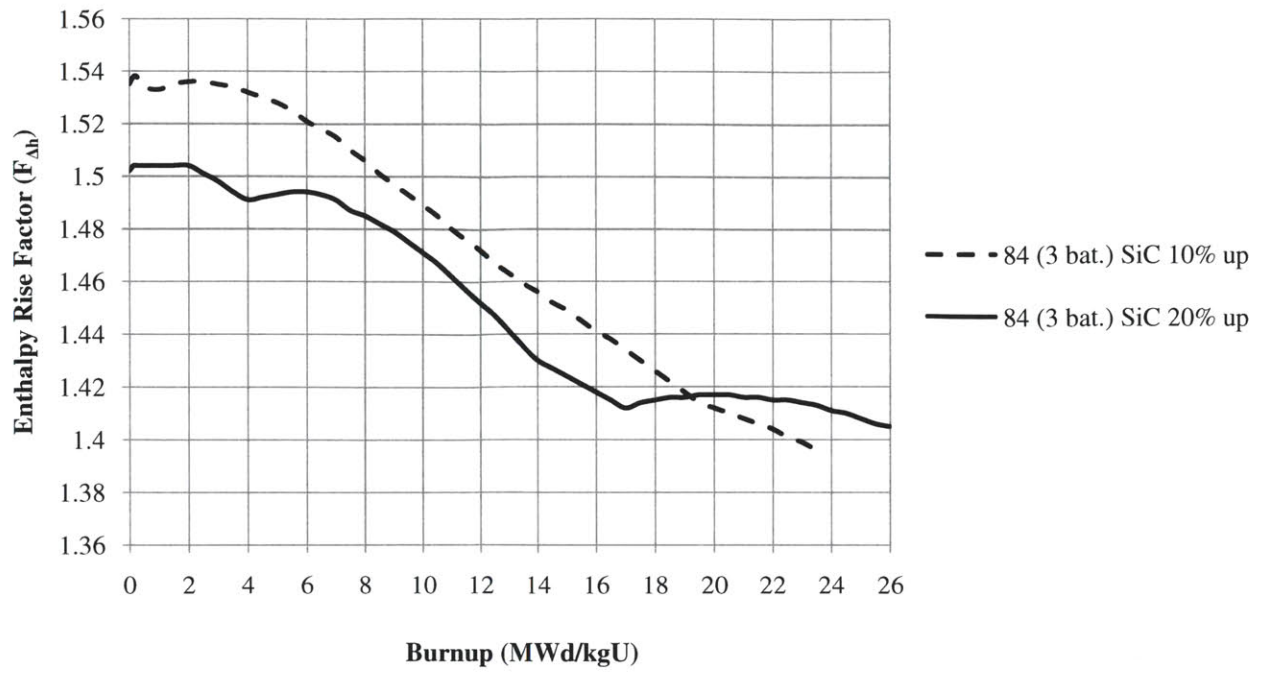


Figure 4.19 F_{Ah} for 84-reload updated core designs.

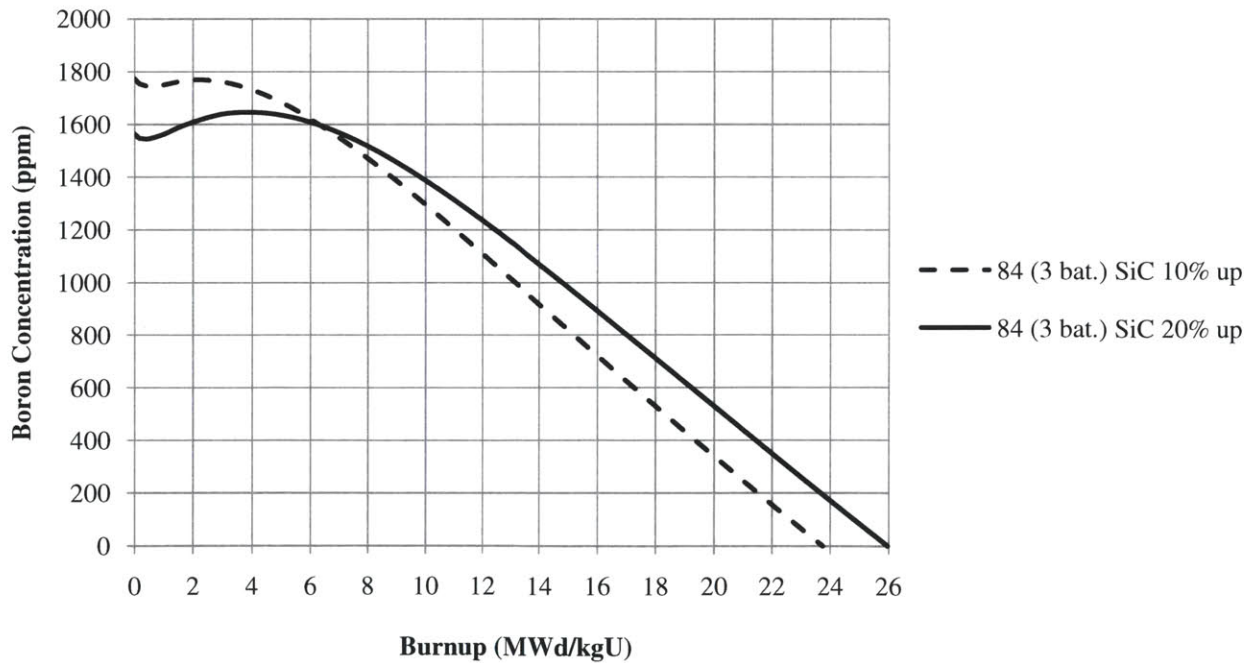


Figure 4.20 Boron concentration (ppm) for 84-reload updated core designs.

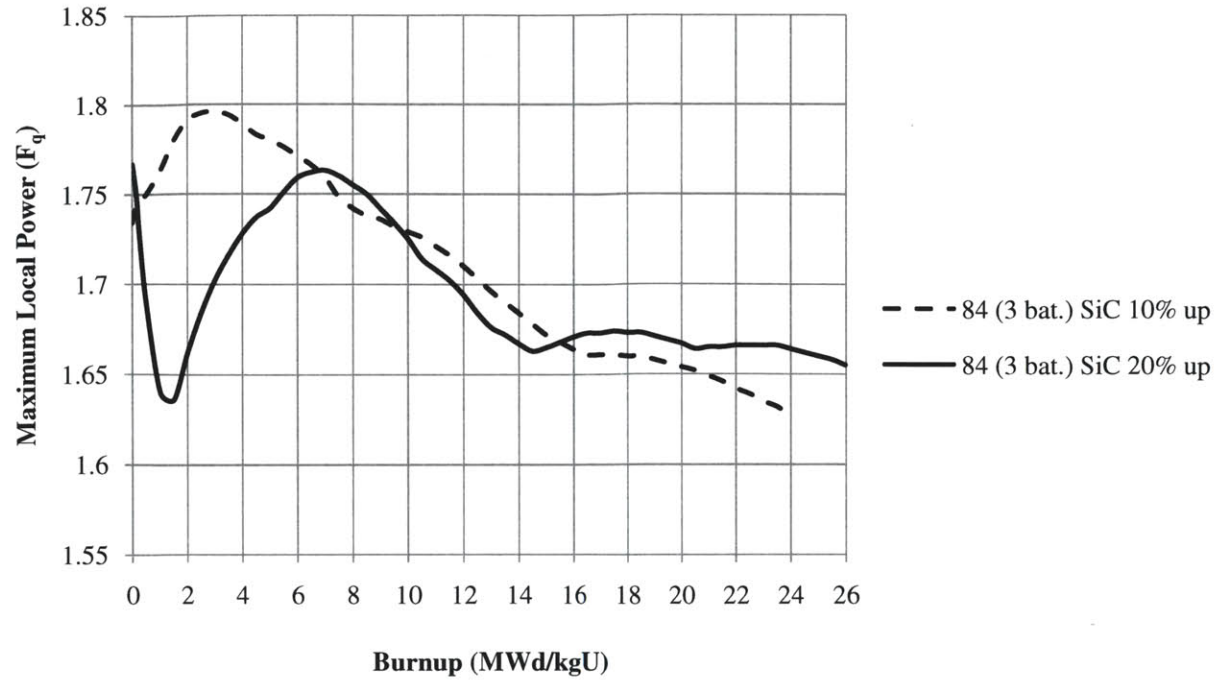


Figure 4.21 F_q for 84-reload updated core designs.

5. 24-MONTH CYCLE CORE DESIGNS

With Zr-clad fuel, operating with a cycle length greater than 18 months introduces significant challenges: 1) increased neutron fluence, 2) higher discharge burnups, and 3) greater leakage rates. In order to achieve longer operating cycles, batch size must be increased, resulting in more fresh fuel ultimately being placed on the core's periphery. With this loading pattern, core parameters were kept below their maximum values but leakage, unfortunately, increased to levels that may lead to a reduction in the pressure vessel's integrity. Further research would have to be conducted specifically on this concern, however, to make an accurate assessment.

Similar to the last chapter's organization, core designs were again discussed on an individual basis. But unlike the chapter describing the 18-month cycles, the 24-month cycles required a few more adjustments to reach an optimal design. Below, Table 5.1 summarizes all the 24-month cores. The core designs in bold represent those designs which represent the most optimal design. The graphs of only those cores in bold can be seen in Figure 5.1 to 5.3.

Table 5.1 Summary of 24-month core designs.

Reload #	Uprate	Avg. w/o	B _C	Avg. B _D	EFPD	#IFBA Rods	Boron (ppm)	F _{Δh}	F _q	Max Pin Burnup
96 SiC (2 bat.)	0%	5.71	29.17	58.6	666	14416 (1.5X)	2037	1.55	1.87	85.1
96 SiC (2 bat.)	0%	5.71	29.26	58.8	668	14416 (2X)	1743	1.59	2.40	85.7
96 SiC (2 bat.)	0%	5.71	29.97	60.3	684	14416 (2X) ⁴	1682	1.62	2.09	88.0
112 SiC (2 bat.)	0%	5.46	29.22	50.4	667	16240 (1.5X)⁵	1718	1.52	1.94	67.4
112 SiC (2 bat.)	0%	5.58	29.94	51.2	684	16240 (1.5X)	1801	1.53	1.97	70.4
112 SiC (2 bat.)	0%	5.58	29.23	50.4	667	16240 (1.5X)	1852	1.54	1.89	68.2
136 SiC (2 bat.)	0%	5.15	29.16	41.3	665	21216 (1.5X)	1534	1.53	2.11	67.2
136 SiC (2 bat.)	0%	7.30	30.25	42.9	666	NA ⁶	1540	1.51	1.94	74.8

⁴ No blankets

⁵ No blankets & re-adjusted enrichment

⁶ 9,792 erbium rods were used

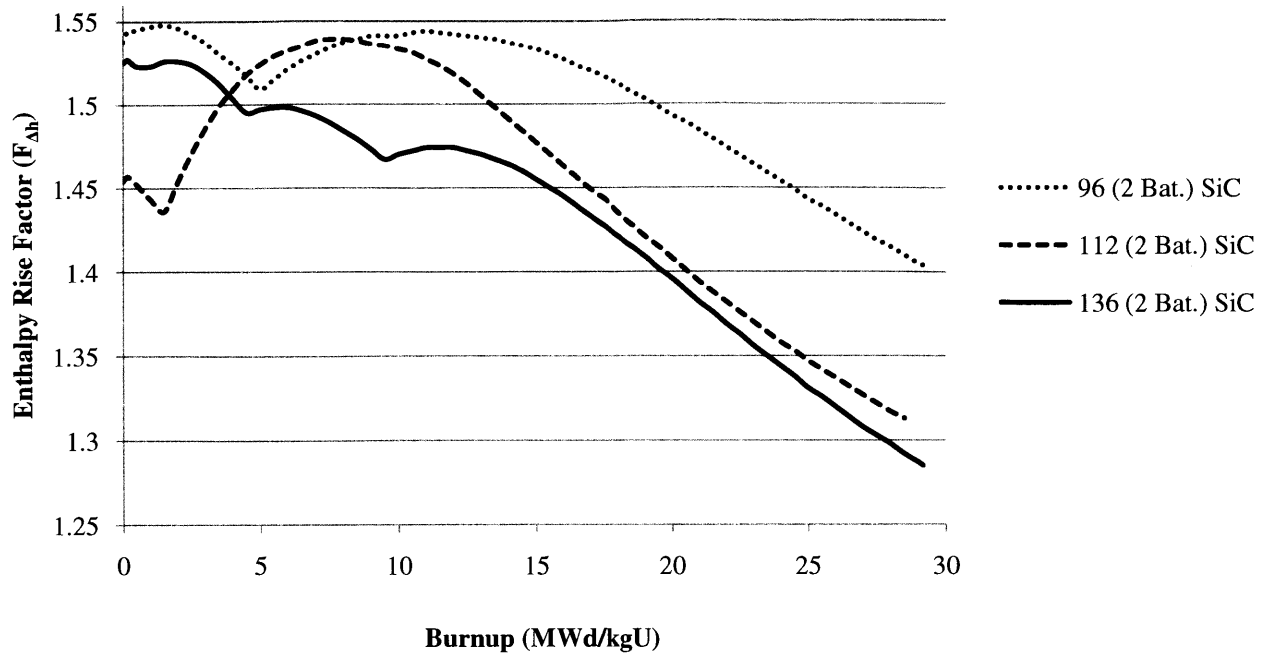


Figure 5.1 F_{Ah} for all 24-month core designs.

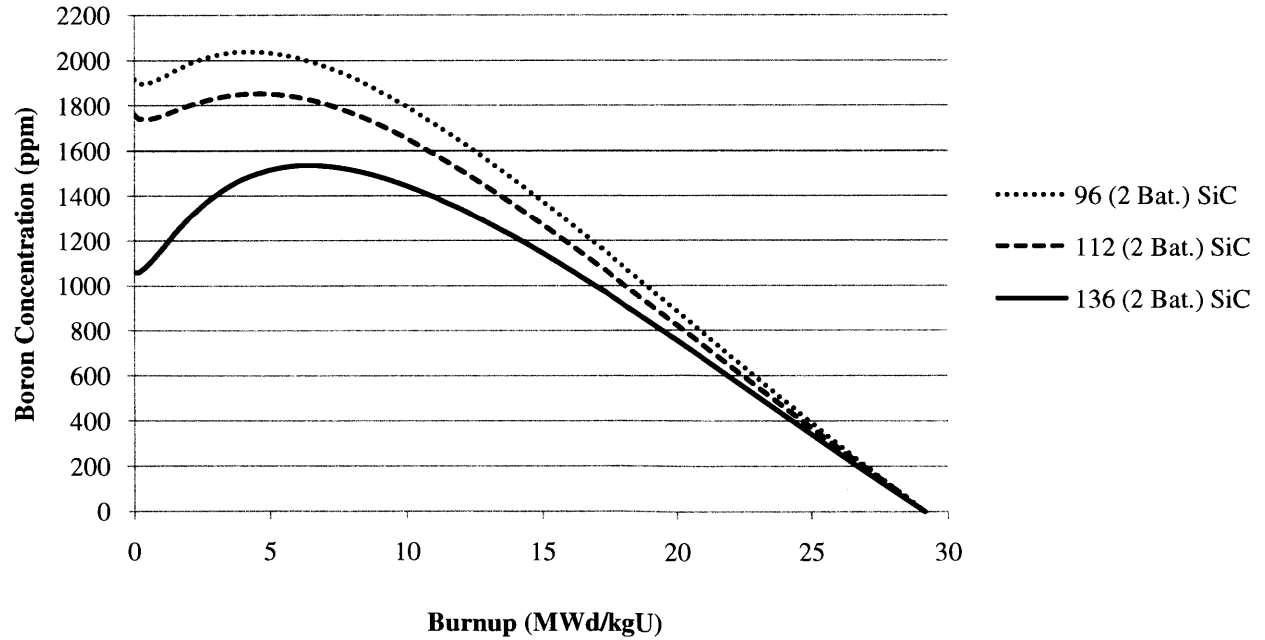


Figure 5.2 Boron concentration (ppm) for all 24-month core designs.

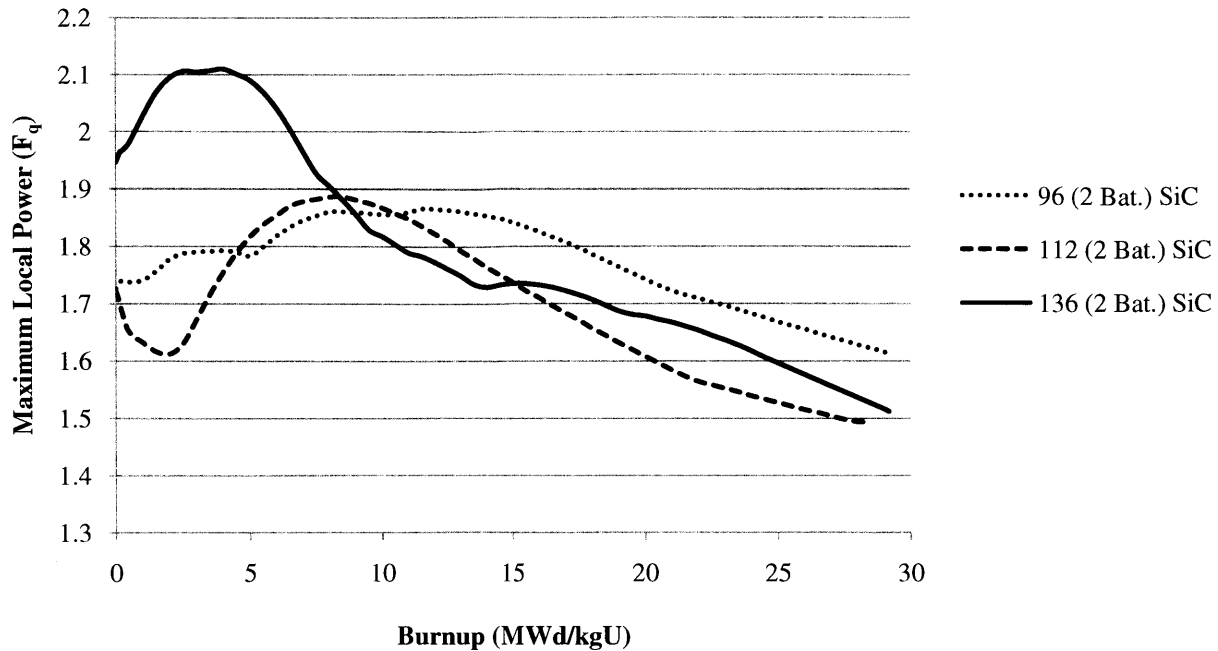


Figure 5.3 F_q for all 24-month core designs.

5.1 96-RELOAD SiC CORE

With 96 assemblies to reload into the core, special exceptions to the general rules of core design had to be made, in particular, loading of fresh assemblies next to each other. As can be seen in Figure 5.4, the most successful pattern involved placing a ring of fresh fuel around the checkerboard of fresh fuel in the center of the core and once-burned fuel on the periphery. Surprisingly, even though fresh fuel was placed side by side, the peaking factors were still lower than the maximum values, except for the soluble boron concentration. This core parameter, however, was loosely related to assembly placement and more strongly related to the amount of burnable poison in the core. In this case, since 1.5X IFBA (2.355 mg $^{10}\text{B}/\text{in}$) is being utilized, a simulation run was completed with 2X IFBA, a type of burnable poison rarely used in current reactor design. As expected, the amount of soluble boron was reduced, the effect of simply increasing the amount of ^{10}B in each fuel rod. But as can be seen in Figure 5.5-5.7, by holding the enrichments and layout of BP rods constant, $F_{\Delta h}$ increased above the limit along with F_q , settling out just below its upper limit.

Another attempt was then made to remove the axial blankets to reduce F_q , which was successful in attaining the required cycle length, but then led to an additional increase in $F_{\Delta h}$. As a result, the core loading pattern would have to be adjusted to lower $F_{\Delta h}$ again. Since few studies have been completed to assess the crud deposition rate of SiC in a PWR environment [Carpenter, 2010], it was assumed that this robust material would have little crud deposition above soluble boron concentrations of 1700 parts per million (ppm). As a result, the first core design with a boron content of 2000 ppm was deemed acceptable by these standards.

Table 5.2 96-reload core design summary of reactor physics parameters.

Reload #	Uprate	Avg. w/o	B_C	Avg. B_D	EFPD	#IFBA Rods	Boron (ppm)	$F_{\Delta h}$	F_q	Max Pin Burnup
96 SiC (2 bat.)	0%	5.71	29.17	58.6	666	14416 (1.5X)	2037	1.55	1.87	85.1
96 SiC (2 bat.)	0%	5.71	29.26	58.8	668	14416 (2X)	1743	1.59	2.40	85.7
96 SiC (2 bat.)	0%	5.71	29.97	60.3	684	14416 (2X) ⁷	1682	1.62	2.09	88.0

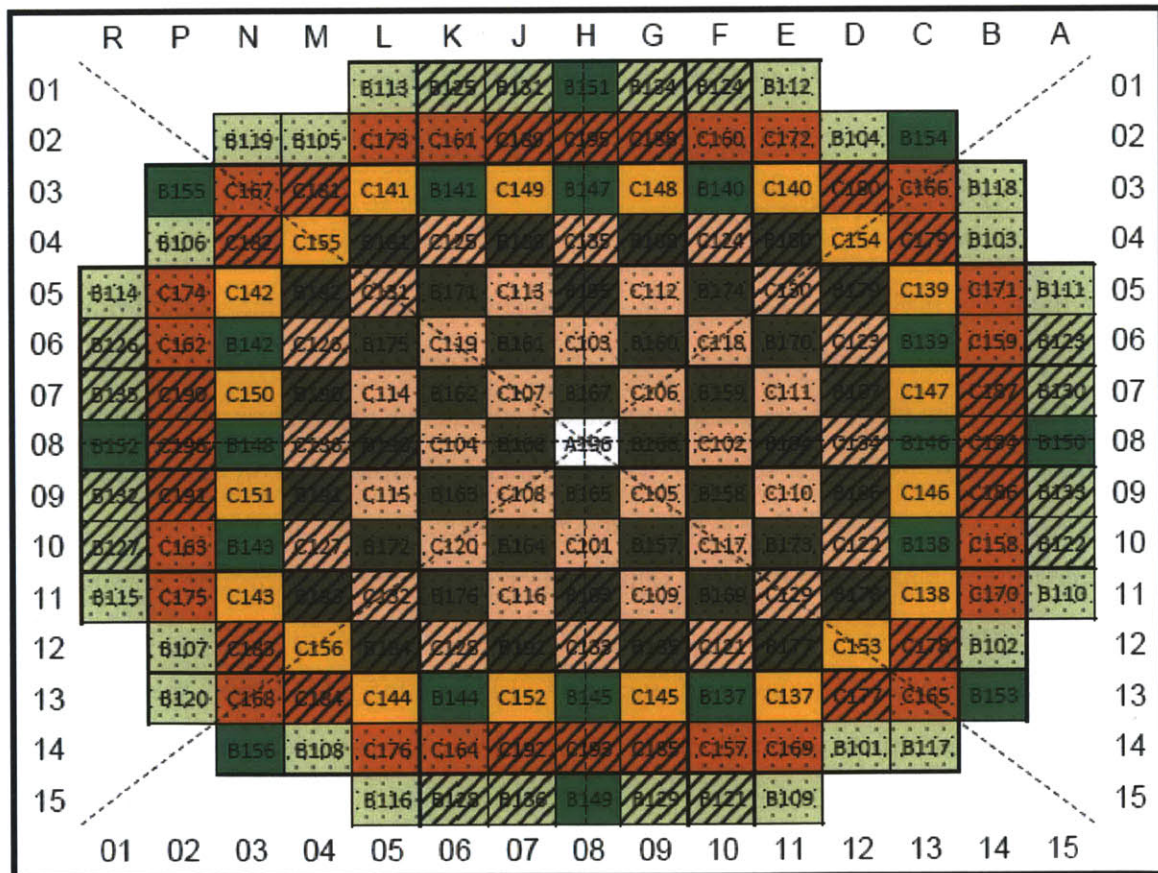




Figure 5.4 96-reload core loading map.

⁷ No blankets

Table 5.3 96-reload core design fuel batch summary.

Fuel	Fuel Batch ID	# ASSYs	ASSY w/o	Blanket w/o	BP Rods per ASSY	IFBA Loading (mg ¹⁰ B/in)
Center	56I156H	1	5.6	3.2	156	2.355
	Once	20	5.6	3.2	156	2.355
	Once	16	6.0	3.2	156	2.355
	Once	20	6.5	3.2	156	2.355
	Once	20	6.0	3.2	128	2.355
	Once	20	5.6	3.2	156	2.355
	Fresh	20	5.6	3.2	156	2.355
	Fresh	16	6.0	3.2	156	2.355
	Fresh	20	6.5	3.2	156	2.355
	Fresh	20	6.0	3.2	128	2.355
	Fresh	20	5.6	3.2	156	2.355

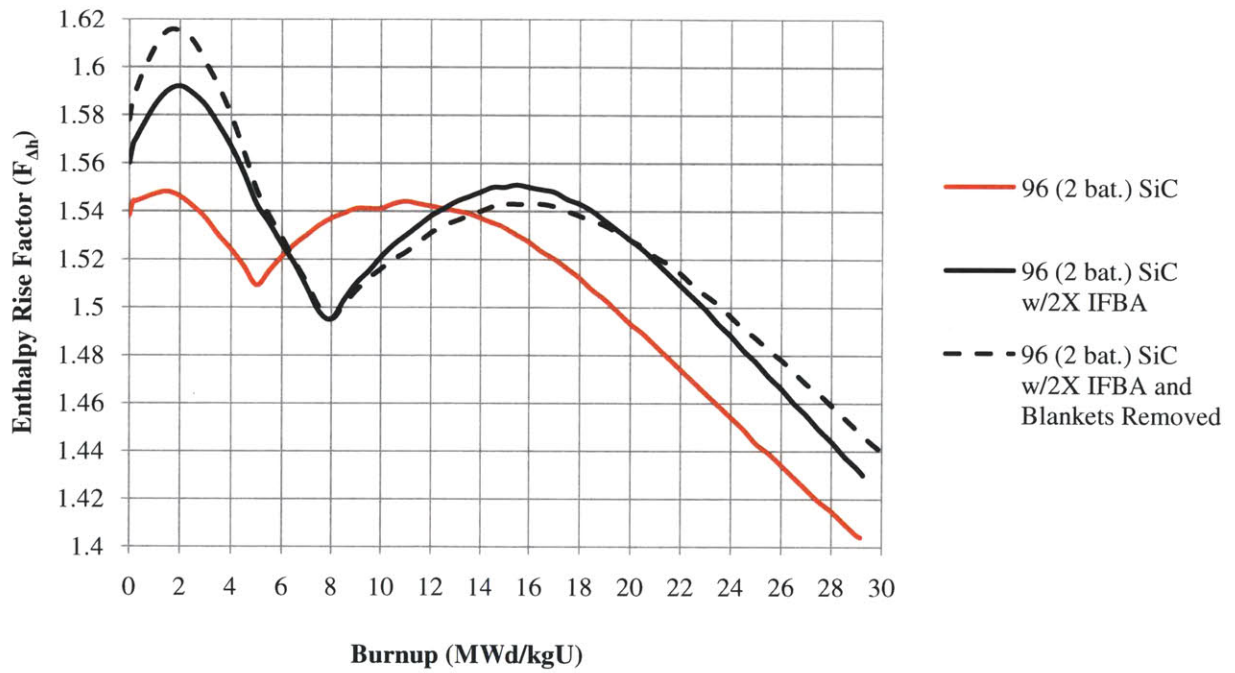


Figure 5.5 F_{Ah} for 96-reload core design.

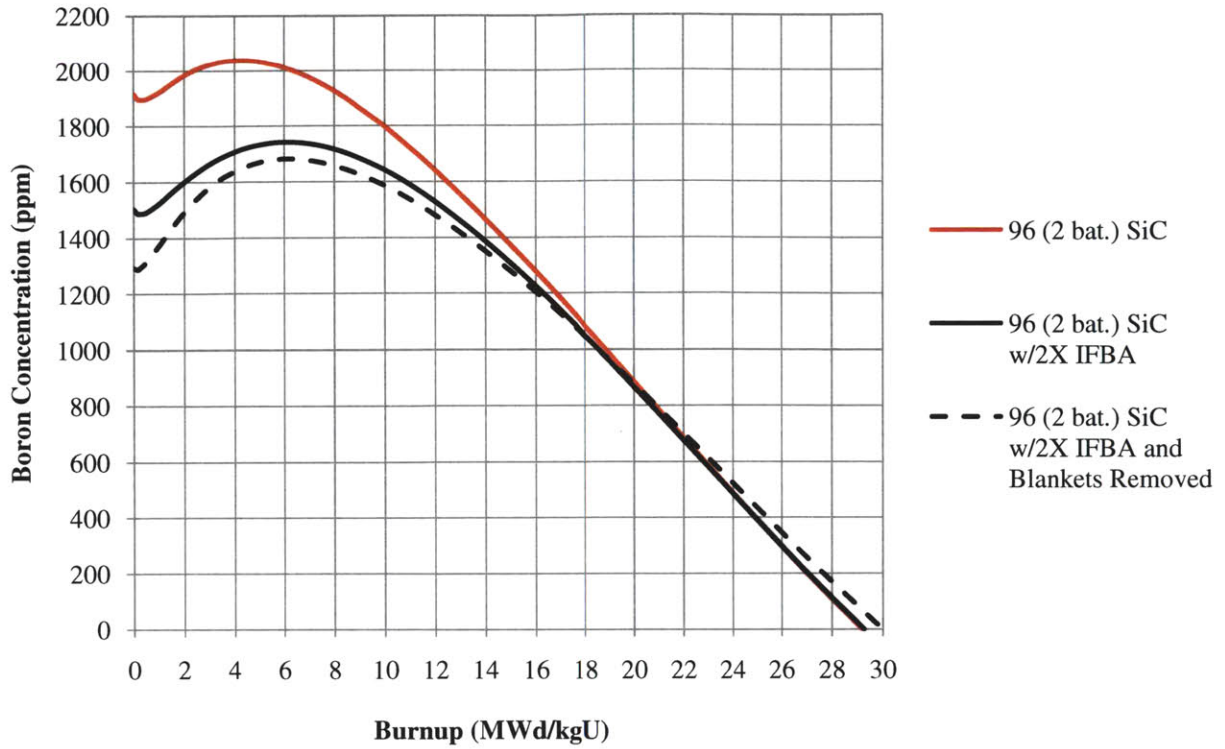


Figure 5.6 Boron concentration (ppm) for 96-reload core design.

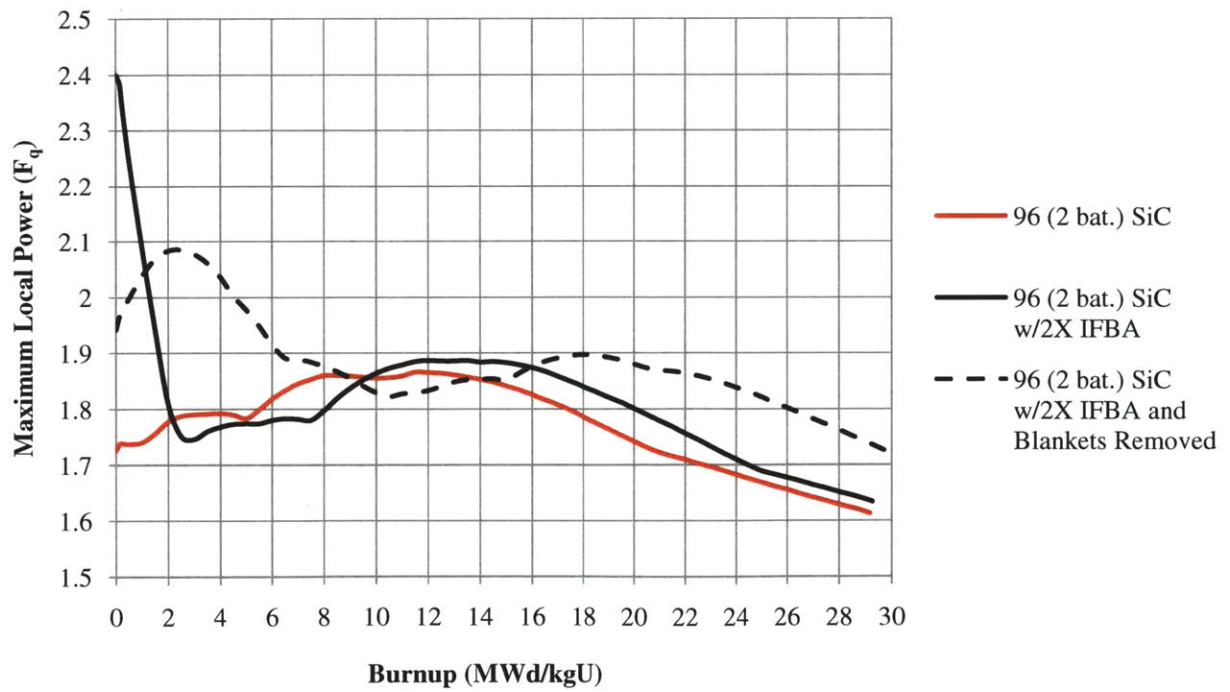


Figure 5.7 F_q for 96-reload core design.

5.2 112-RELOAD SiC CORE

Juxtaposed against the 96-reload core, the 112-reload core proved the advantages of removing axial blankets. In this design, since there were so many fresh assemblies to load at one time into the core, once-burned fuel could no longer be loaded around the periphery. As a result, significant increases in the leakage rate occurred but peaking still remained less than the established limits. Since there were more fresh assemblies, the average enrichment per reload was lower than the 96-reload core, as expected, but could have been lower if not for the additional enrichment needed as a result of more neutrons escaping the system. Figures 5.9-5.11 demonstrated how the removal of the axial blankets lowered $F_{\Delta h}$ and increased F_q , the opposite trend observed with the 96-reload core. After removing the blankets, the enrichments were also adjusted to reveal the total advantages in this type of assembly modification.

Table 5.4 112-reload core design summary of reactor physics parameters.

Reload #	Uprate	Avg. w/o	B_c	Avg. B_D	EFPD	#IFBA Rods	Boron (ppm)	$F_{\Delta h}$	F_q	Max Pin Burnup
112 SiC (2 bat.)	0%	5.58	29.23	50.4	667	16240 (1.5X)	1852	1.54	1.89	68.2
112 SiC (2 bat.)	0%	5.58	29.94	51.2	684	16240 (1.5X) ⁸	1801	1.53	1.97	70.4
112 SiC (2 bat.)	0%	5.46⁹	29.22	50.4	667	16240 (1.5X)	1718	1.52	1.94	67.4

⁸ No Blankets

⁹ Enrichment adjusted to achieve 24-month cycle length (~ 666 EFPD)

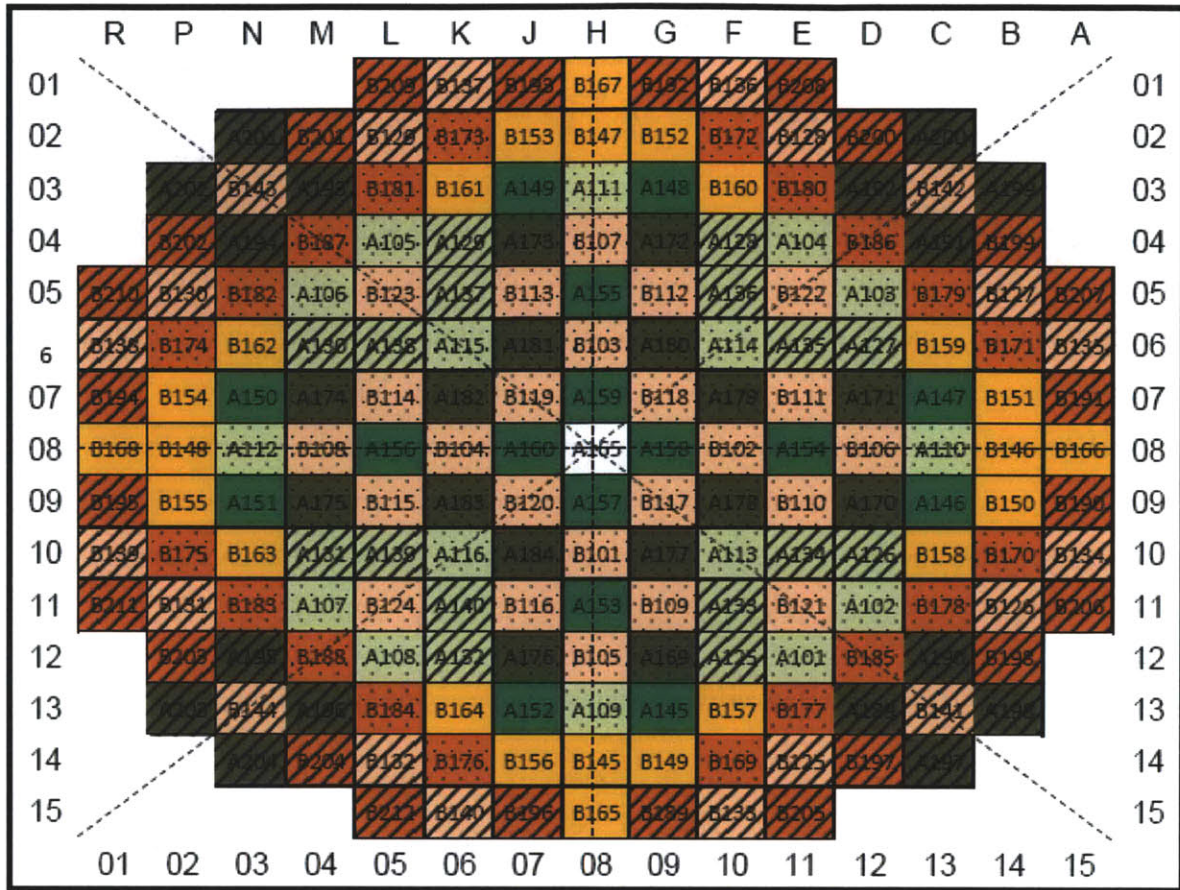


Figure 5.8 112-reload core loading map.

Table 5.5 112-reload core design fuel batch summary.

Fuel	Fuel Batch ID	# ASSYs	ASSY w/o	Blanket w/o	BP Rods per ASSY	IFBA Loading (mg ¹⁰ B/in)
Once	59I156H	16	5.9	3.2	156	2.355
Once	60I128H	16	6.0	3.2	128	2.355
Once	56I128H	16	5.6	3.2	128	2.355
Once	56I156H	16	5.6	3.2	156	2.355
Once	59I156H	16	5.9	3.2	156	2.355
Fresh	59I156H	24	5.9	3.2	156	2.355
Fresh	60I128H	20	6.0	3.2	128	2.355
Fresh	56I128H	24	5.6	3.2	128	2.355
Fresh	56I156H	20	5.6	3.2	156	2.355
Fresh	59I156H	24	5.9	3.2	156	2.355

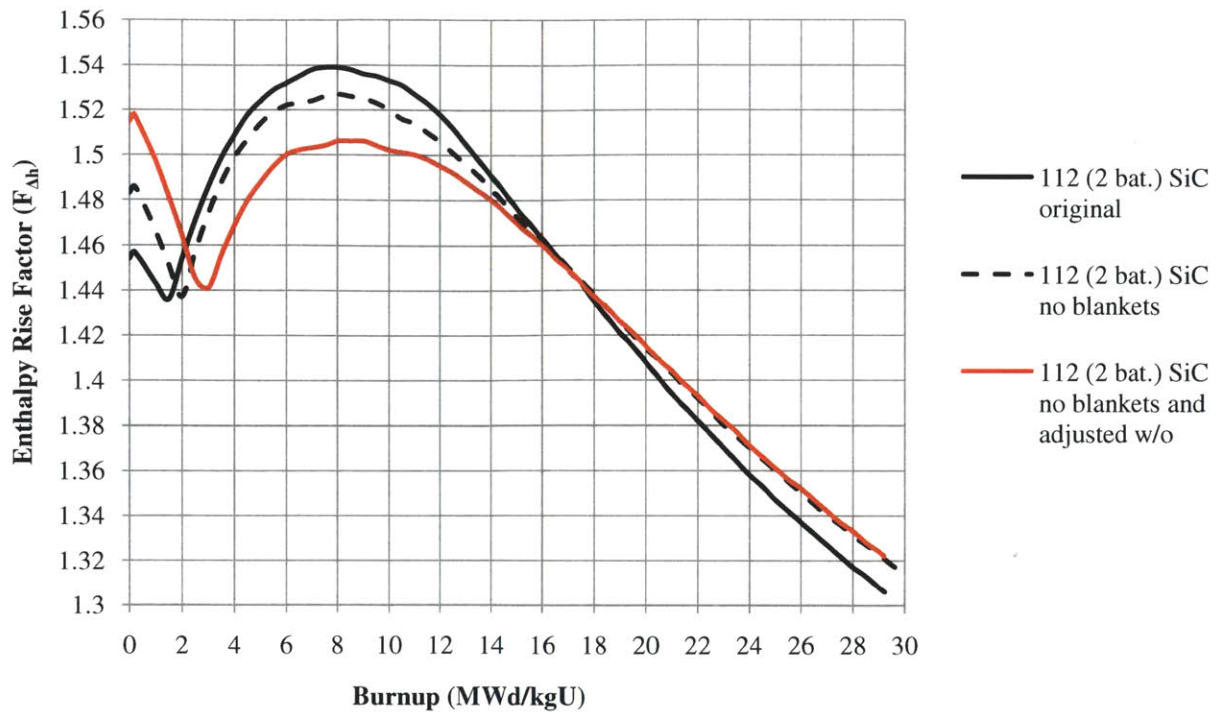


Figure 5.9 F_{Ah} for 112-reload core design.

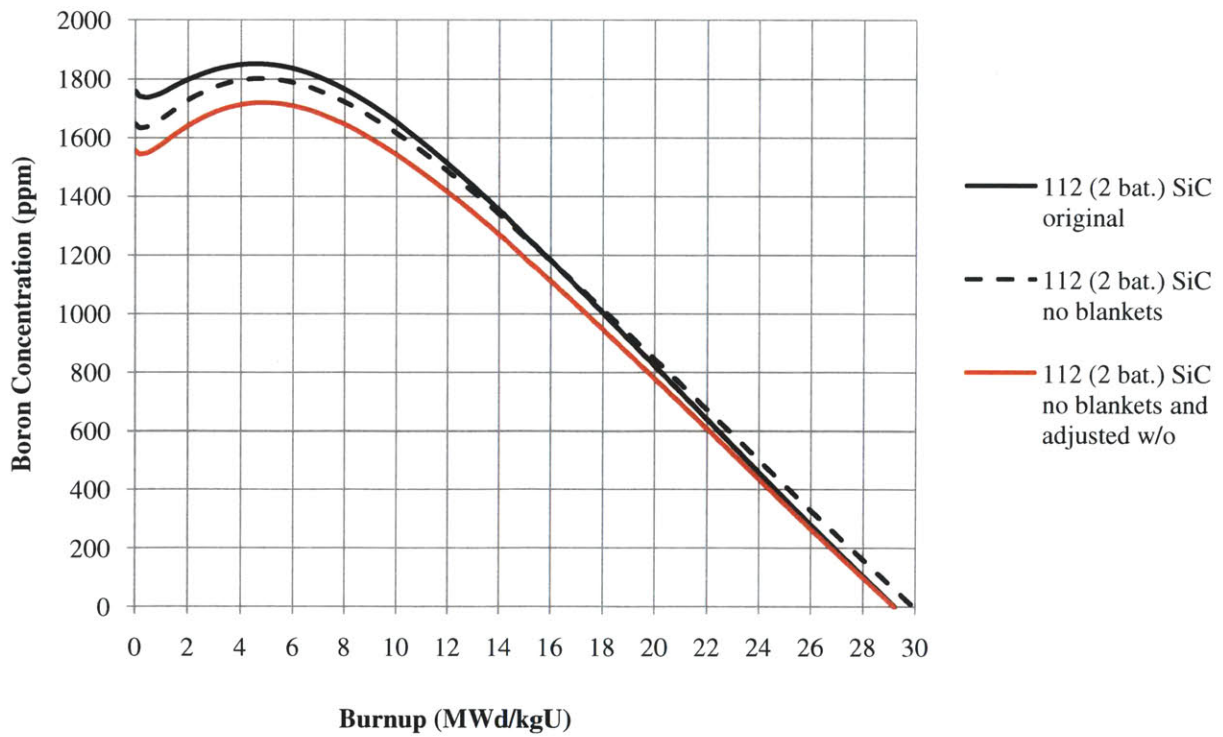


Figure 5.10 Boron concentration (ppm) for 112-reload core design.

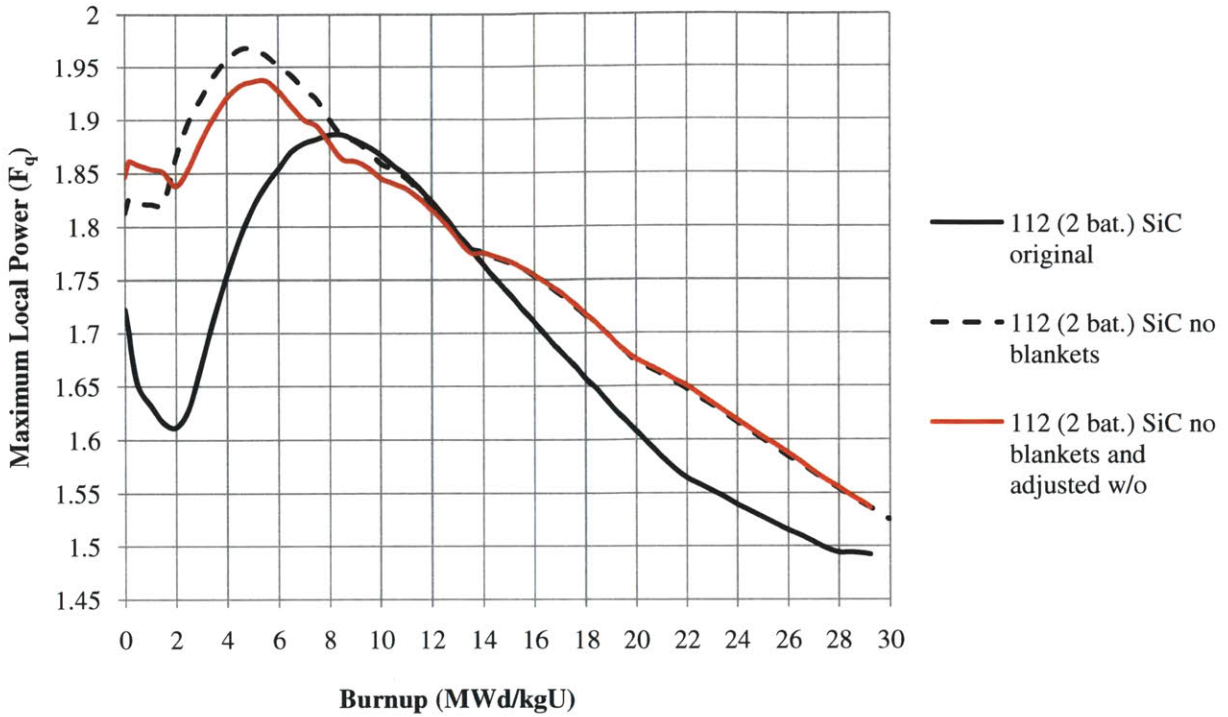


Figure 5.11 F_q for 112-reload SiC core design.

5.3 136-RELOAD SiC CORE

Designing a 136-reload core involved loading over two-thirds of the core with SiC-clad fuel. In this design, the highest leakage rates were observed, but only near the end of cycle (EOC). The lower average enrichment in the 136-reload core most likely led to the lower leakage rates experienced earlier in the cycle. Figure 5.12 compares the leakage rates over the cycle length of each core. As can be seen, leakage rates were not strictly a function of batch size or cycle length. In general, as more assemblies were placed near the periphery or driven to higher discharge burnups, leakage was increased.

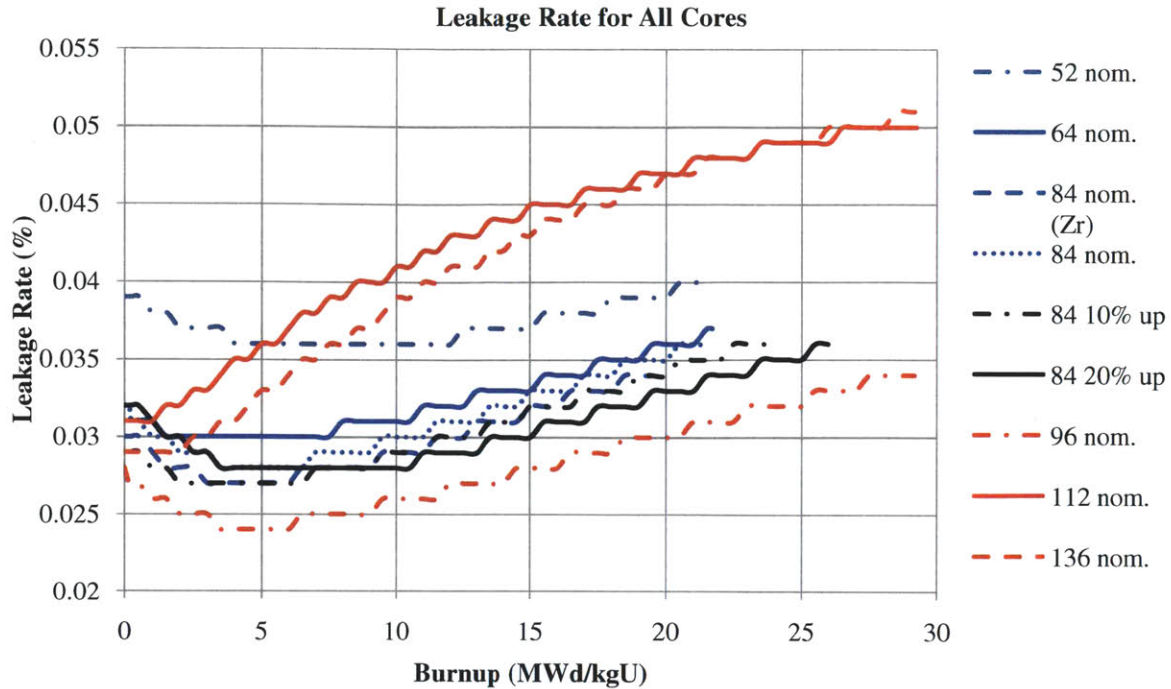


Figure 5.12 Leakage rates for all core designs.

Given the previous success in removing axial blankets in the 112-reload core, the same procedure was followed for the 136-reload core. As can be seen in Table 5.6, the $F_{\Delta h}$ values were at acceptable levels, but the F_q was slightly higher compared to other cores. In an effort to lower this core parameter, the burnable poison (IFBA) was replaced with erbium. A difference in the reactivity hold-down of erbium and IFBA can be seen in Chapter 2 (Figure 2.3). The different amount of reactivity held-down also contributed to the different F_q , $F_{\Delta h}$, and boron concentration curves in Figure 5.14-5.16. Additionally, as discussed in Chapter 2, erbium's lower isotopic cross-sections, compared to gadolinium and boron-10, led to a greater number of BP rods being needed in the core, about 70 erbium rods per assembly. The burnable poison layouts of erbium can be seen in Appendix A. Tables 5.7 and 5.8 summarize the assemblies reloaded into the core.

Table 5.6 136-reload core design summary of reactor physics parameters.

Reload #	Uprate	Avg. w/o	B_C	Avg. B_D	EFPD	#IFBA Rods	Boron (ppm)	$F_{\Delta h}$	F_q	Max Pin Burnup
136 SiC (2 bat.)	0%	5.15	29.16	41.3	665	21216 (1.5X)	1534	1.53	2.11	67.2
136 SiC (2 bat.)	0%	7.30	30.25	42.9	666	NA ¹⁰	1540	1.51	1.94	74.8

¹⁰ 9,792 erbium rods were used

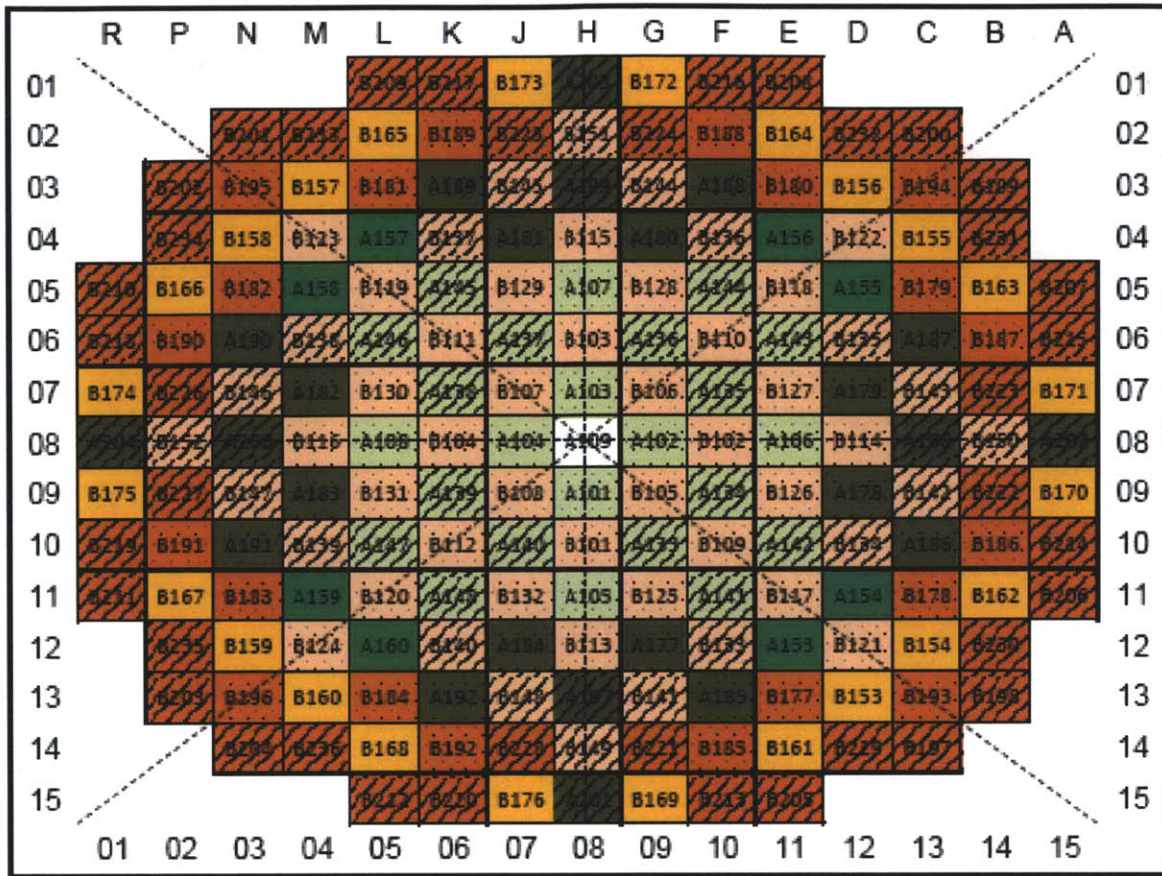


Figure 5.13 136-reload core loading map.

Table 5.7 136-reload core design (with IFBA) fuel batch summary.

Fuel	Fuel Batch ID	# ASSYs	ASSY w/o	Blanket w/o	BP Rods per ASSY	IFBA Loading (mg ¹⁰ B/in)
Once	49I156H	16	-	3.2	156	2.355
	49I156H	16	-	3.2	156	2.355
	53I156H	16	-	3.2	156	2.355
	53I156H	16	-	3.2	156	2.355
	53I156H	16	-	3.2	156	2.355
Fresh	49I156H	24	-	3.2	156	2.355
	49I156H	20	-	3.2	156	2.355
	53I156H	24	-	3.2	156	2.355
	53I156H	20	-	3.2	156	2.355
	53I156H	24	-	3.2	156	2.355

Table 5.8 136-reload core design (with Er) fuel batch summary.

Fuel	Fuel Batch ID	# ASSYs	ASSY w/o	Blanket w/o	BP Rods per ASSY	Er Loading (% Er ₂ O ₃)
Once	E187372H	16	7.3	-	72	10
Once	E187372H	16	7.3	-	72	10
Once	E187372H	16	7.3	-	72	10
Once	E187372H	16	7.3	-	72	10
Once	E187372H	16	7.3	-	72	10
Fresh	E187372H	24	7.3	-	72	10
Fresh	E187372H	20	7.3	-	72	10
Fresh	E187372H	24	7.3	-	72	10
Fresh	E187372H	20	7.3	-	72	10
Fresh	E187372H	24	7.3	-	72	10

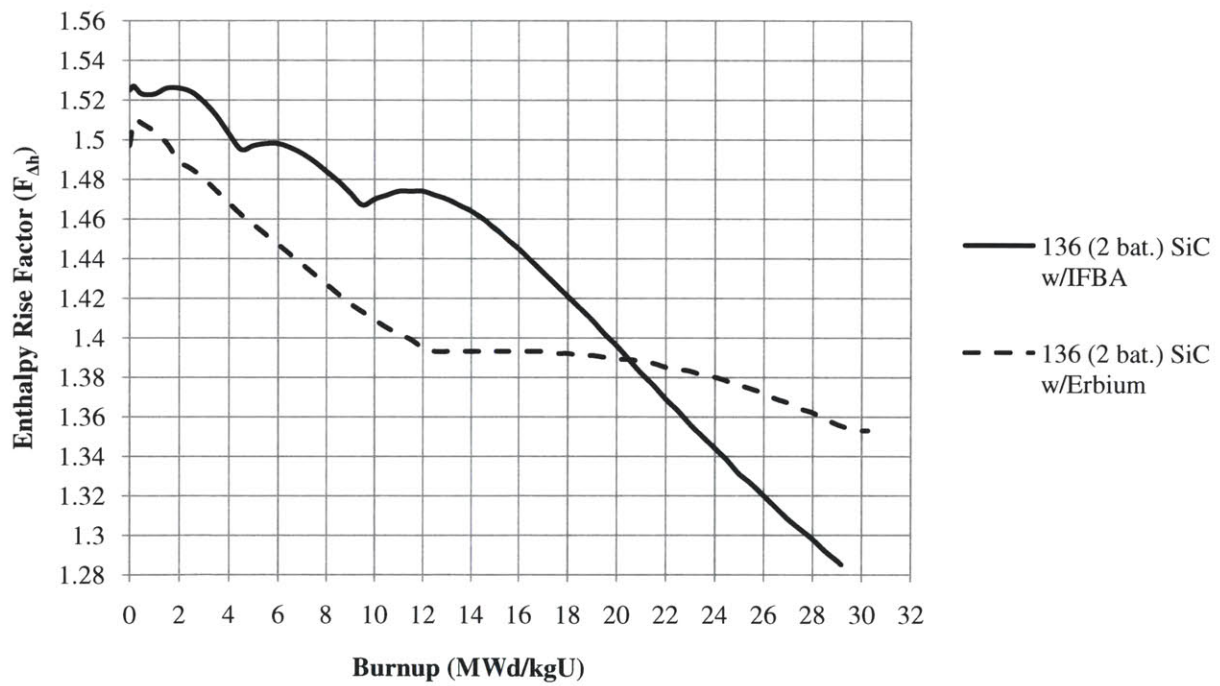


Figure 5.14 F_{Ah} for 136-reload core design.

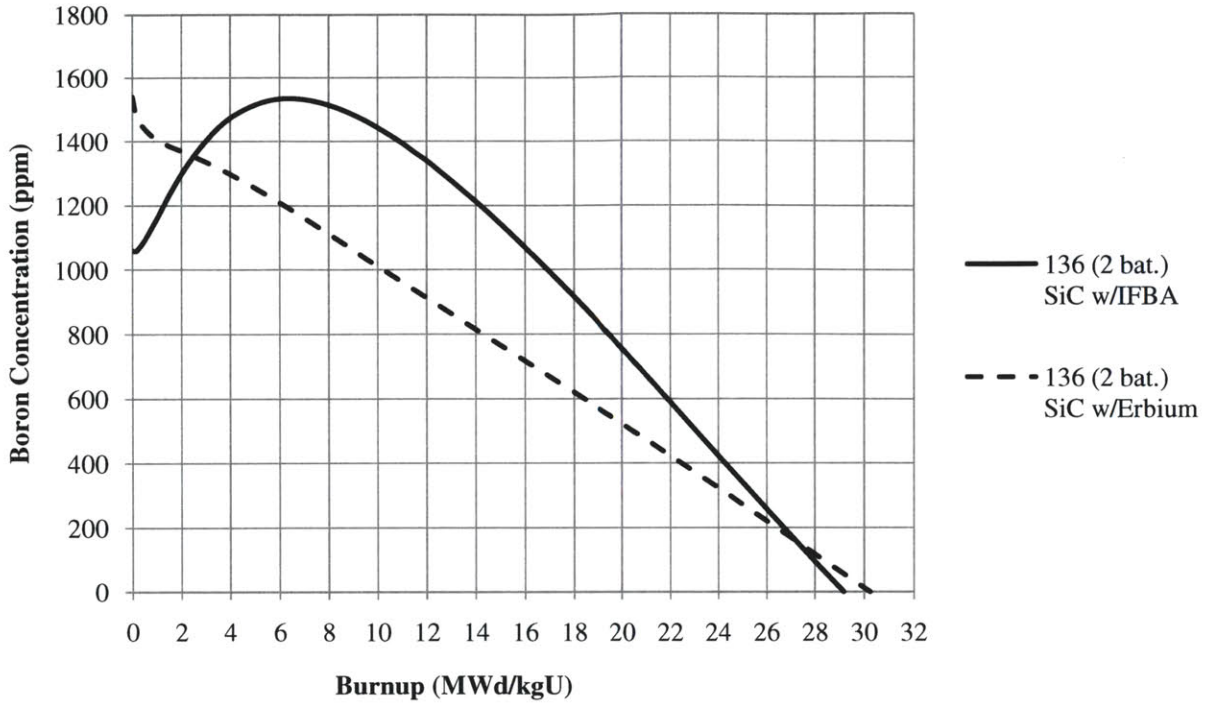


Figure 5.15 Boron concentration (ppm) for 136-reload core.

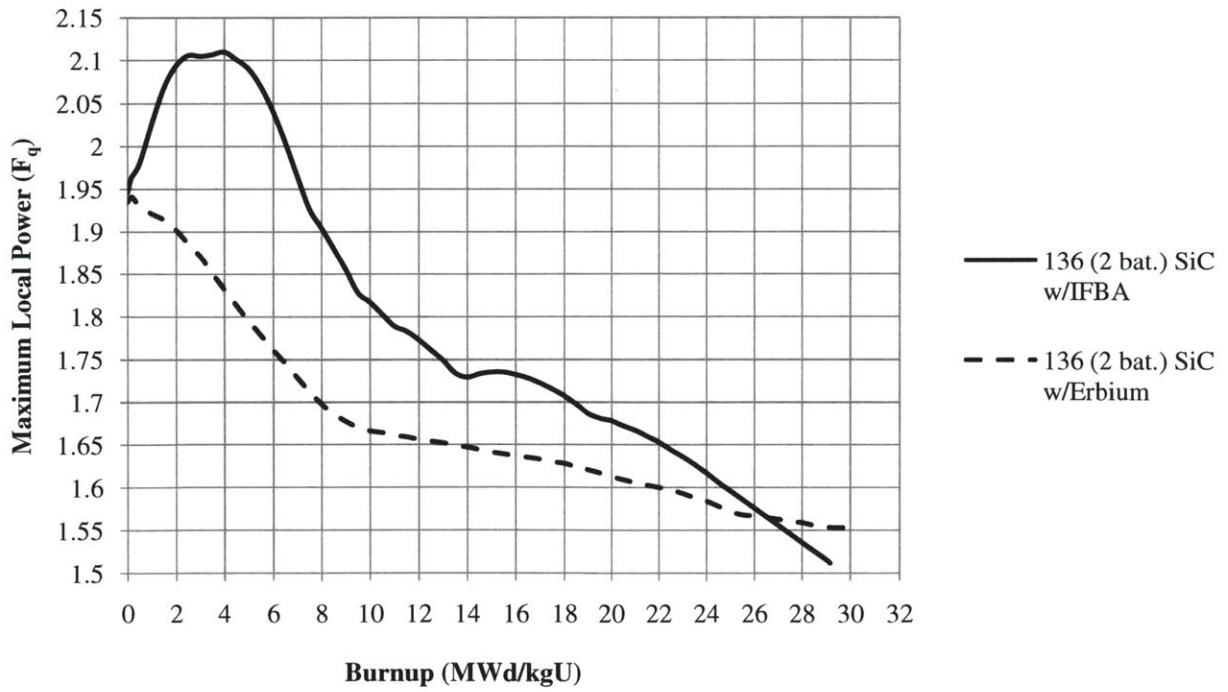


Figure 5.16 F_q for 136-reload core design.

6. REACTIVITY CONTROL AND COEFFICIENT ANALYSIS

In addition to designing cores capable of achieving and maintaining criticality with appropriate peaking factors, reactivity and control parameters must also be calculated to ensure reactor safety during operation. For this study, the particular assessments performed were the moderator temperature coefficient (MTC), isothermal temperature coefficient (ITC), uniform doppler coefficient (UDC), boron coefficient, and power coefficient. Additionally, the shutdown margin was calculated for each core.

While a regulatory body would require even transient response calculations, like a loss-of-coolant accident (LOCA) transient analysis, these basic parameters reveal the core's likelihood to survive any type of accident scenario required in the licensing process. Additionally, they may be utilized as inputs for future transient analyses. For convenience, Table 6.1 summarizes the steady-state characteristics of core designs subjected to the safety parameter analysis. In particular, the 96-reload case was analyzed without 2X IFBA, the 112-reload case without axial blankets, and the 136-reload case with IFBA and not erbium as a burnable poison.

Table 6.1 Core designs evaluated for transient analysis

Reload #	Uprate	Avg. w/o	B _C	Avg. B _D	EFPD	#IFBA Rods	Boron (ppm)	F _{ΔH}	F _q	Max Pin Burnup
52 SiC (4 bat.)	0%	6.84	21.61	80.2	493	8112 (1.5X)	1465	1.55	1.78	96.0
64 SiC (3 bat.)	0%	5.74	21.70	65.5	495	6656 (1.5X)	1654	1.55	1.81	81.3
84 Zr (3 bat.)	0%	4.52	19.45	44.7	492	12208 (1X)	1477	1.53	1.80	66.8
84 SiC (3 bat.)	0%	4.79	21.56	49.6	492	12208 (1X)	1509	1.50	1.76	74.7
84 SiC (3 bat.)	10%	5.30	23.74	54.5	492	12208 (1X)	1773	1.54	1.80	83.2
84 SiC (3 bat.)	20%	5.78	25.97	59.7	494	12208 (1.5X)	1647	1.50	1.82	88.8
96 SiC (2 bat.)	0%	5.71	29.17	58.6	666	14416 (1.5X)	2037	1.55	1.87	85.1
112 SiC (2 bat.)	0%	5.46	29.22	50.4	667	16240 (1.5X)	1718	1.52	1.94	67.4
136 SiC (2 bat.)	0%	5.15	29.16	41.3	665	21216 (1.5X)	1534	1.53	2.11	67.2

6.1 MODERATOR TEMPERATURE COEFFICIENT (MTC)

The reactivity difference associated with an intentional adjustment to the moderator inlet temperature divided by the subsequent change in the averaged moderator temperature may be defined as the moderator temperature coefficient (MTC). In SIMULATE-3, the inlet moderator temperature was increased by 5 degrees Fahrenheit, while the power, fuel temperature, and

xenon and samarium distributions were kept constant. The new reactivity was then subtracted from the previous reactivity and divided by the moderator temperature change, giving MTC in units of pcm/°F. In general, the MTC was a function of moderator temperature, boron concentration, cycle exposure, and control rod position. For licensed LWRs, the MTC should be negative over the entire cycle length at HFP. Despite the soluble boron concentration having been shown in previous studies to have a positive effect on the MTC, all cases were negative throughout their entire life. As expected, however, the 96-reload case was the least negative, most likely as a result of the very high boron concentration (around 2000 ppm) at BOC. While the MTC should be negative, it should be noted that too negative of a value may be harmful during large reactivity insertions under cold water injection scenarios [Zhang, 2010].

Figure 7.1 illustrates the negative MTC for each core during its cycle. This is primarily a result of reduced water density from the increase in moderator temperature, leading to a decrease in overall core reactivity. This simple effect provides a nuclear reactor with an ability to shut itself down in the event of a SCRAM – a coincidence of nature and design that increases the safety of nuclear power.

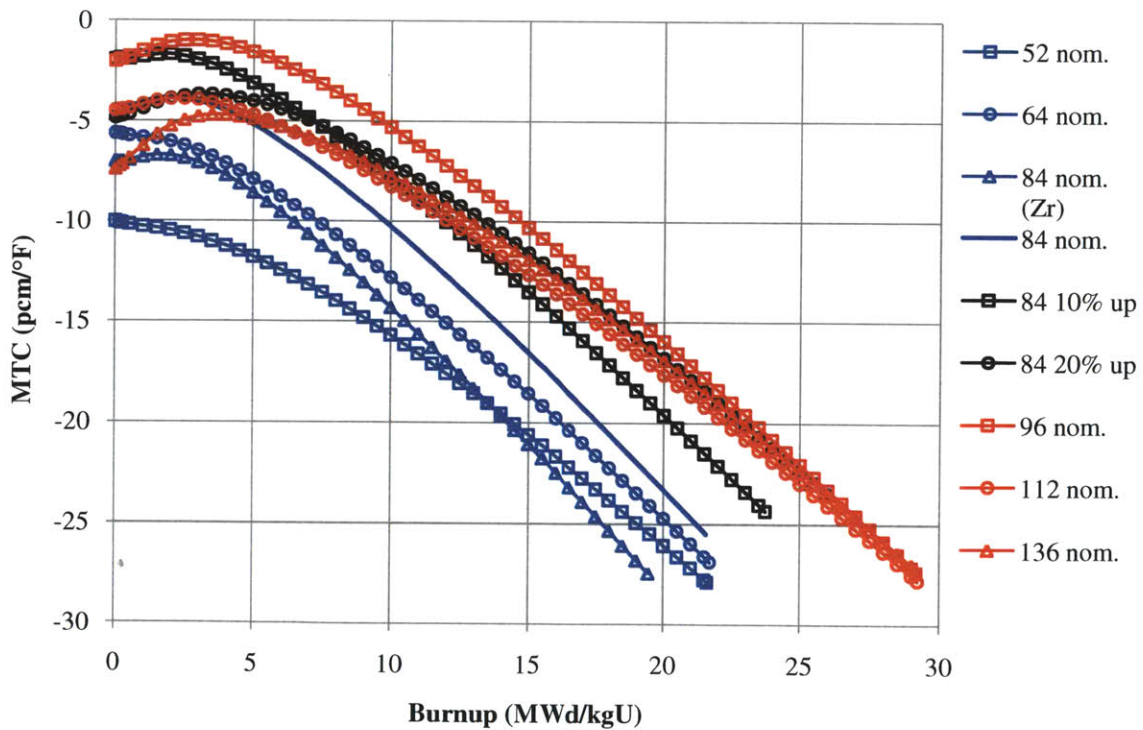


Figure 6.1 Moderator temperature coefficients for all 18- and 24-month core designs.

6.2 ISOTHERMAL TEMPERATURE COEFFICIENT (ITC)

Defined as the reactivity change associated with a uniform change in the fuel and moderator inlet temperatures divided by the change in the averaged moderator temperature, the isothermal temperature coefficient provides a very similar but slightly more practical value compared to the MTC. Described more clearly, the ITC assumes the same fuel temperature across the fuel, enabling the effect of the moderator to be measured more directly. As expected, the ITC was found to be slightly more negative than the MTC in all core designs evaluated.

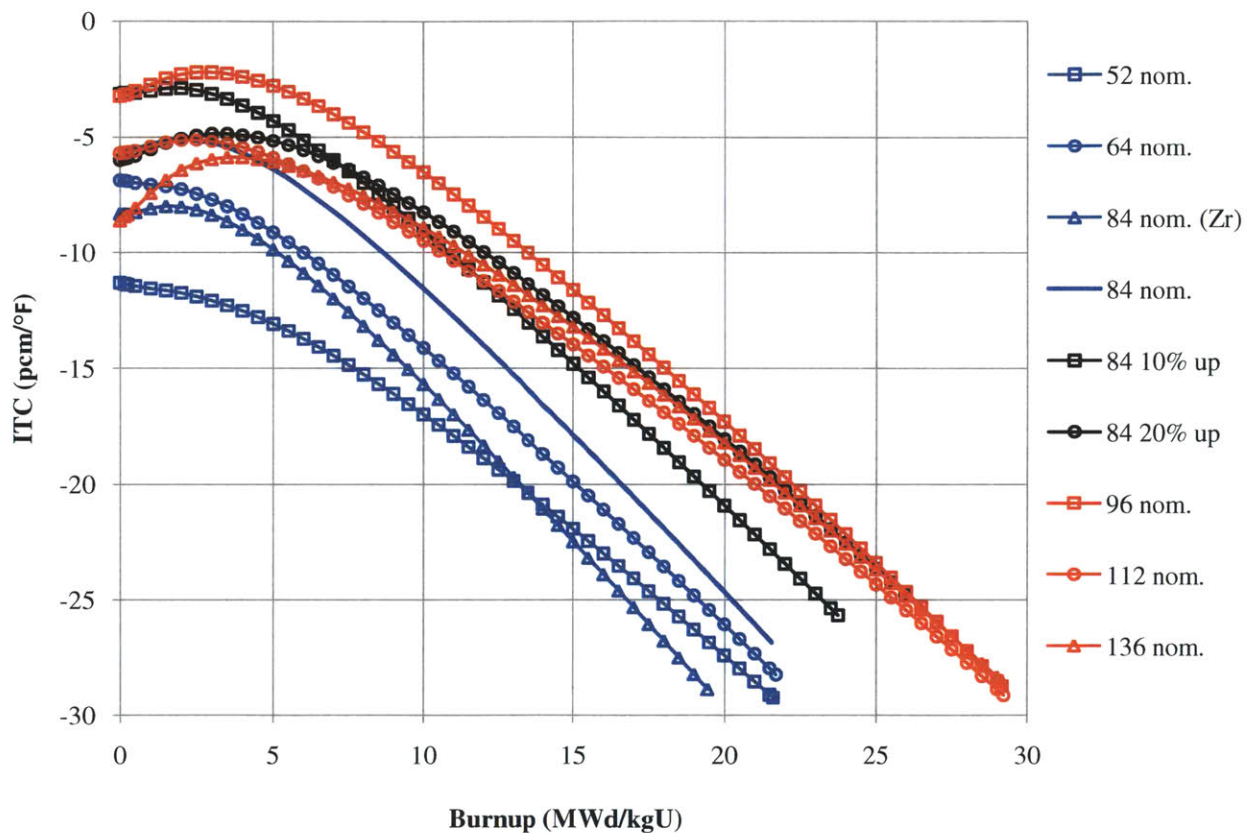


Figure 6.2 Isothermal temperature coefficient for all 18- and 24-month core designs.

6.3 UNIFORM DOPPLER COEFFICIENT (UDC)

The uniform doppler coefficient was calculated by SIMULATE-3 as the reactivity change associated with a uniform change in fuel temperature divided by the change in the averaged fuel temperature. As expected, these values were also negative, primarily as a result of the Doppler effect.

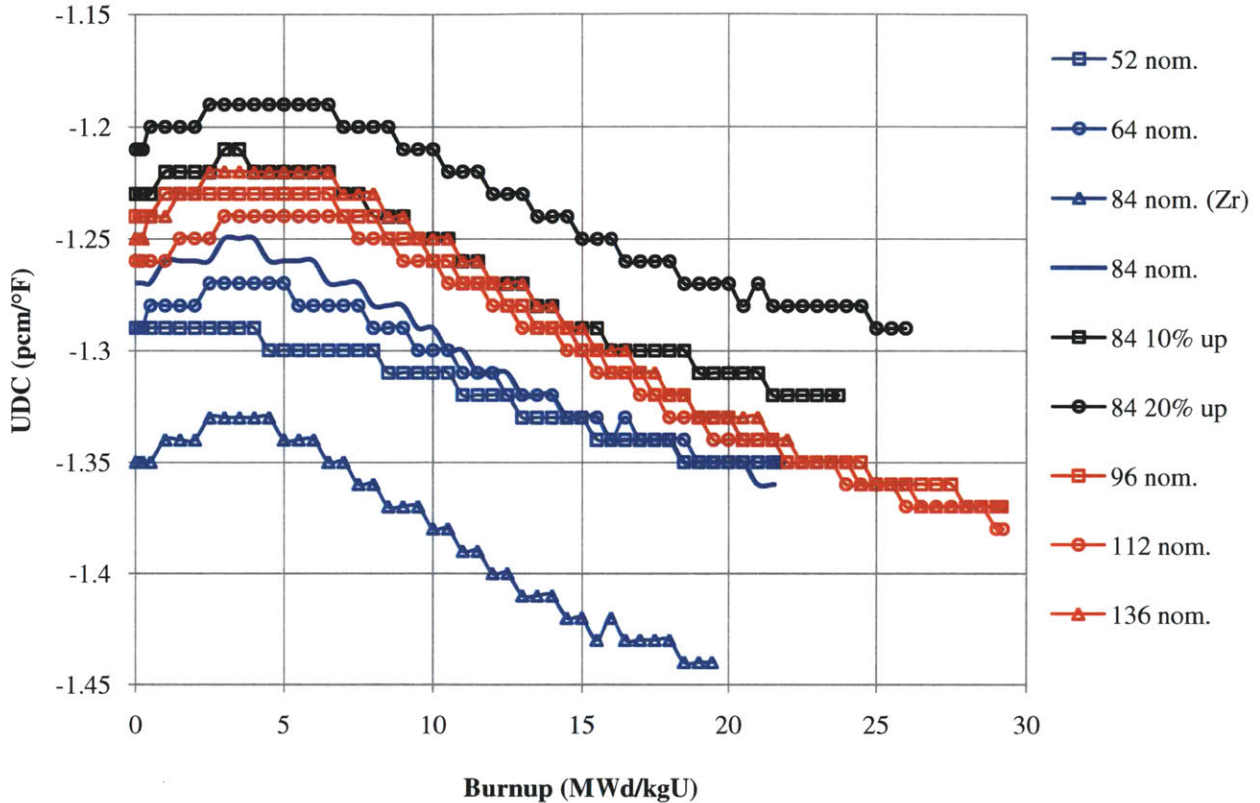


Figure 6.3 Uniform doppler coefficient for all 18- and 24-month core designs.

6.4 BORON COEFFICIENT

In order to calculate the boron coefficient, the reactivity change associated with a uniform perturbation of the boron concentration was divided by the boron change. With this value, the amount of reactivity held down by each ppm of boron may be determined for each step in the cycle. As expected, boron held down slightly more boron as EOC was approached in all core designs.

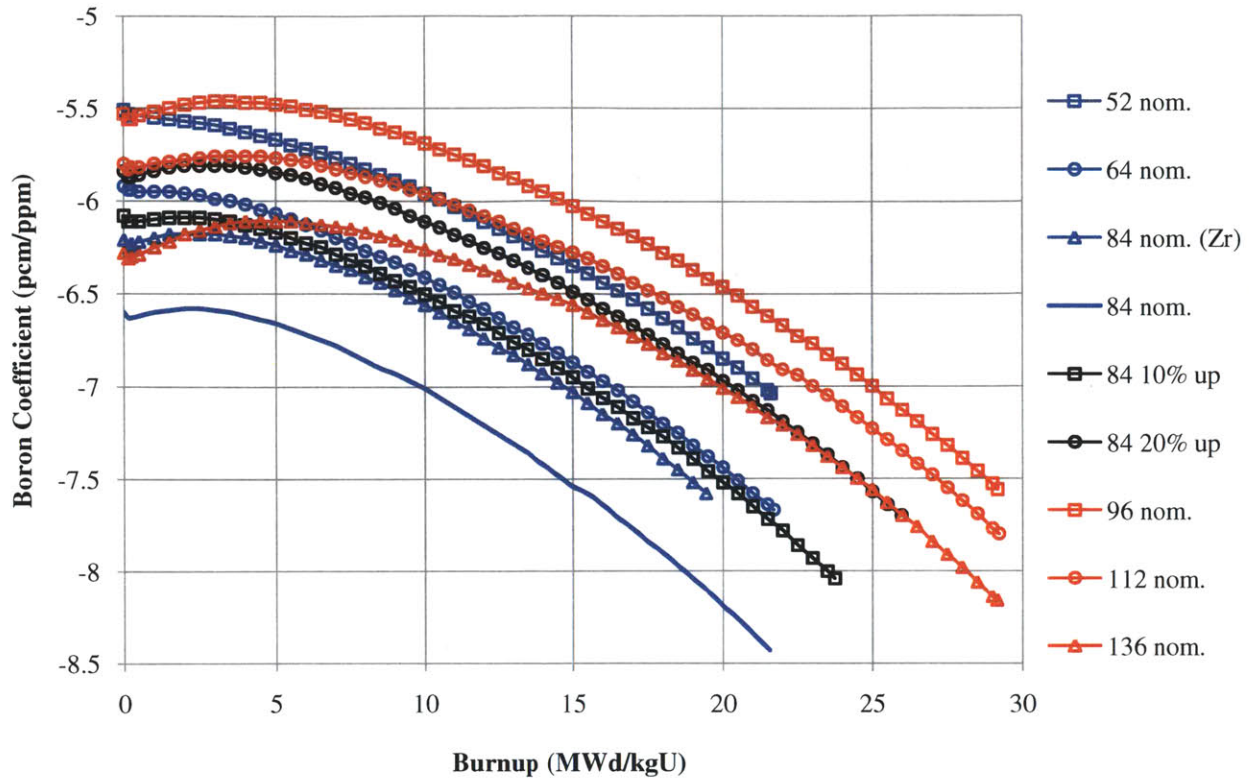


Figure 6.4 Boron coefficient for all 18- and 24-month core designs.

6.5 POWER COEFFICIENT

Finally, the power coefficient was determined by taking the reactivity change associated with a uniform change in the power level divided by the percent change in power. As noted in the SIMULATE-3 manual, the power distribution utilized to evaluate each cross section remained unchanged.

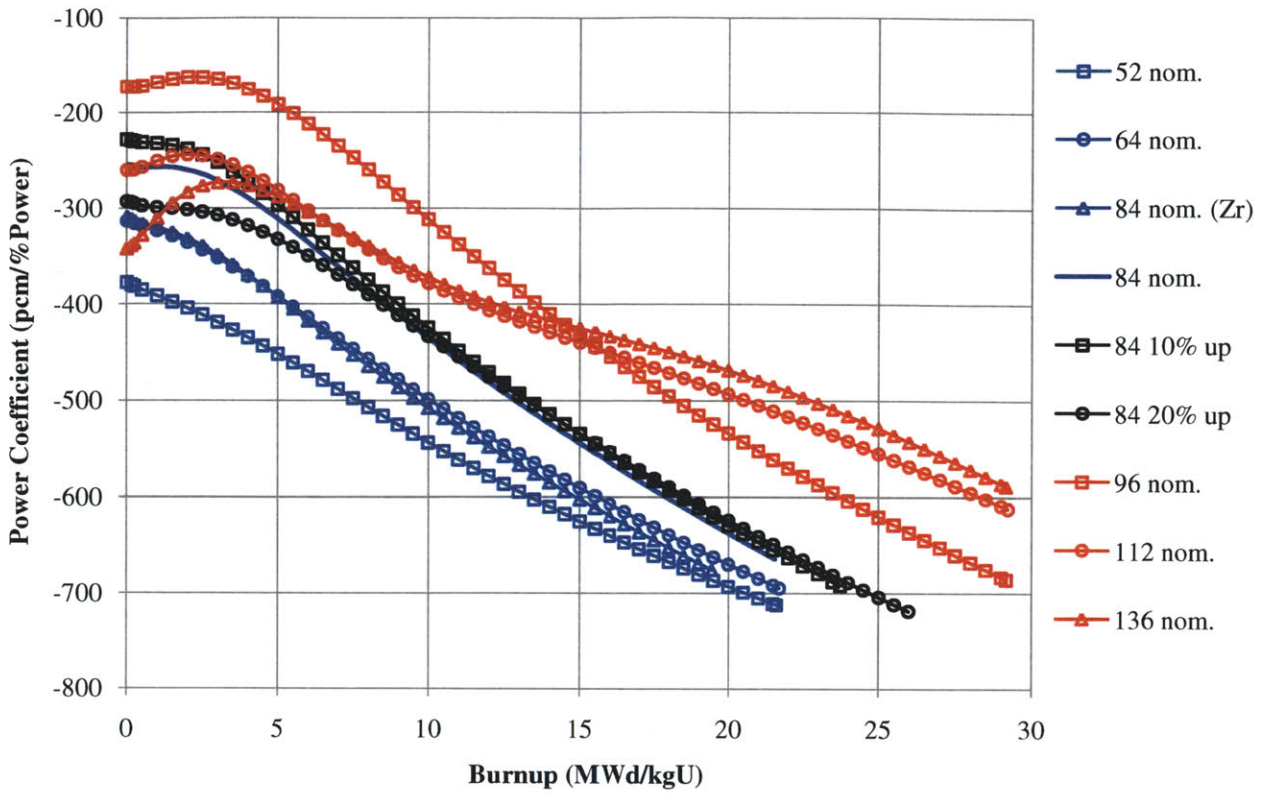


Figure 6.5 Power coefficient for all core designs.

6.6 SHUTDOWN MARGIN

Unlike the previous reactivity parameters which dealt with temperature, power, and boron perturbations, the shutdown margin quantifies the amount of reactivity that may be held down with control rods and other subcritical events during the powering down of a nuclear reactor. For this work (and also for industry), a value of negative reactivity of 1.3% or -1300 pcm, was considered acceptable. As can be seen in Table 6.2, all cores met the shutdown margin except for the 20% uprated core near EOL. In this case, adequate shutdown margin may require the control rod material or configuration to be altered. Regardless, shutdown margin usually decreases toward the end of cycle, but in some cases, related to a harder neutron spectrum in more enriched batches like the 52-reload case, the shutdown margin may actually increase at EOL.

Table 6.2 Shutdown margin for all cores

Reload #	Uprate	Enrichment	SDM (pcm)		SDM (%)	
			BOL	EOL	BOL	EOL
52 SiC (4 bat.)	0%	6.84	-2544	-2735	2.5	2.7
64 SiC (3 bat.)	0%	5.74	-2889	-1776	2.9	1.8
84 Zr (3 bat.)	0%	4.52	-2737	-1928	2.7	1.9
84 SiC (3 bat.)	0%	4.79	-2784	-2203	2.8	2.2
84 SiC (3 bat.)	10%	5.30	-2192	-1657	2.2	1.7
84 SiC (3 bat.)	20%	5.78	-2009	-1219	2.0	1.2
96 SiC (2 bat.)	0%	5.71	-2275	-2823	2.3	2.8
112 SiC (2 bat.)	0%	5.58	-2555	-2562	2.6	2.6
136 SiC (2 bat.)	0%	5.15	-2496	-2803	2.5	2.8

For all the cores described above, a control rod map was utilized from the Seabrook nuclear power plant, keeping the same position of shutdown and control rod banks in the core. As will be described, only the control rod banks were assumed to be inserted when calculating the “insertion allowance.”

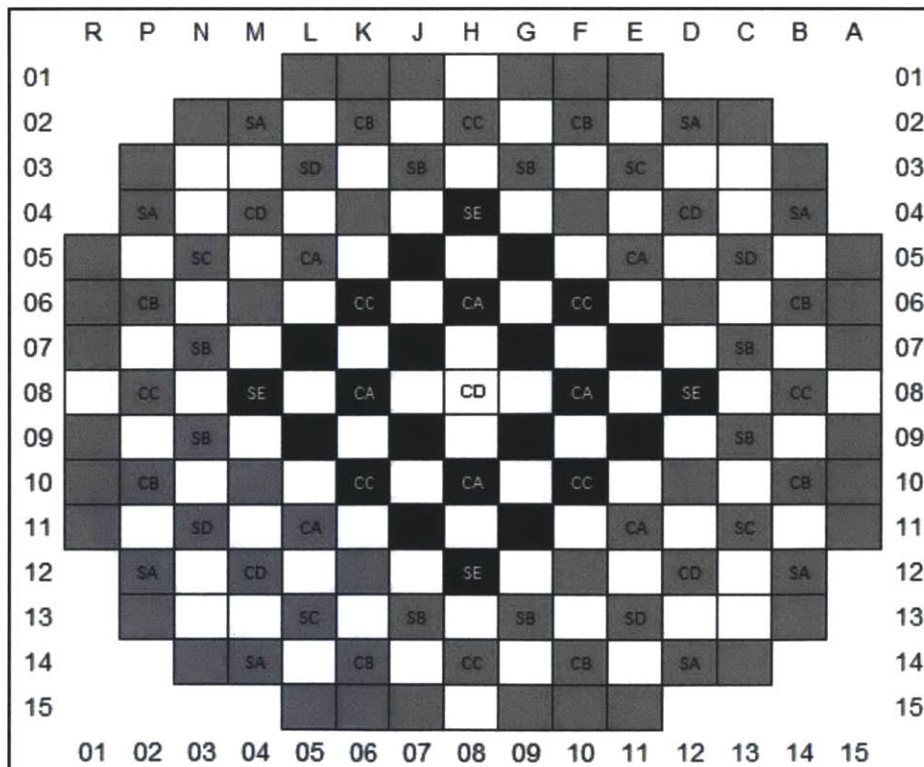


Figure 6.6 Labels that start with “S” refer to *shutdown* banks and are either completely inserted or withdrawn during operation. Labels that start with “C” refer to *control* banks and have variable insertion/withdrawal levels.

The shutdown margin was calculated in a series of seven steps described below in Table 6.3

Table 6.3 Step-by-step description of shutdown margin calculation

Step 1	<i>The “insertion allowance” worth of control rods was determined by utilizing SIMULATE-3 to calculate the reactivity of the core when only 30% of the control banks were inserted into the equilibrium core with xenon.</i>	+ $\Delta\rho$
Step 2	<i>When the reactor shuts down, it goes from hot full power (HFP) to hot zero power (HZP). The reactivity difference of the core at HFP to HZP was calculated without the reactivity hold-down of equilibrium xenon.</i>	+ $\Delta\rho$
Step 3	<i>The total positive reactivity experienced during a shutdown was calculated by adding the values found in Step 1 and Step 2 together.</i>	+ $\Delta\rho$
Step 4	<i>SIMULATE-3 was utilized to insert all control rods into the reactor (ARI) with equilibrium xenon accounted for.</i>	- $\Delta\rho$
Step 5	<i>The HWR card in SIMULATE-3 was utilized to determine the high worth rod (HWR) in the equilibrium cycle with xenon and then calculate its reactivity worth by removing all control rods from the reactor core except the HWR. This value was then added to Step 4, reducing the total negative reactivity in the core.</i>	- $\Delta\rho$
Step 6	<i>The total negative reactivity in the core was further reduced by multiplying it by a “conservatism factor” of 0.9.</i>	- $\Delta\rho$
Step 7	<i>Shutdown Margin was calculated by adding Step 3 and Step 6 together.</i>	

Figure 6.7 graphically demonstrated the negative and positive reactivity insertions from the steps above for the nominal, 84-reload SiC case.

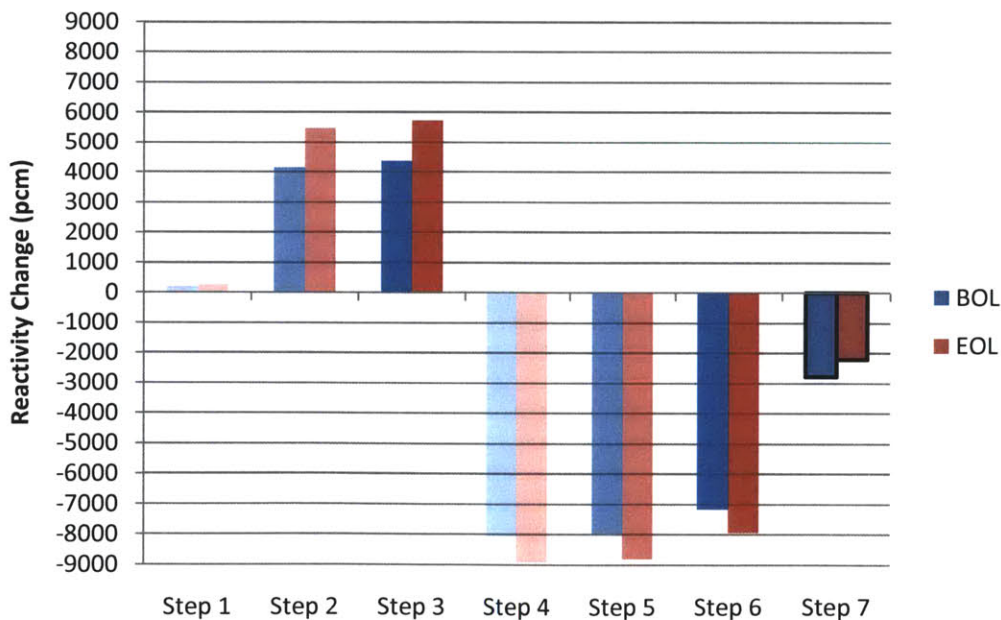


Figure 6.7 Graphic representation of reactivity gains and losses from steps during a shutdown margin calculation.

Shutdown margin (SDM) can also be described mathematically.

$$SDM = \rho_{positive} + \rho_{negative} = (\rho_{CRD\ 30\% In} + \rho_{HFP \rightarrow HZP}) + 0.9 \cdot [\rho_{ARI} + \rho_{HWR}]$$

Where:

$$\rho_{CRD\ 30\% In} = \text{Step 1 (+}\rho\text{)}$$

$$\rho_{HFP \rightarrow HZP} = \text{Step 2 (+}\rho\text{)}$$

$$\rho_{ARI} = \text{Step 4 (-}\rho\text{)}$$

$$\rho_{HWR} = \text{Step 5 (-}\rho\text{)}$$

Tables 6.4 and 6.5 provide the values calculated in the steps above for the nominal 84-reload core design's shutdown margin.

Table 6.4 Shutdown and control rod bank worth for the nominal 84-reload SiC case

Bank #	Row	Col	BOL HFP (pcm)	EOL HFP (pcm)
1	11	11	101.8	104.7
2	8	12	93.3	104.7
3	12	8	93.3	99.2
4	12	12	92.8	97.1
5	9	13	92.4	91.1
6	13	9	88.9	91.1
7	10	10	88.9	87.9
8	8	10	77.7	87.7
9	10	8	80.3	88.6
10	13	11	73.6	81.2
11	11	13	76.0	73.7
12	8	14	75.8	76.0
13	14	8	73.1	75.8
14	10	14	72.3	73.7
15	14	10	58.4	62.6
16	8	8	58.2	62.6
17	14	12	29.7	42.8
18	12	14	29.7	43.0

Table 6.5 Reactivity balance for nominal 84-reload SiC case.

Description	BOL (k_{eff})	BOL (pcm)	EOL (k_{eff})	EOL (pcm)
Rod insertion allowance worth	0.99792	208	0.99748	253
Total decrement HFP to HZP (excluding Xe)	1.04331	4151	1.05791	5474
HFP to HZP + Rod insertion allowance	-	4360	-	5727
Total Rod Worth (HFP)	0.92559	-8039	0.91814	-8916
Total Rod Worth - Most Effective Rod (HFP)	-	-7937	-	-8811
Rod Conservatism factor (90%)	-	-7144	-	-7930
Shutdown Margin	-	-2784	-	-2203

7. DIVERSE BURNABLE POISON CORE DESIGNS

With so many variables that may be adjusted in refueling a reactor core, one critical choice was the type of burnable poison utilized. As mentioned in Chapter 2, every burnable poison helps “hold down” reactivity in some fashion at BOC. Depending on the absorption cross-sections of various isotopes in BP, this reactivity may be initially held down at varying rates, illustrated in Figure 7.1.

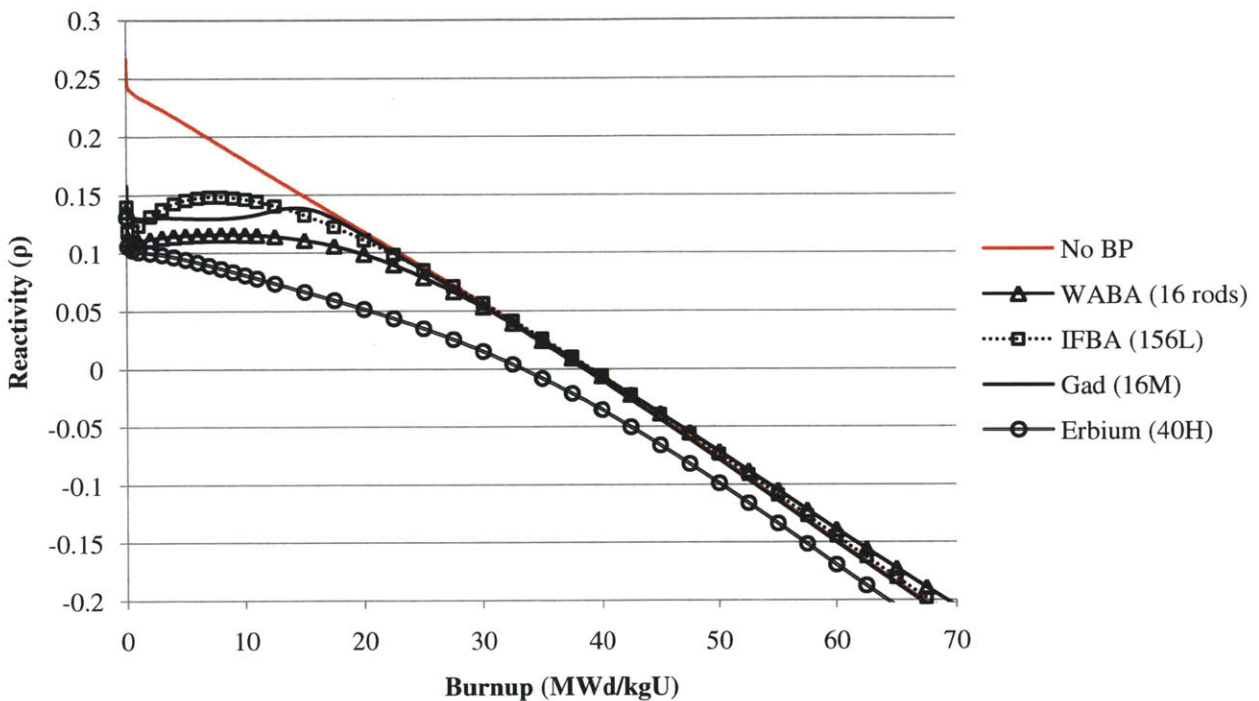


Figure 7.1 Burnable poisons hold down reactivity in varying ways As a result of different isotopic abundances.

In this research, a gadolinium core will be constructed as well as cores with both IFBA and Gd, and IFBA and WABA.

7.1 GADOLINIUM CORE

Designing a core with Gd followed the same procedure as the previous core designs discussed in Chapters 4 and 5. The only differences in the computer modeling were at the assembly level, in CASMO-4E, the BP material and rod location needed to be changed

appropriately. This was a relatively straightforward process, but involved the creation of a library of new types of assemblies with various rod layouts, which can be found in Appendix A.

Table 7.1 84-reload core design (with Gd) summary of reactor physics parameters.

Reload #	Uprate	Avg. w/o	B _C	Avg. B _D	EFPD	#Gd Rods	Boron (ppm)	F _{Δh}	F _q	Max Pin Burnup
84 SiC (3 bat.)	0%	4.89	21.65	49.8	492	1216	1676	1.544	1.81	72.9

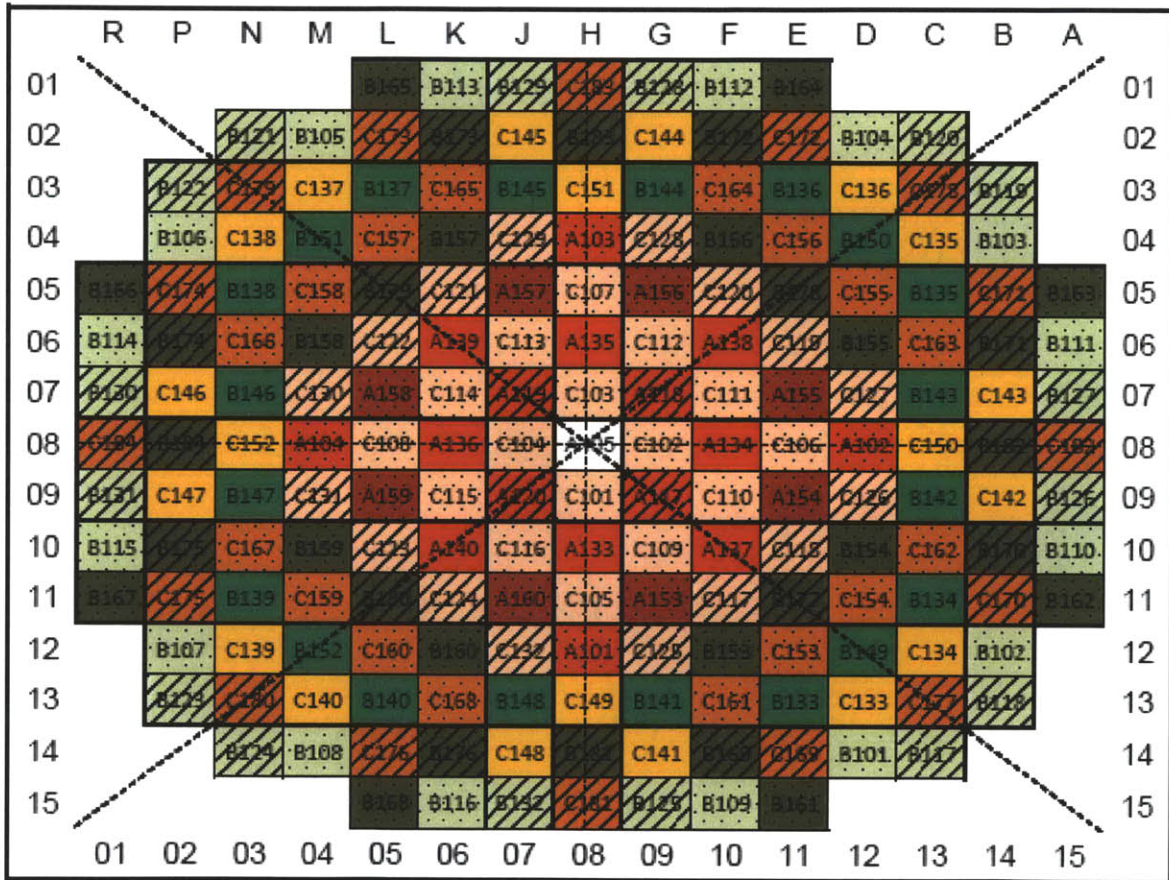


Figure 7.2 84-reload (with Gd) core loading map.

Table 7.2 84-reload core design (with Gd) fuel batch summary.

Fuel	Fuel Batch ID	# ASSYs	ASSY w/o	Blanket w/o	# Gd Rods per ASSY	Gd Loading (% Gd ₂ O ₃)
Twice	G185516M	4	5.5	3.2	16	7.0
	G184812L	4	4.8	3.2	12	4.0
	G184816M	8	4.8	3.2	16	7.0
	G184716M	8	4.7	3.2	16	7.0
Once	G185516M	16	5.5	3.2	16	7.0
	G184812L	16	4.8	3.2	12	4.0
	G184816M	20	4.8	3.2	16	7.0
	G184716M	16	4.7	3.2	16	7.0
	G185512L	16	5.5	3.2	12	4.0
Fresh	G185516M	16	5.5	3.2	16	7.0
	G184812L	16	4.8	3.2	12	4.0
	G184816M	20	4.8	3.2	16	7.0
	G184716M	16	4.7	3.2	16	7.0
	G185512L	16	5.5	3.2	12	4.0

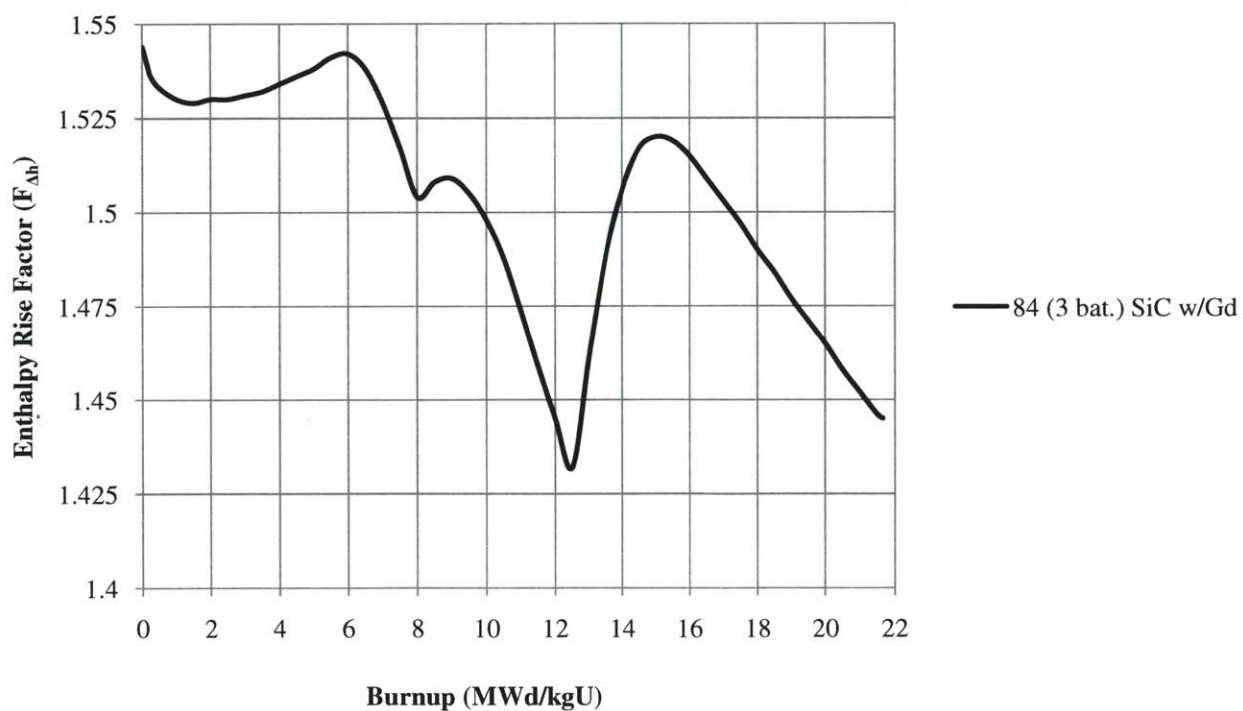


Figure 7.3 F_{Ah} for 84-reload core (with Gd).

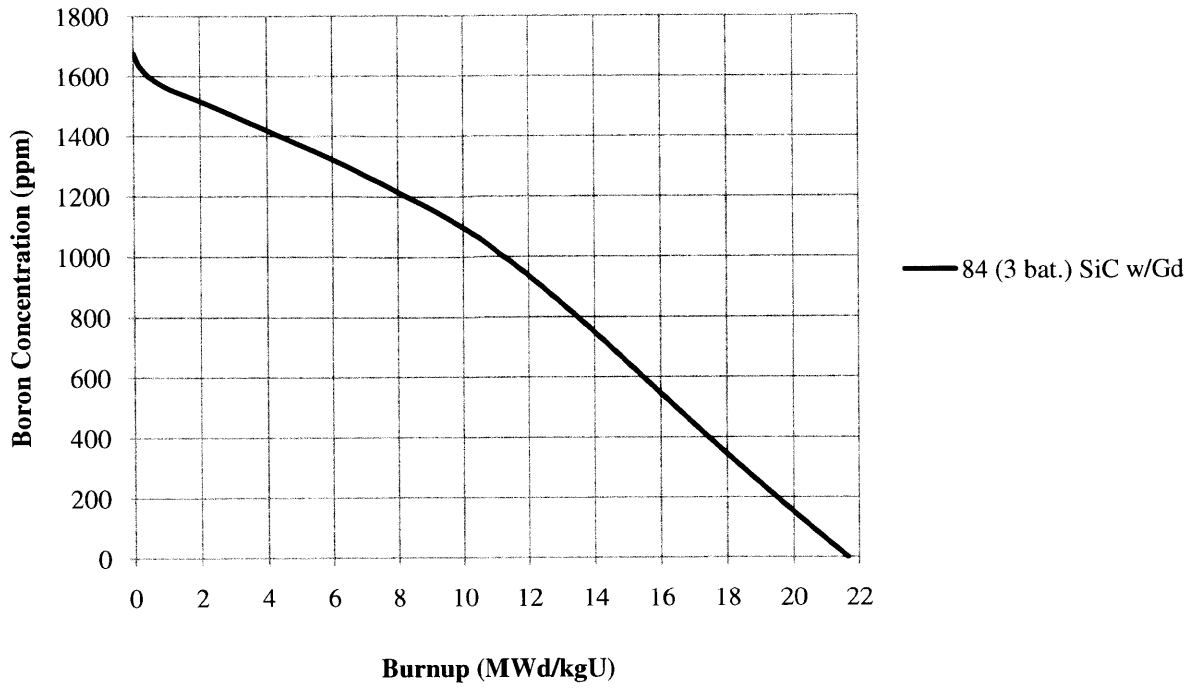


Figure 7.4 Boron concentration (ppm) for 84-reload core (with Gd).

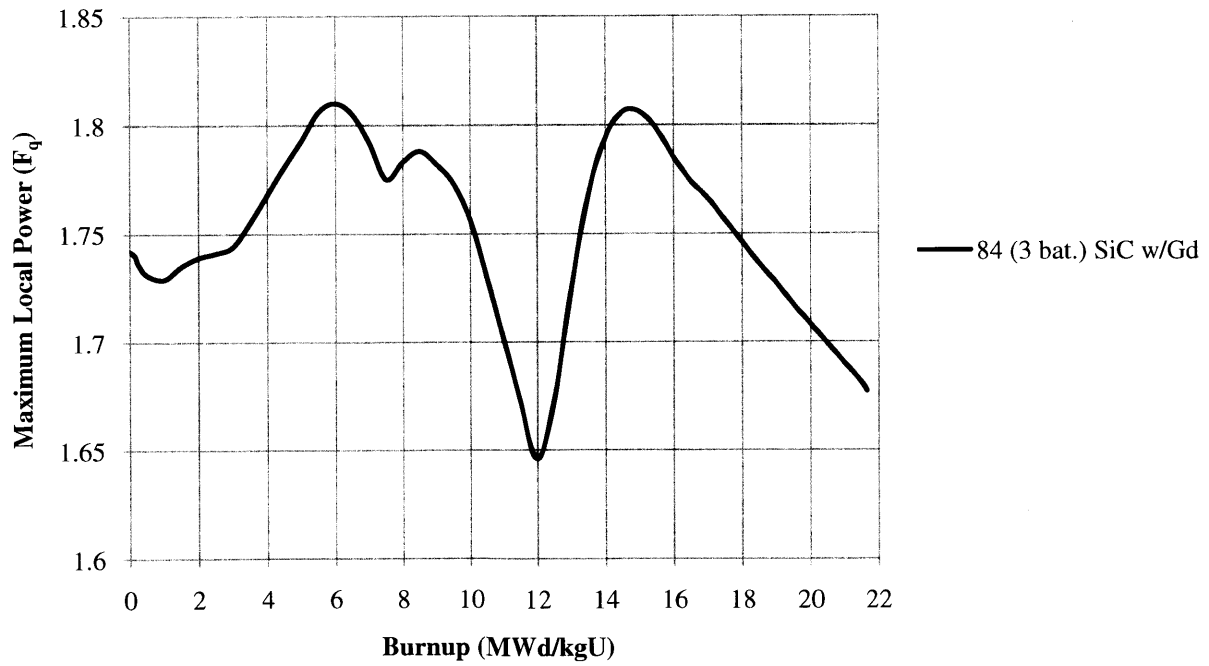


Figure 7.5 F_q for 84-reload core (with Gd).












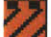


7.2 GADOLINIUM-IFBA CORE

In this design, assemblies with 156-IFBA rods were inserted into the core loading pattern utilized in the previous section. With this approach, the idea was to minimize, or save, the number of IFBA rods inserted into the core. As a result of this design, 4096 IFBA rods could be replaced with only 512 Gd rods. This may be an economic benefit to the utility if a fabrication company imposes a limit on the number of IFBA rods given as a convenience for a large order of assemblies. Figures 7.6-7.8 provide the values of $F_{\Delta h}$, boron concentration needed, and F_q , respectively. All parameters stay within allowable bounds.

Table 7.3 Target core parameters for 84-reload SiC case with Gd & IFBA BP.

Reload #	Uprate	Avg. w/o	B_C	Avg. B_D	EFPD	#Gd/IFBA Rods	Boron (ppm)	$F_{\Delta h}$	F_q	Max Pin Burnup
84 SiC (3 bat.)	0%	4.88	21.72	49.9	495	512 8112 (1X)	1470	1.532	1.758	72.0

Table 7.4 Fuel Loading for 84-reload SiC case with Gd & IFBA BP.

Fuel	Fuel Batch ID	# ASSYs	ASSY w/o	Blanket w/o	BP Type	# BP Rod	Gd Loading (% Gd_2O_3)	IFBA Loading (mg $^{10}B/in$)
 Twice	57I156L	4	5.7	3.2	IFBA	156	-	1.57
 Twice	G184516M	4	4.5	3.2	Gd	16	7.0	-
 Twice	48I156L	8	4.8	3.2	IFBA	156	-	1.57
 Twice	G184516M	8	4.5	3.2	Gd	16	7.0	-
 Once	57I156L	16	5.7	3.2	IFBA	156	-	1.57
 Once	G184516M	16	4.5	3.2	Gd	16	7.0	-
 Once	48I156L	20	4.8	3.2	IFBA	156	-	1.57
 Once	G184516M	16	4.5	3.2	Gd	16	7.0	-
 Once	57I156L	16	5.7	3.2	IFBA	156	-	1.57
 Fresh	57I156L	16	5.7	3.2	IFBA	156	-	1.57
 Fresh	G184516M	16	4.5	3.2	Gd	16	7.0	-
 Fresh	48I156L	20	4.8	3.2	IFBA	156	-	1.57
 Fresh	G184516M	16	4.5	3.2	Gd	16	7.0	-
 Fresh	57I156L	16	5.7	3.2	IFBA	156	-	1.57

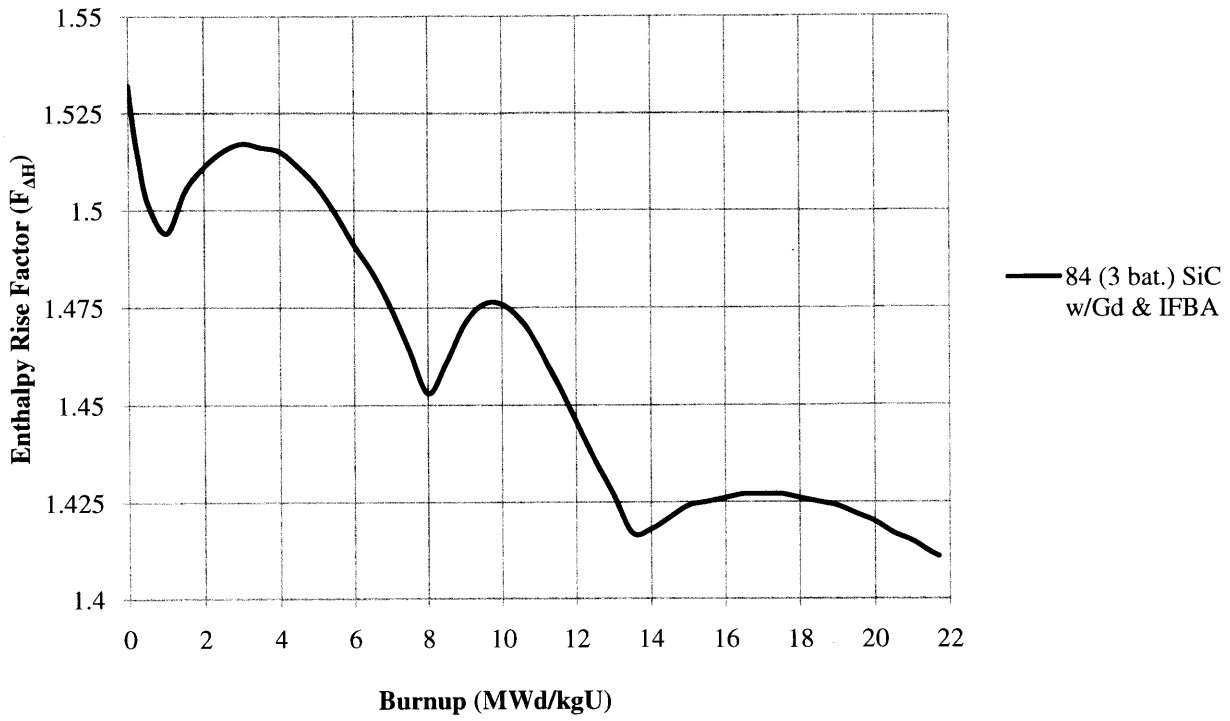


Figure 7.6 F_{Ah} for 84-reload core with Gd & IFBA.

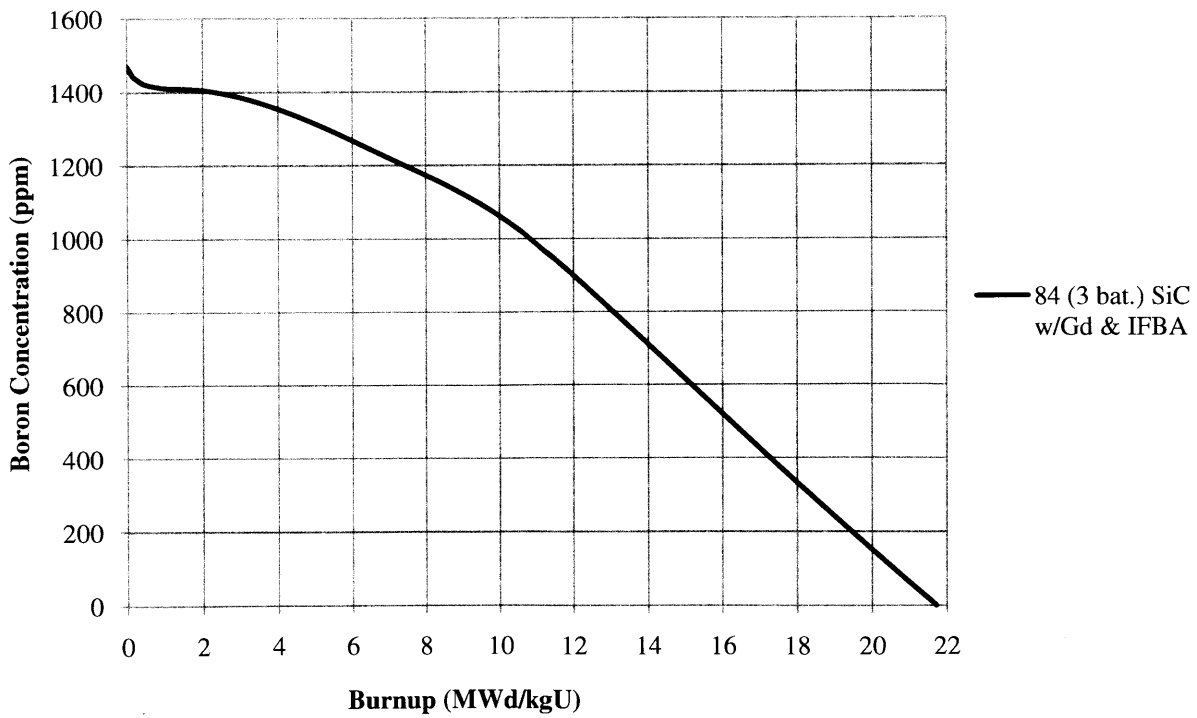


Figure 7.7 Boron concentration for 84-reload core with Gd & IFBA.

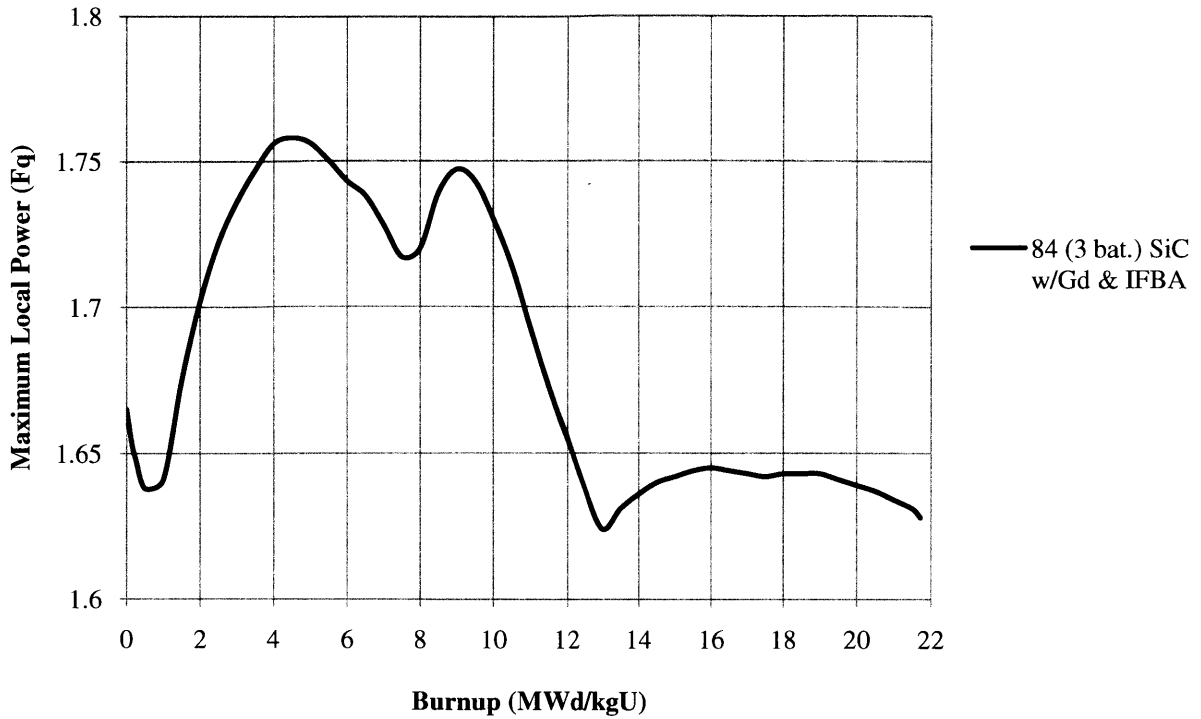


Figure 7.8 F_q for 84-reload core with Gd & IFBA.

7.3 IFBA-WABA CORE

Implementing WABA into the core presented several unique challenges to the PWR computer modeling. First, new pins and material cards had to be utilized to describe the unique structure of the WABA rod, depicted previously in Figure 2.3. Second, assemblies with WABA could not be placed in a location of a shutdown or control bank. This was a logical limitation, since control rods had to maintain the ability to be inserted into the guide tubes on the operator's command. Finally, unlike IFBA, erbium, and gadolinium, WABA rods had to be removed after only one cycle because of their high reactivity hold-down in the core. Fortunately, in this simulation the same loading pattern for the nominal 84-reload core design could be utilized. As can be seen in Figure 7.9, "X's" were placed on the assembly locations that did not contain WABA. These locations corresponded to the control rod locations given earlier in Figure 2.11. In the end, the WABA rods successfully held down reactivity, but the F_q value saw a noticeable increase, however, it remained under the conservative limit of 2.0.

Table 7.5 84-reload core physics parameters with WABA as additional burnable poison.

Reload #	Uprate	Avg. w/o	B _C	Avg. B _D	EFPD	# IFBA/WABA Rods	Boron (ppm)	F _{Δh}	F _q	Max Pin Burnup
84 SiC (3 bat.)	0%	4.86	21.62	49.7	493	12208 (1X) 2016	1491	1.500	1.971	75.1

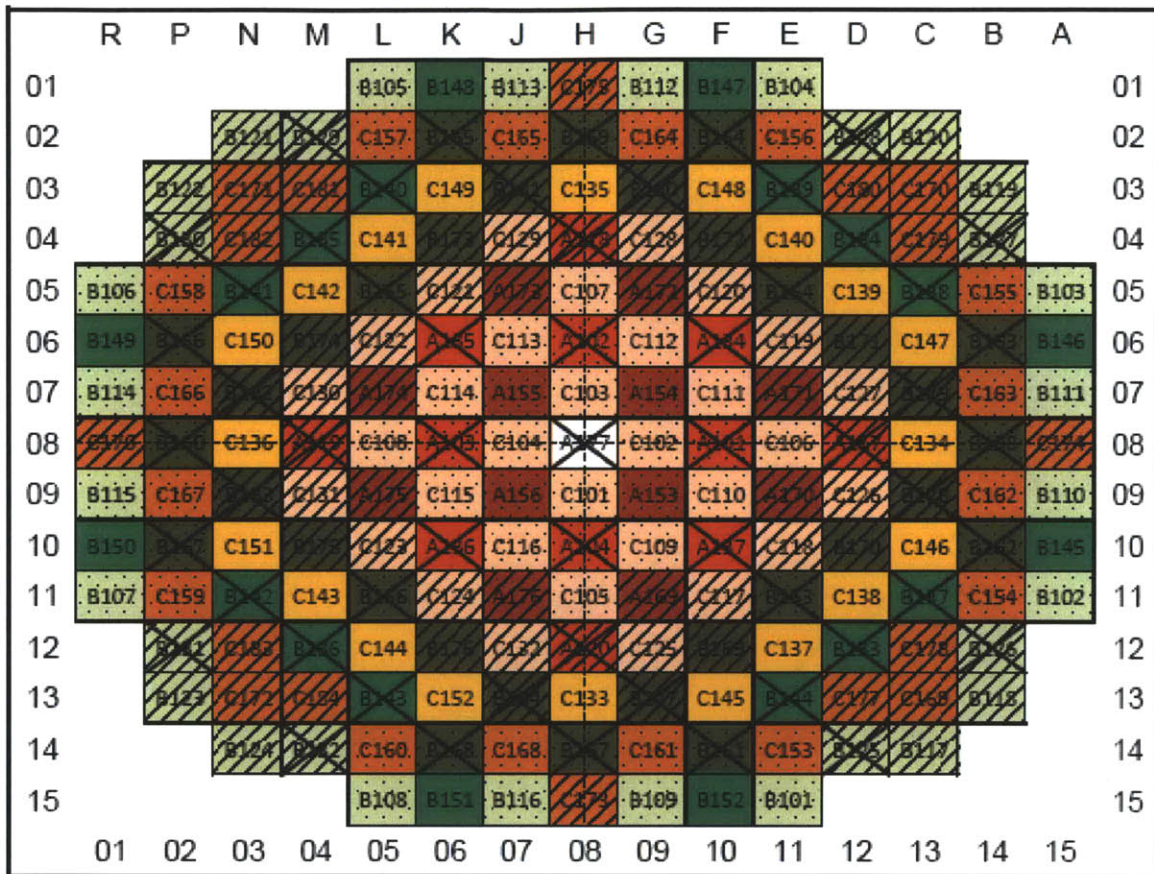


Figure 7.9 84-reload core reloading map for WABA. An “X” over an assembly location demarcates a shutdown or control bank location.

Table 7.6 84-reload refueling summary with WABA as additional burnable poison.

Fuel	Fuel Batch ID	# ASSYs	ASSY w/o	Blanket w/o	# WABA Rods	# IFBA Rods	IFBA Loading (mg ¹⁰ B/in)
Twice	56I156L	4	5.6	3.2	24	156	1.57
	45I156L	4	4.5	3.2	24	156	1.57
	45I156L	4	4.5	3.2	24	156	1.57
	50I128L	4	5.0	3.2	24	128	1.57
	56I128L	9	5.6	3.2	24	128	1.57
Once	56I156L	16	5.6	3.2	24	156	1.57
	45I156L	16	4.5	3.2	24	156	1.57
	45I156L	20	4.5	3.2	24	156	1.57
	50I128L	16	5.0	3.2	24	128	1.57
	56I128L	16	5.6	3.2	24 </td <td>128</td> <td>1.57</td>	128	1.57
Fresh	56I156L	16	5.6	3.2	24	156	1.57
	45I156L	16	4.5	3.2	24	156	1.57
	45I156L	20	4.5	3.2	24	156	1.57
	50I128L	16	5.0	3.2	24	128	1.57
	56I128L	16	5.6	3.2	24	128	1.57

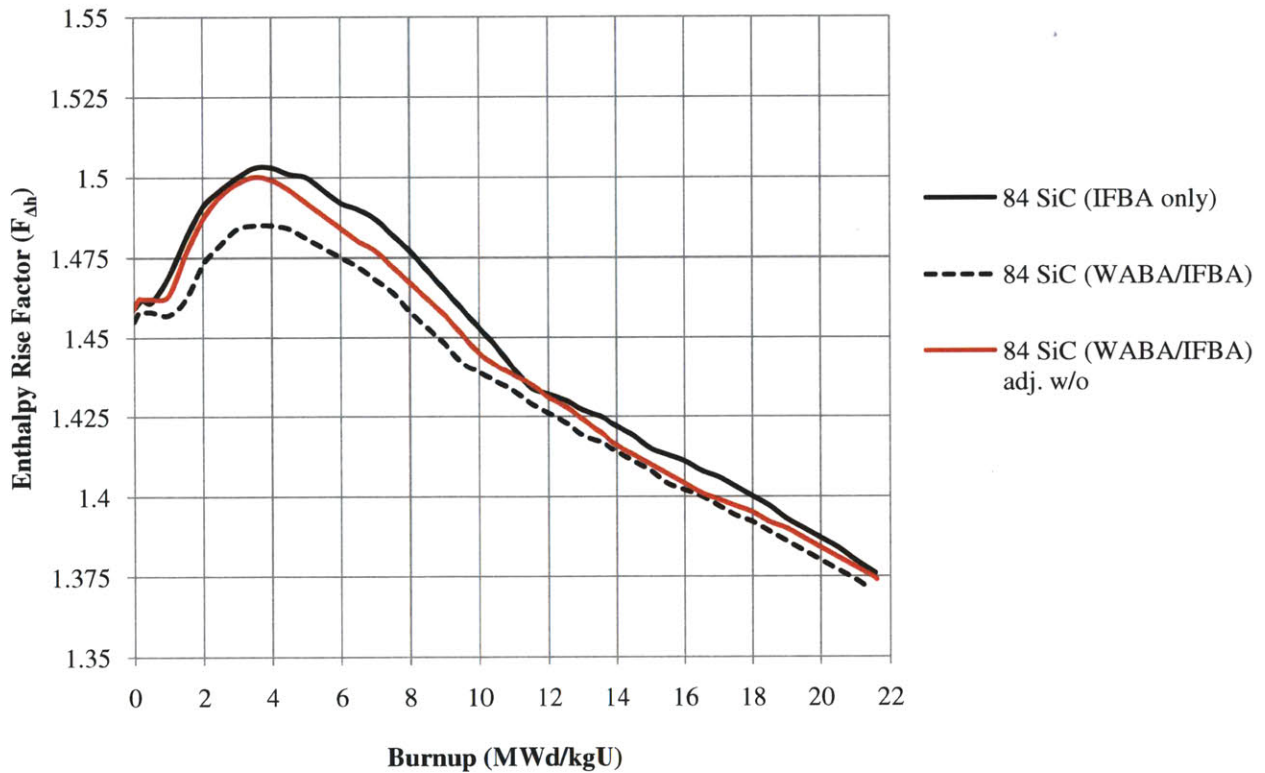


Figure 7.10 F_{Ah} throughout cycle length of 84-reload design with WABA.

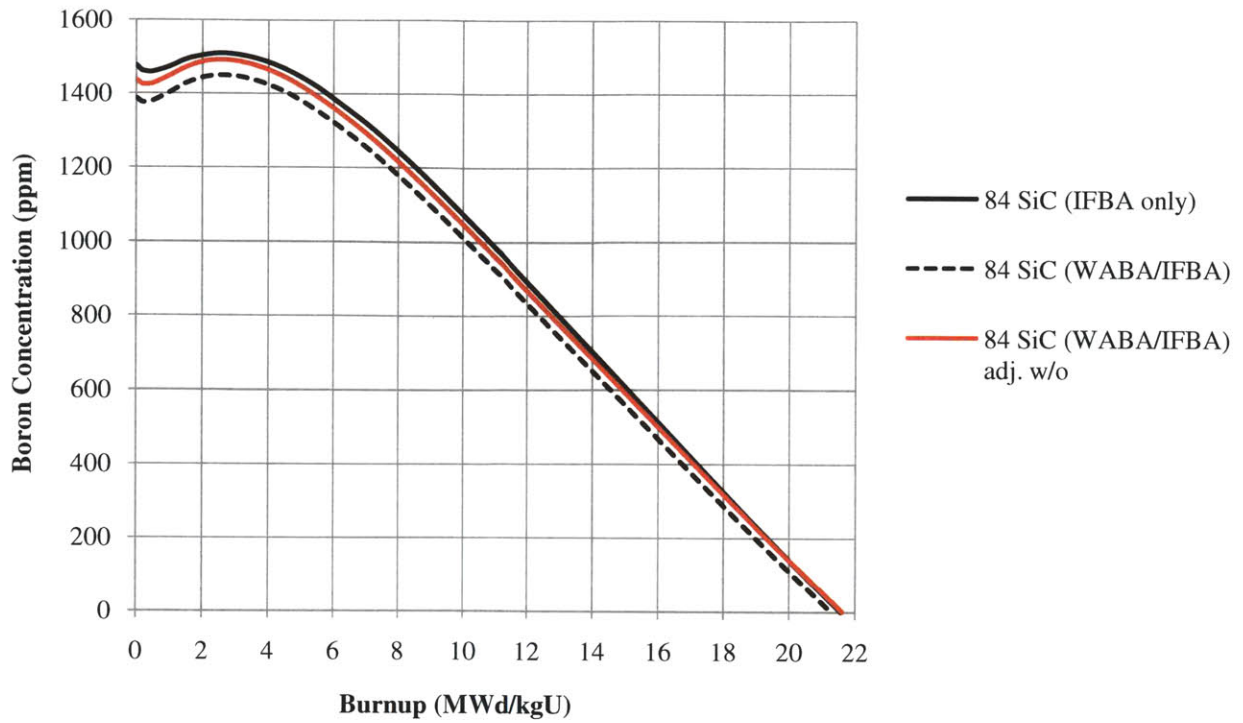


Figure 7.11 Boron Concentration throughout cycle length of 84-reload design with WABA.

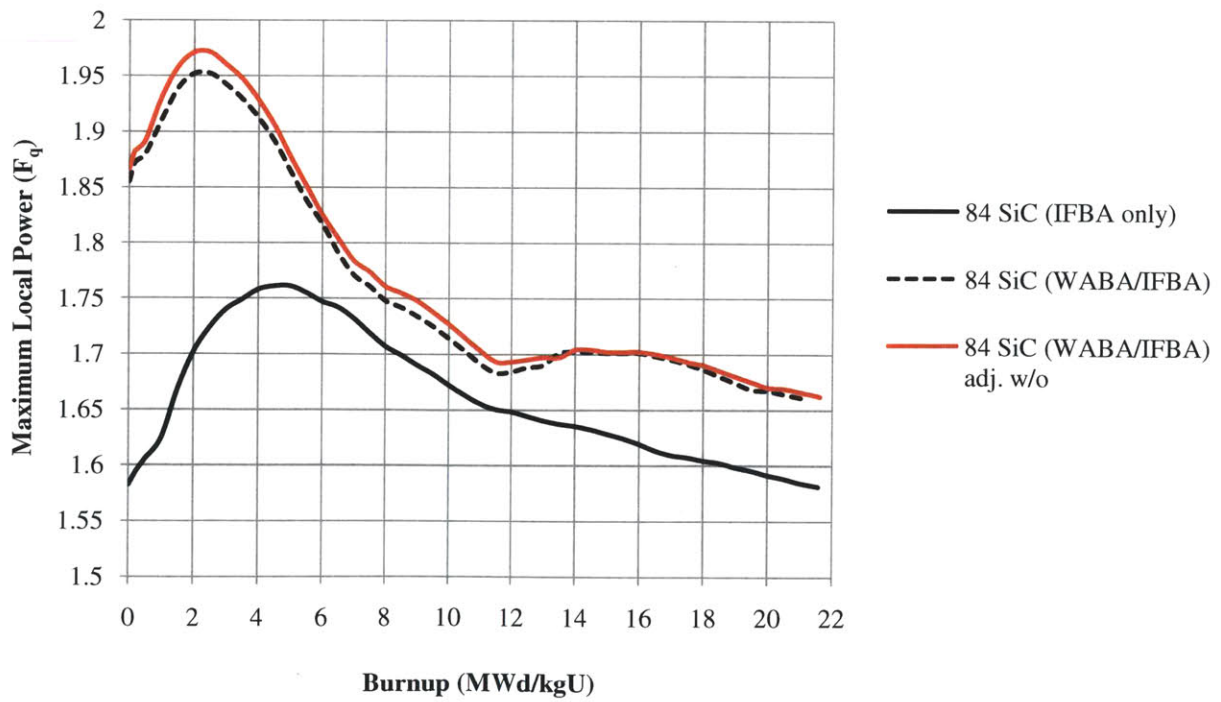


Figure 7.12 F_q throughout cycle length of 84-reload design with WABA.

7.4 SAFETY COEFFICIENTS OF DIVERSE BURNABLE POISONS

As performed in previous sections, a safety coefficient analysis was performed for the unique core designs described in Chapter 7. This included examining the MTC, ITC, boron coefficient, power coefficient, and UDC throughout the entire cycle. In addition, the shutdown margin was calculated for each core design. Every core demonstrated acceptable reactivity feedback coefficients and margins, except for the WABA design at EOC. With WABA, while the shutdown margin was well above the limit at BOC, by EOC, it had plummeted to under 600 pcm, suggesting that WABA should be removed earlier than EOC in order to maintain safety and stability in the core.

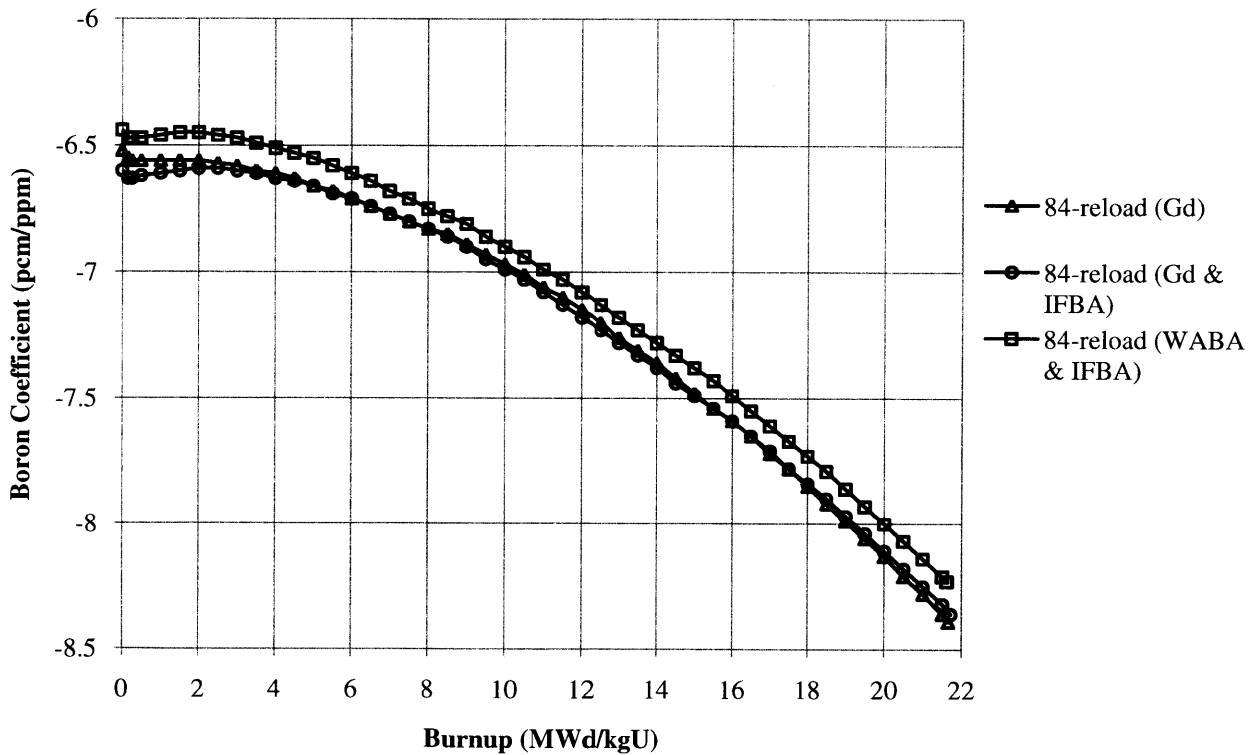


Figure 7.13 Boron coefficient for all cores with additional burnable poison.

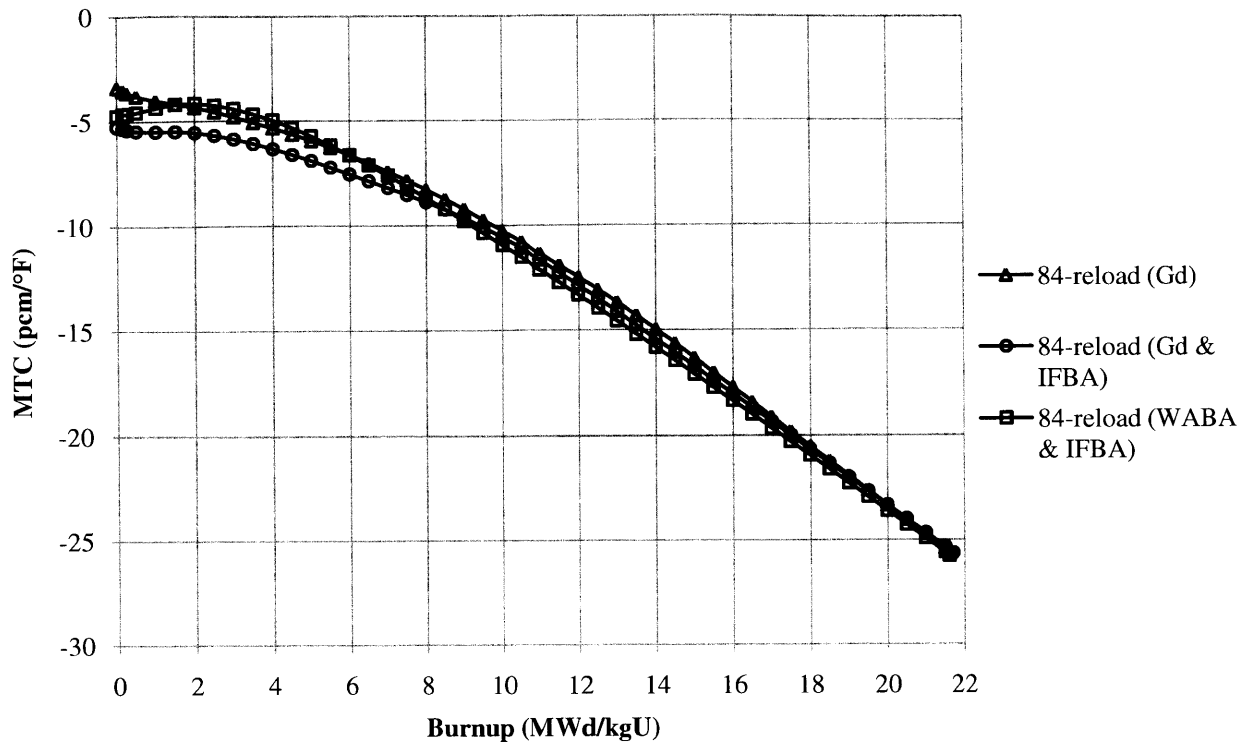


Figure 7.14 MTC for all cores with additional burnable poison.

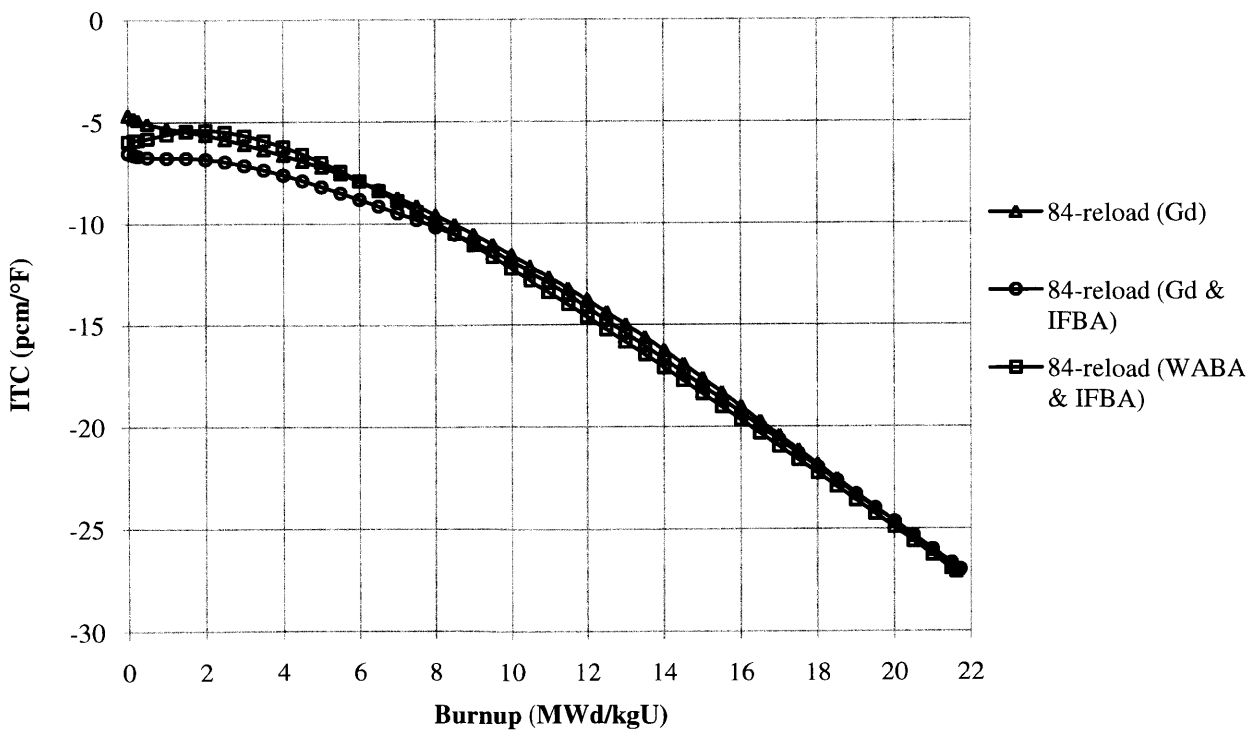


Figure 7.15 ITC for all cores with additional burnable poison.

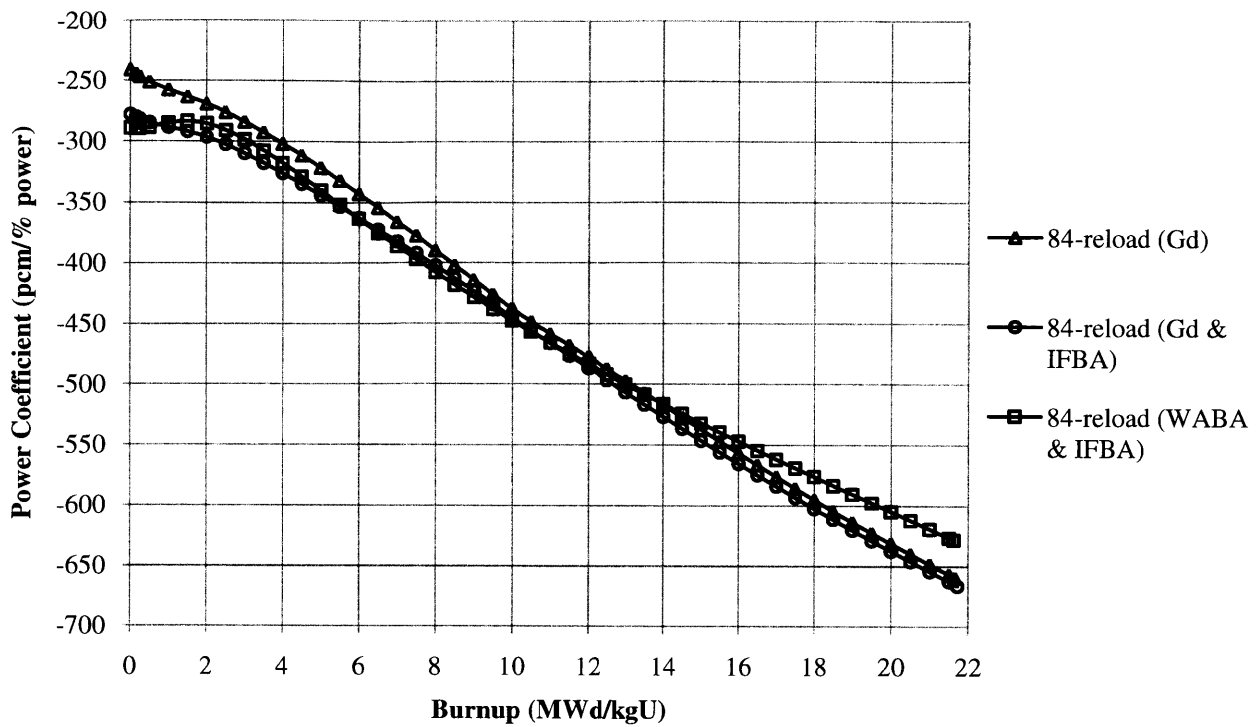


Figure 7.16 Power coefficient for all cores with additional burnable poison.

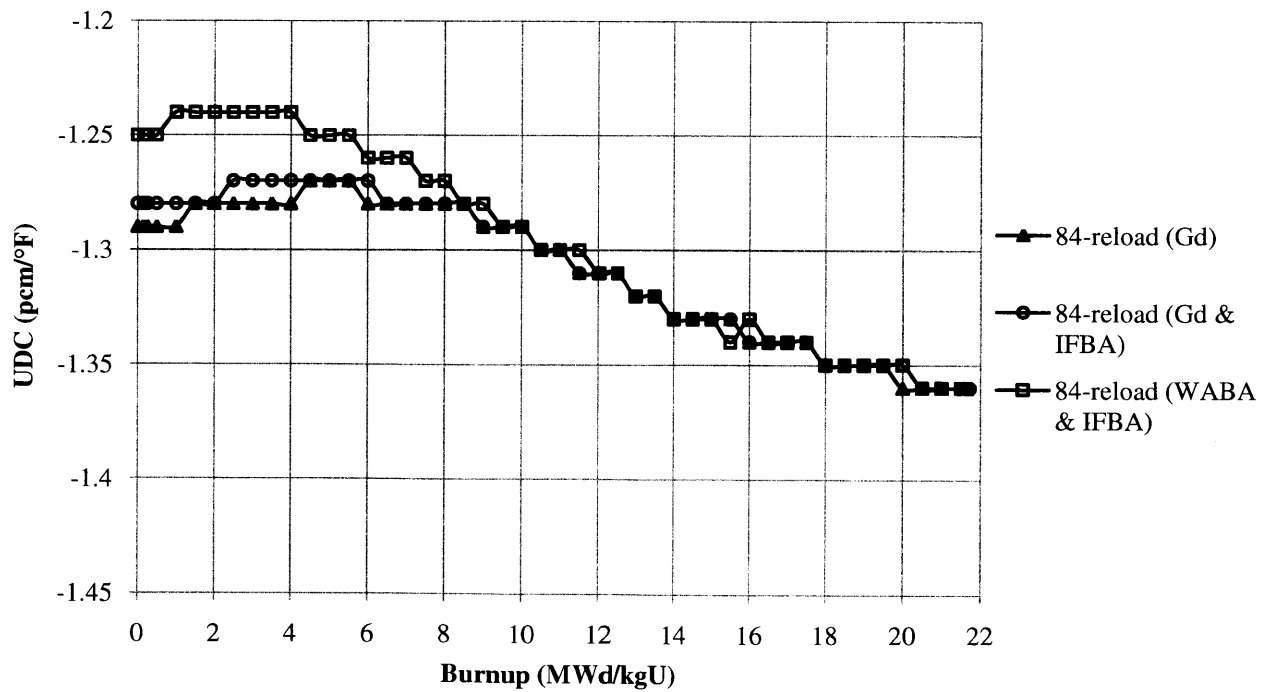


Figure 7.17 UDC for all cores with additional burnable poison.

Table 7.7 Shutdown margin for all cores with additional burnable poison.

Case	Uprate	Enrichment	SDM (pcm)		SDM (%)	
			BOL	EOL	BOL	EOL
84 SiC (IFBA only)	0%	4.79	-2784	-2203	2.78	2.20
84 SiC (Gd only)	0%	6.84	-3013	-2269	3.01	2.27
84 SiC (Gd & IFBA)	0%	5.74	-3113	-2318	3.11	2.32
84 SiC (WABA & IFBA)	0%	4.52	-2347	-518	2.35	0.52

8. TRANSITION CYCLE CORE DESIGN

Assuming constant power production, realistic implementation of SiC cladding will involve some type of transition cycle where both new and old cladding material must exist in the same core. As a result, a transition cycle analysis was performed on the 3-batch, nominal 84-reload case to prove that safety margins and reactor physics parameters were satisfied throughout the appropriate cycles.

8.1 REACTOR PHYSICS CONSIDERATIONS

As described in Section 4.4, the transition cycle analysis began with the equilibrium core of the 84-reload Zr case. From there, a cycle was run with one batch of SiC loaded into the core, then another, and finally, the last batch, leading to a core with only SiC-clad fuel with a 10% void. The identical loading pattern described in Figure 4.1 was utilized in this analysis. Figure 8.1 shows how fresh assemblies with SiC cladding replaced Zr-clad assemblies in three cycles.

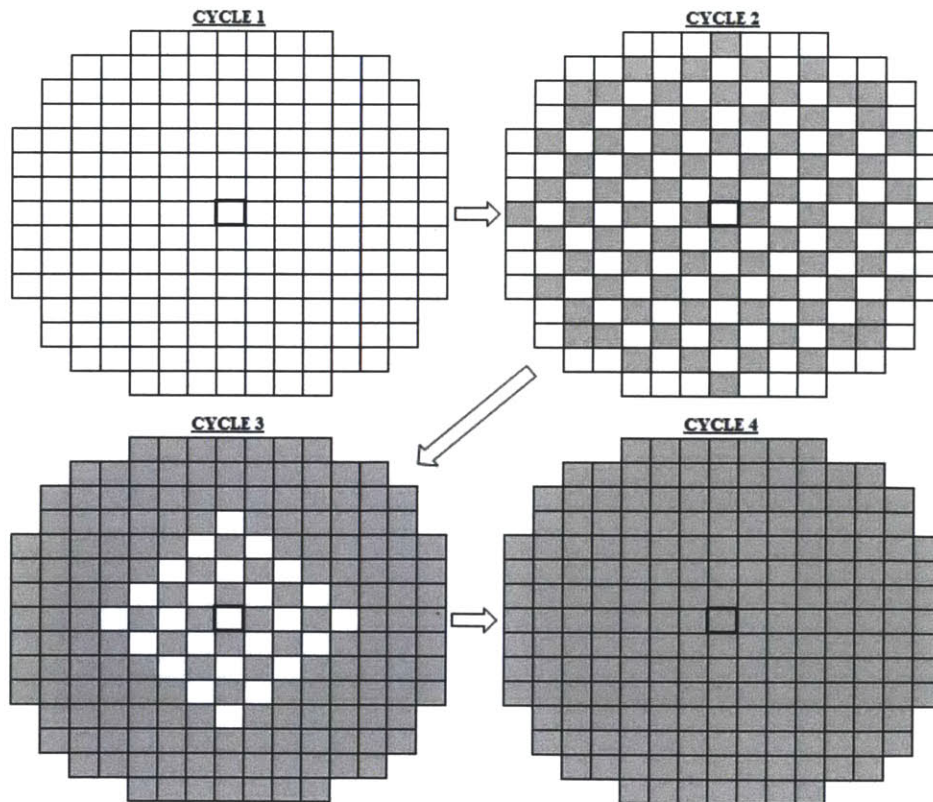


Figure 8.1 Transition Cycles from Initial Core (Cycle 1) with all Zr assemblies (white) to final core (Cycle 4) with all SiC assemblies (gray).

The most challenging cycle, in regards to satisfying the reactor physics limitations, occurred during the third cycle. At this stage, the majority of SiC-clad fuel was loaded on the periphery, creating a slightly higher $F_{\Delta h}$, but still lower than the initial core with only Zr cladding. Table 8.1 summarizes the reactor physics parameters.

Table 8.1 Reactor Physics parameters for the transition cycles

Cycle #	U^{235} w/o	Reload (MT)	B_c	Avg. B_D	EFPD	#IFBA Rods	Boron (ppm)	$F_{\Delta h}$	F_q	Max Pin Burnup
1	4.52	90.8	19.45	44.7	492	12208 (1X)	1477	1.533	1.801	66.8
2	4.66	86.9	20.31	46.7	492	12208 (1X)	1478	1.476	1.717	67.9
3	4.81	83.0	21.28	48.9	492	12208 (1X)	1510	1.518	1.765	68.4
4	4.80	81.8	21.60	49.6	493	12208 (1X)	1506	1.481	1.735	74.6

Compared to the equilibrium cores in Table 4.1, it should be noted that some of the core physics parameters have subtly changed compared to the transition core of the nominal 84-reload case with SiC cladding. This difference was primarily a result of slightly different power distributions and peaking factors in transition cycles 1 to 3. In addition, the average reload enrichments and amount of loaded fuel (in metric tons) varied slightly to account for the 10% void in the SiC-clad fuel. The reload fuel summaries for each cycle can be found in Appendix C. Cycle 3 also recorded a slightly higher average enrichment from additional SiC assemblies (with higher average enrichment per rod compared to Zr-clad rods) loaded on the periphery, which can be seen above in Figure 8.1. This additional enrichment acted to balance out the elevated leakage rates experienced in Cycle 3. Figures 8.2-8.4 show a few of the core physics parameters over the cycle length.

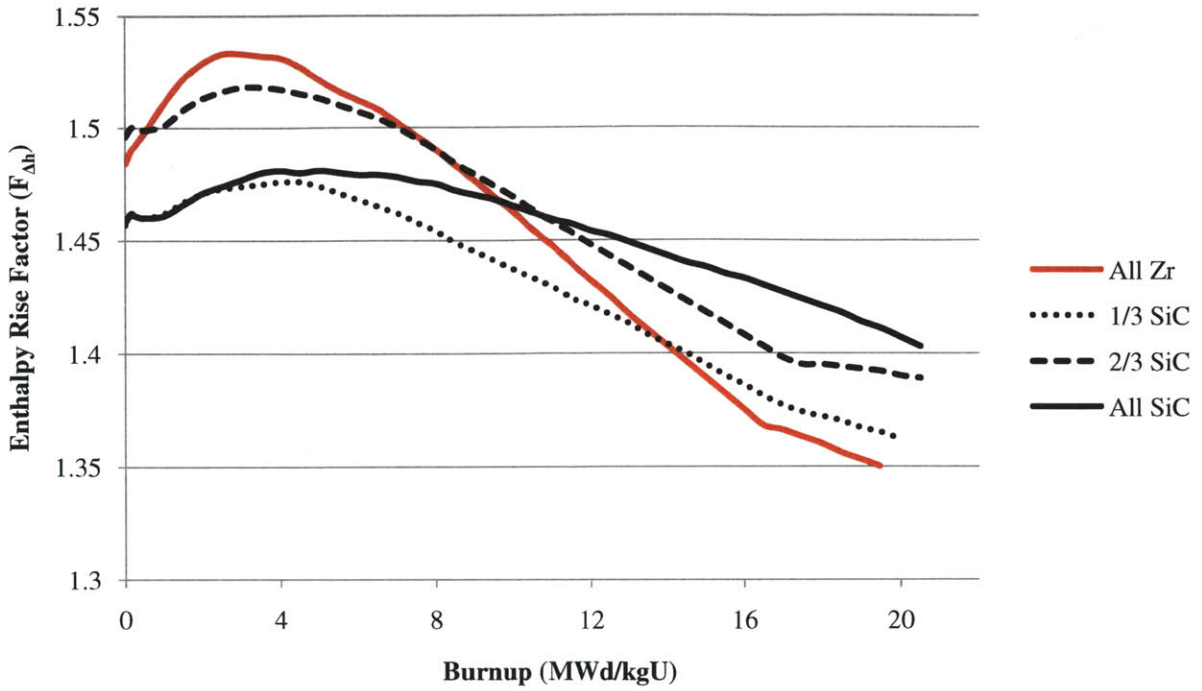


Figure 8.2 $F_{\Delta h}$ for all transition cycles.

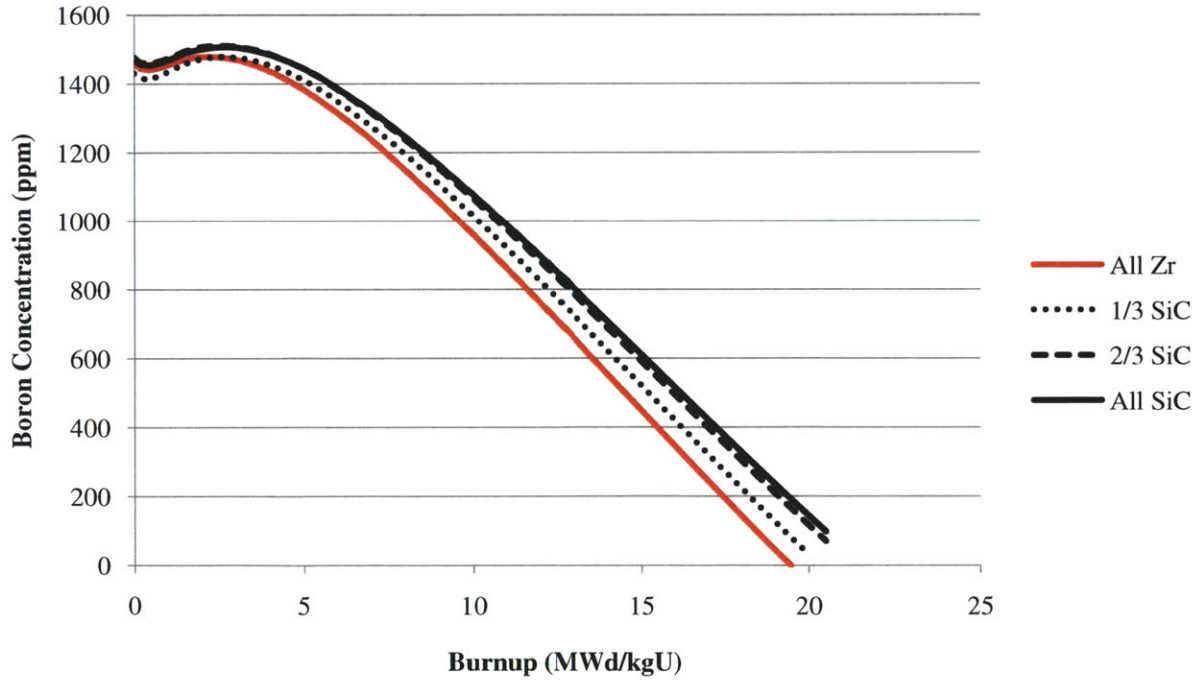


Figure 8.3 Boron concentration (ppm) for all transition cycles.

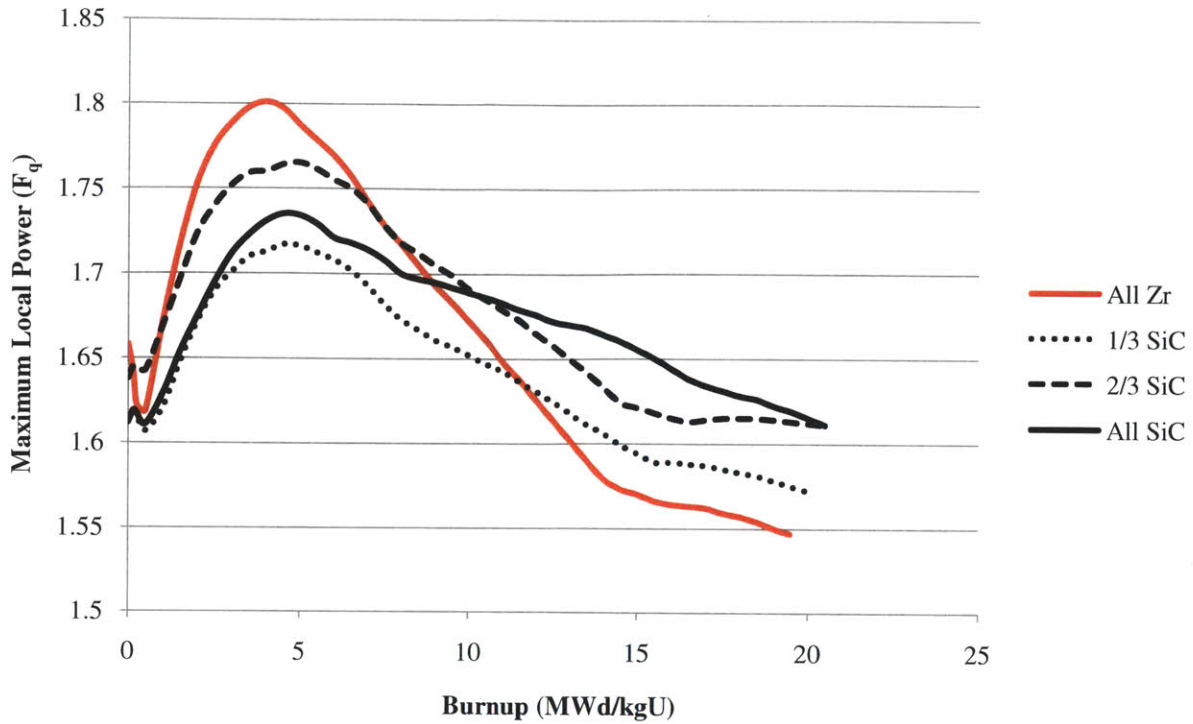


Figure 8.4 F_q for all transition cycles.

8.2 SAFETY PARAMETERS OF TRANSITION CYCLE

In addition to ensuring that all reactor physics parameters were appropriate, a perturbation analysis was performed to ensure that all coefficients and reactivity feedbacks were negative. These results can be seen in Figures 8.5 to 8.9. The shutdown margin was also calculated for each transition core, revealing an acceptable level of core reactivity in the event of a power loss or SCRAM.

Table 8.2 Shutdown margin for all transition cycles.

Cycle #	Uprate	Avg. w/o	SDM (pcm)		SDM (%)	
			BOL	EOL	BOL	EOL
1	0%	6.84	-2737	-1928	2.7	1.9
2	0%	5.74	-2652	-2009	2.7	2.0
3	0%	4.52	-2645	-2135	2.6	2.1
4	0%	4.79	-2752	-2201	2.8	2.2

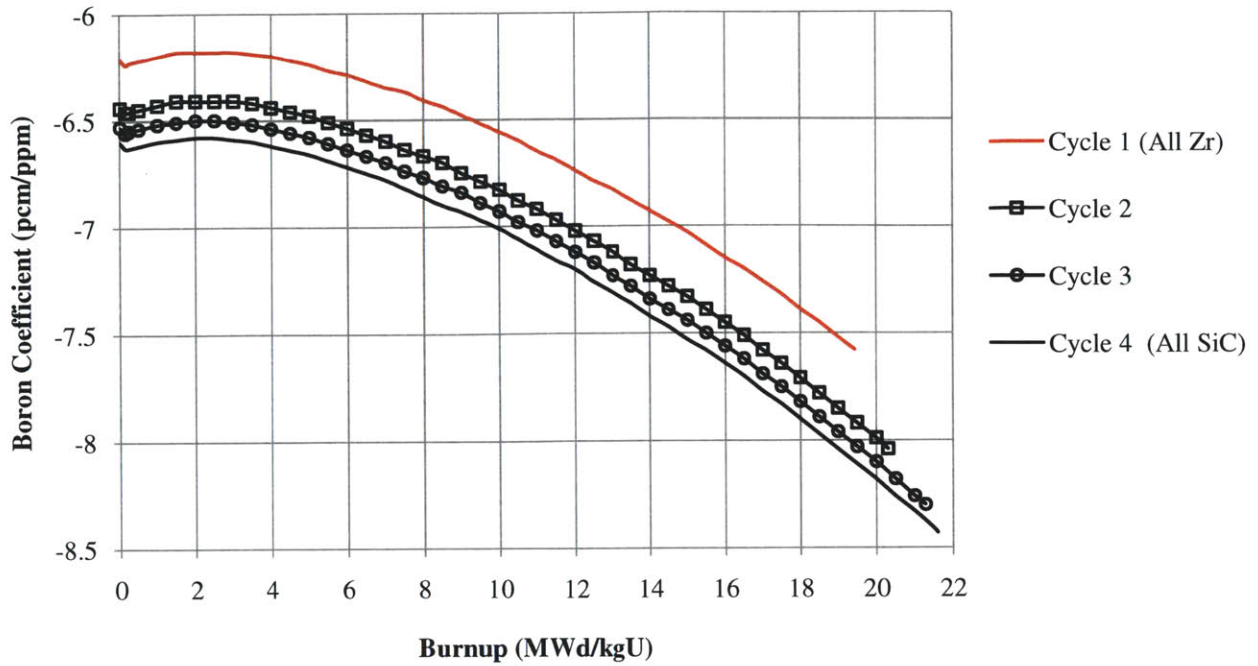


Figure 8.5 Boron coefficients for all transition cycles.

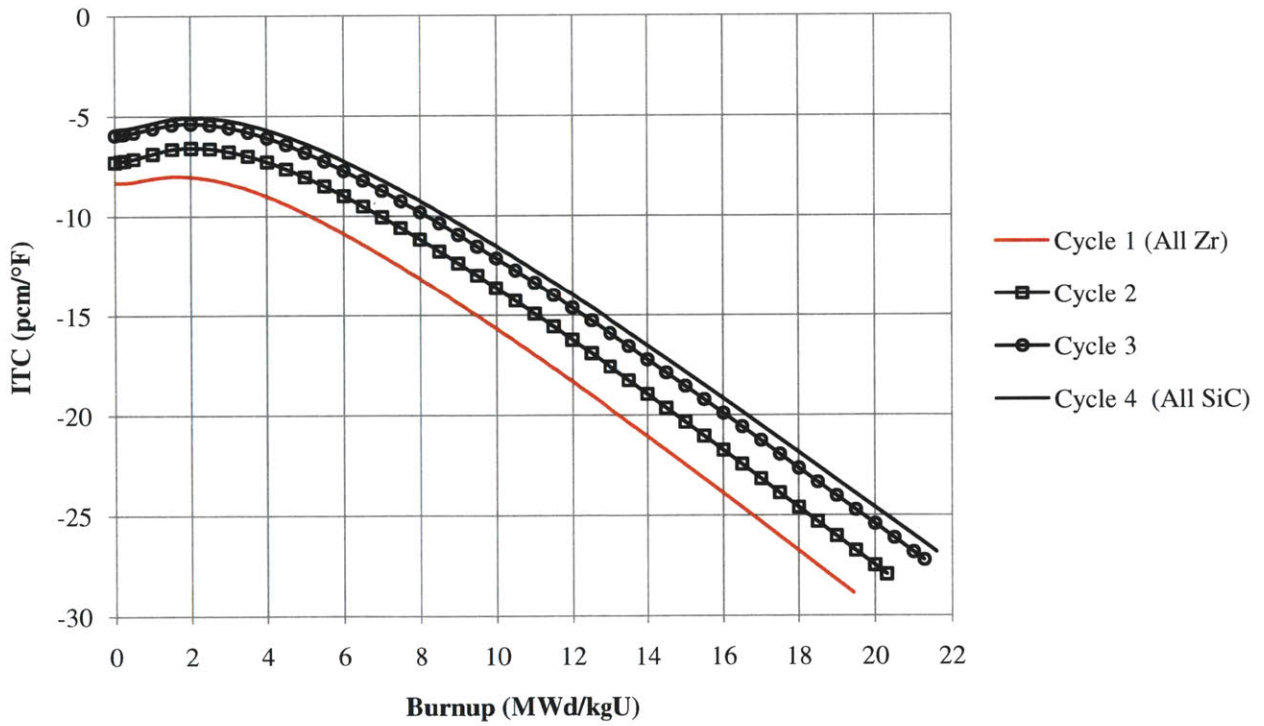


Figure 8.6 ITC for all transition cycles.

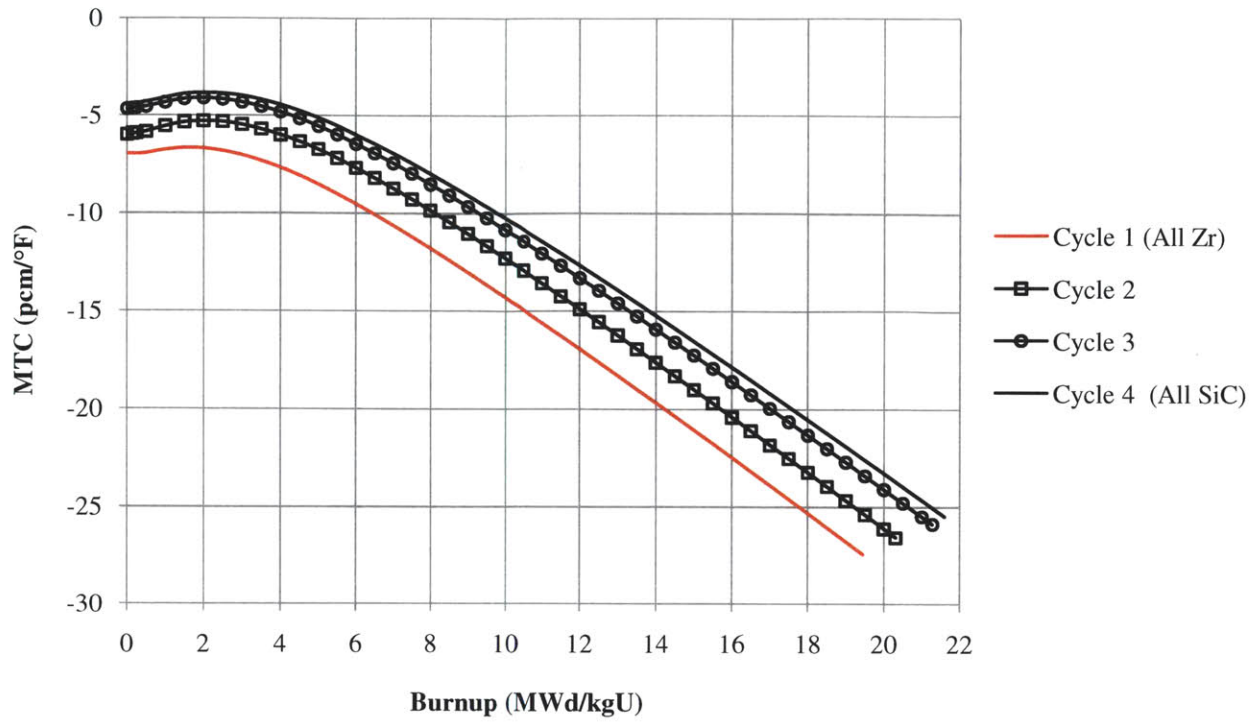


Figure 8.7 MTC for all transition cycles.

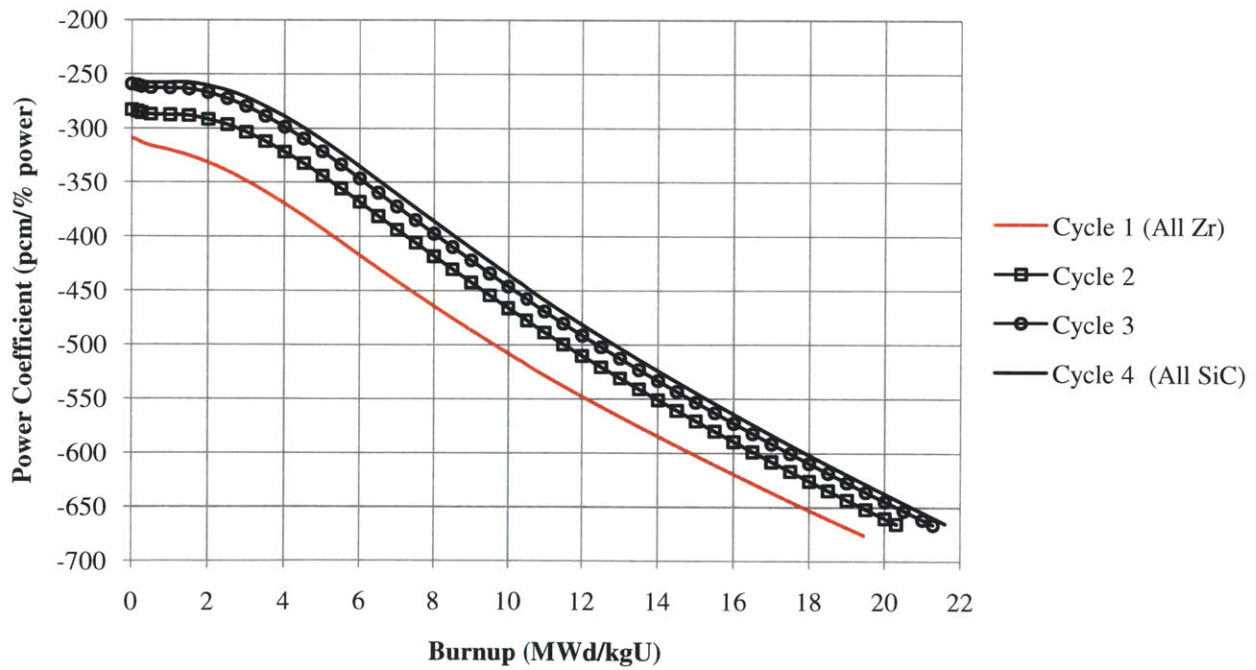


Figure 8.8 Power Coefficient for all transition cycles.

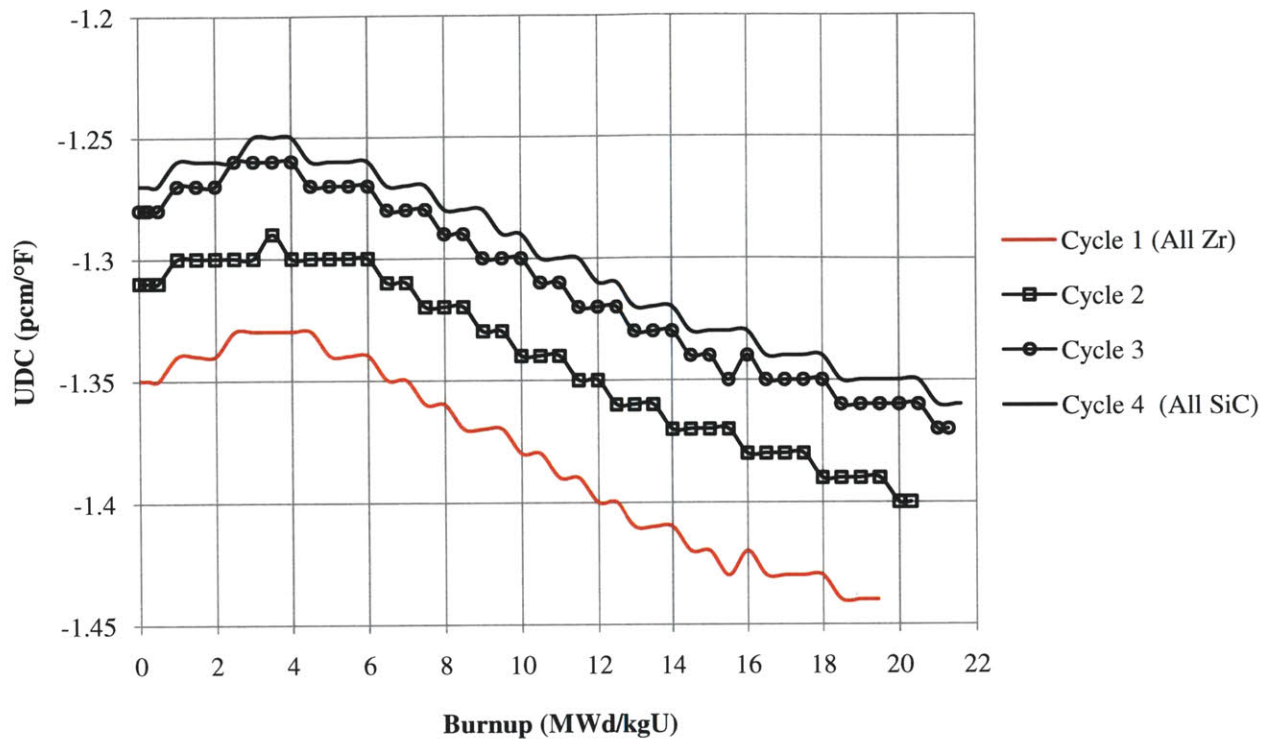


Figure 8.9 Uniform doppler coefficient for all transition cycles

9. SUMMARY AND RECOMMENDATIONS FOR FUTURE WORK

9.1 SUMMARY OF CORE DESIGN

Operating under standard PWR conditions, all 16 core designs demonstrated their ability to reach a desired cycle length of 18 or 24 months with traditional core management techniques. In addition, the guidelines set forth by the NRC were met throughout the entire cycle length, assuming of course that the maximum allowable burnup for assemblies and the peak rod were raised to accommodate SiC's robustness.

As for power uprates, SiC-clad fuel has an ability to satisfy the reactor physics guidelines, while still operating at the higher power level. The 10% uprated design met all reactor physics requirements and still possessed an adequate shutdown margin while the 20% uprated core design did not meet the shutdown margin at EOC, which will be discussed at greater lengths in the next section. As a result, economic gains could be made for utilities if they implemented silicon carbide cladding, by deriving more power from their plants.

As expected, SiC-clad fuel followed the same fuel management principles as the Zr-clad fuel. When the number of reloaded assemblies increased (assuming the same power level and desired cycle length), the enrichment decreased in a linear fashion. This can be seen in Table 4.1 and 5.1. However, it should be noted that the leakage, described in Figure 5.12, may pose a concern for actual implementation in two-year cycles. An industry core design usually targeted a leakage rate around 3%, but with some cores demonstrating leakages above 5%, this raises some concerns over the possible integrity of the pressure vessel being compromised over the years of plant operation.

Additionally, the high boron concentration of the 96-reload case exceeded the boron target value by over 17%. While the prolonged effects of soluble boron on SiC cladding is not yet known, it is likely to be more tolerant of borated water than Zr cladding. As was indicated in section 5.1, the concentration of BP in some cores would have to be increased, leading to re-shuffling, and re-optimization of the core. As with all these designs, an industry-level optimization program would be required to achieve the lowest peaking factors, leakage rate, and highest discharge burnup.

9.2 SUMMARY OF SAFETY PARAMETER ANALYSIS

The safety coefficients evaluated in this research consisted of calculating the shutdown margin and reactivity feedback and control mechanisms for each core. Every core successfully demonstrated negative reactivity coefficients, but the shutdown margin was a problem for the 20% uprated core and the core design with WABA rods. In the case of 20% uprate design, the shutdown margin dropped below the 1.3% limit by the EOC, but was well above the level at BOC. This indicated that the control rod material or position should be changed in order to possibly enhance the margin. However, previous work has shown that a 20% uprate may be a limiting power increase for some cores, and in this case, that result may prove true. As for the WABA core design, the shutdown safety margin was also well above the limit at BOC, but then dropped to less than 600 pcm at EOC. This could be improved by simply removing the WABA rods before the end of one cycle, but this would be an undesirable request since it would require additional outage days in the plant's operating cycle. As a result, an industry-level core optimization program should be utilized to decide the best location and implementation of the WABA rods.

9.3 FUTURE WORK

Several areas of future work have become more apparent after the present work. First, a loss-of-coolant (LOCA) analysis and any other transient analyses required for an NRC operating license should be performed. This will prove to the industry, at least through simulation, that there should be no unexpected consequences of introducing SiC into the core for a modest increase in the core power level. Second, all the models should be run again with the exact composition of the silicon carbide cladding (beyond simply stoichiometric SiC), including any isotopes of elements added for corrosion protection or other preventative measures. Unfortunately, this exact composition may not be known for a while, or at least until the end plugs can be welded together and a whole SiC-clad fuel rod (including fuel) is irradiated in the core for at least one cycle length. Third, the crud deposition rate caused by soluble boron interacting with SiC should be investigated. This will help set an upper limit on the amount of soluble boron that can be diluted into the water at BOC. And finally, access to an industry-level code should be given to allow these cores to produce optimized results, not just the best results

from trial-and-error. With this type of analysis, the full benefits of SiC could be understood before it is implemented into the fleet of current PWRs.

REFERENCES

- 10 CFR § 50.46, “Acceptance criteria for emergency core cooling systems for light-water nuclear power reactors,” U.S. Code of Federal Regulations (2007).
- Bahadir, T., “CMS-Link, User’s Manual,” Studsvik of America, Inc. (1997).
- Beccherle, J., Hejzlar, P., and Kazimi, M.S., “PWR Transition to a Higher Power Core Using Annular Fuel,” *Center for Advanced Energy Systems* MIT-NFC-TR-095 (September 2007).
- Berna, G.A., et. al., “FRAPCON-3: A Computer Code for the Calculation of Steady-State, Thermal-Mechanical Behavior of Oxide Fuel Rods for High Burnup,” NUREG/CR-6534 (1997).
- Carpenter, D.M., *Assessment of Innovative Fuel Designs for High Performance Light Water Reactors*, S.M. Thesis, Massachusetts Institute of Technology (2006).
- Carpenter, D.M., et. al., “An Assessment of Silicon Carbide as a Cladding Material for Light Water Reactors,” *Center for Advanced Nuclear Energy Systems*, MIT-ANP-TR-132 (2010).
- Cochran, R.G. and Tsoulfanidis, N. The Nuclear Fuel Cycle: Analysis and Management. American Nuclear Society, La Grange Park, IL (1990).
- Cooper, K., “EWI Developments in Silicon Carbide Joining,” EPRI-Sponsored Meeting on Silicon Carbide for Nuclear Applications, Orlando, FL (September 2010).
- DiGiovine, A.S. and Rhodes, J.D., “SIMULATE-3 User’s Manual,” Studsvik of America, Inc. (1995).
- Edenius, M., et.al., “CASMO-4: A Fuel Assembly Burnup Program, User’s Manual,” Studsvik of America, Boston, MA (1995).
- EPRI, “Optimum Cycle Length and Discharge Burnup for Nuclear Fuel: Phase I: Results Achievable Within the 5% Enrichment Limit,” EPRI Report 1003133, Palo Alto, CA (2001).
- EPRI, “Optimum Cycle Length and Discharge Burnup for Nuclear Fuel: Phase II: Results Achievable with Enrichments Greater than 5.0 w/o,” EPRI Report 1003217, Palo Alto, CA, and U.S. Department of Energy, Washington, D.C. (2002).
- EPRI, “Parametric Study of Front-End Nuclear Fuel Cycle Costs Using Reprocessed Uranium,” EPRI, Palo Alto, CA (2009).

Feng, B., Kazimi, M.S., and Hejzlar, P., “Innovative Fuel Designs for High Power Density Pressurized Water Reactor,” *Center for Advanced Energy Systems* MIT-NFC-TR-075 (September 2005).

Feng, B., Hejzlar, P., and Kazimi, M.S., “On the Use of High Performance Annular Fuel in PWRs,” *Center for Advanced Energy Systems* MIT-NFC-TR-100 (June 2008).

Franceschini F. and Lahoda, E.J., “Neutronic Behavior and Impact on Fuel Cycle Cost of Silicon Carbide Clad,” 2010 ANS Winter Meeting, Las Vegas, NV (2010).

Griffith, G., and Garnier, J., “INL Program Plan Overview: CMC Channel Box,” EPRI-Sponsored Meeting on Silicon Carbide for Nuclear Applications, Orlando, FL (September 2010).

Johnson, S.C., “SiC/SiC Bond Development for Application to SiC End Plugs,” EPRI-Sponsored Meeting on Silicon Carbide for Nuclear Applications, Orlando, FL (September 2010).

Kazimi, M.S., “PWR Cores with Silicon Carbide Cladding,” *Center for Advanced Nuclear Energy Systems* (December 2010a).

Kazimi, M.S., Hejzlar, P., et. al., “Evaluation of High Power Density Annular Fuel for Korean OPR-1000 Reactor: Final Report,” *Center for Advanced Nuclear Energy Systems* MIT-NFC-TR-114 (March 2010b).

Locke, D.H., “Review of experience with water reactor fuels 1968-1973,” *Nuclear Engineering and Design* **33** (1975) 94.

Long, Y., “Modeling the Performance of High Burnup Thoria and Urania PWR Fuel,” Ph. D. thesis, MIT Department of Nuclear Engineering, 2002.

NRC, “Nuclear Design,” NUREG-0800, Section 4.3 (March 2007).

NRC, *Extended Burnup Evaluation, BAW-10186-A Topical Report*, U.S. Nuclear Regulatory Commission (1997).

Olander, D.R., “Light water reactor fuel design and performance,” *Encyclopedia of Materials: Science and Technology*, Elsevier Science (2001) 4490.

Ott, L.J. and Spellman, D.J., “Advanced Fuel/Cladding Testing Capabilities in the ORNL High Flux Isotope Reactor,” EPRI-Sponsored Meeting on Silicon Carbide for Nuclear Applications, 30 September 2010.

- Rusch, C.A., "Nuclear fuel performance: Trends, remedies, and challenges," *Journal of Nuclear Materials* **383** (2008) 41.
- Seabrook, "Application for Stretch Power Uprate," License Amendment Request 04-03 (March 2004).
- Seabrook, Revision 11 to UFSAR, Chapter 4, ML071430575, Table 4.3-1 (March 2007).
- Snead, L.L., et al., "Handbook of SiC properties for fuel performance modeling," *Journal of Nuclear Materials* **371** (2007) 329.
- Studsvik Scandpower, "CASMO-4E: Extended Capability CASMO-4, User's Manual," Studsvik Scandpower (2009).
- Thomas, D.E., "History of zircaloy development," *Transactions of the American Nuclear Society* **18** (1974) 111.
- Todreas, N.E., and Kazimi, M.S. Nuclear Systems II: Elements of Thermal Hydraulic Design. Taylor & Francis, Hemisphere, NY (1990).
- Westinghouse, "Zirconium Diboride Integral Fuel Burnable Absorbers," Online available http://westinghousenuclear.com/Products_&_Services/docs/flysheets/NF-FE-0028.pdf (2006).
- Yagnik, S., "Falcon-based Assessment of SiC-clad Fuel Rod," EPRI-Sponsored Meeting on Silicon Carbide for Nuclear Applications, Orlando, FL (September 2010).
- Yang, R., et al., "Fuel R & D to improve fuel reliability," *Journal of Nuclear Science and Technology* **43** (2006) 951.
- Yueh, K., "SiC For Nuclear Applications: Core Design Feasibility Evaluation," EPRI-Sponsored Meeting on Silicon Carbide for Nuclear Applications, Orlando, FL (September 2010a).
- Yueh, K., Carpenter, D., and Feinroth, H., "Clad in Clay," *Nuclear Engineering* (2010b).

APPENDIX A: BURNABLE POISON LAYOUTS

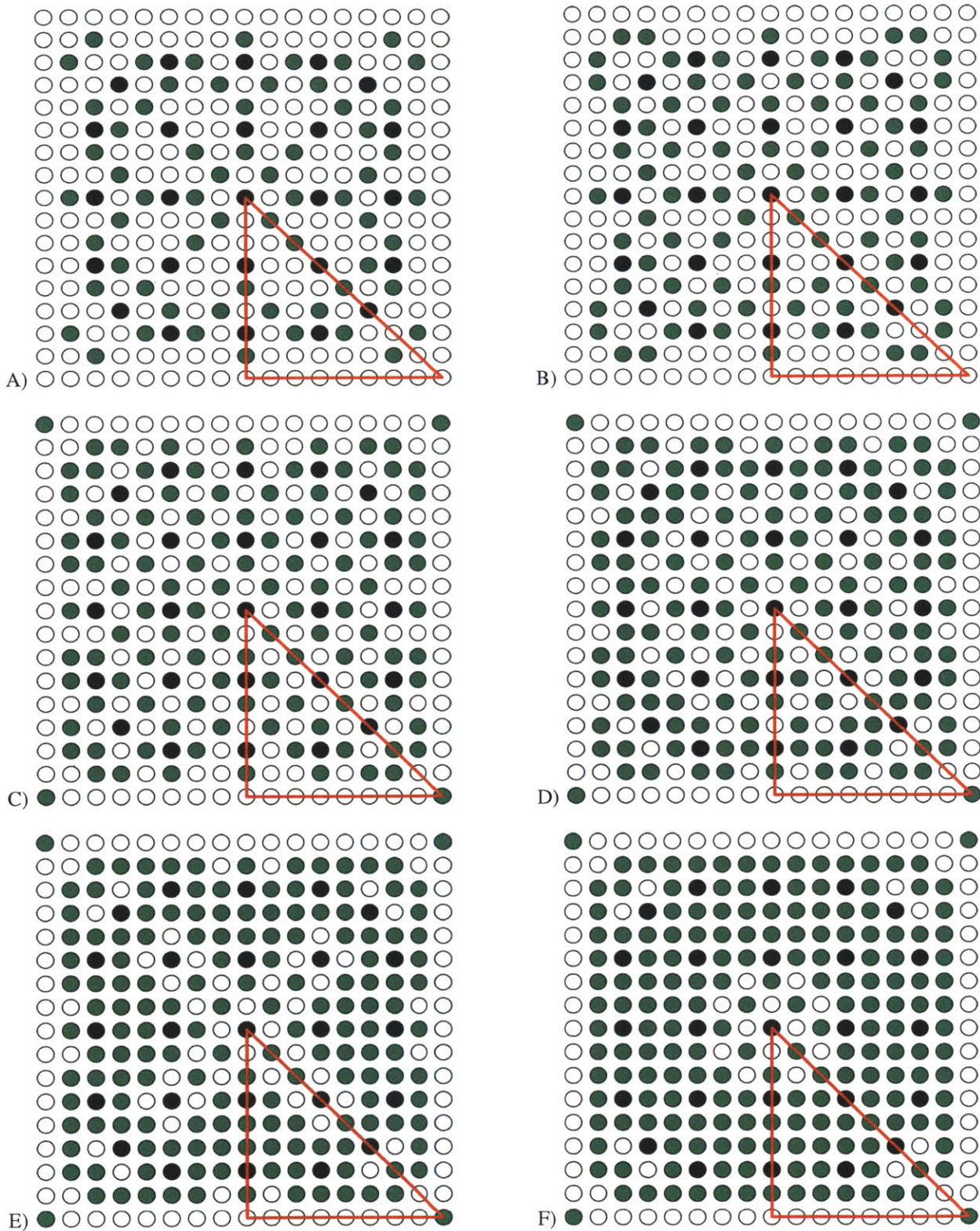


Figure A.1 A) 64-IFBA B) 80-IFBA C) 104-IFBA D) 128-IFBA E) 156-IFBA F) 180-IFBA rod layouts.

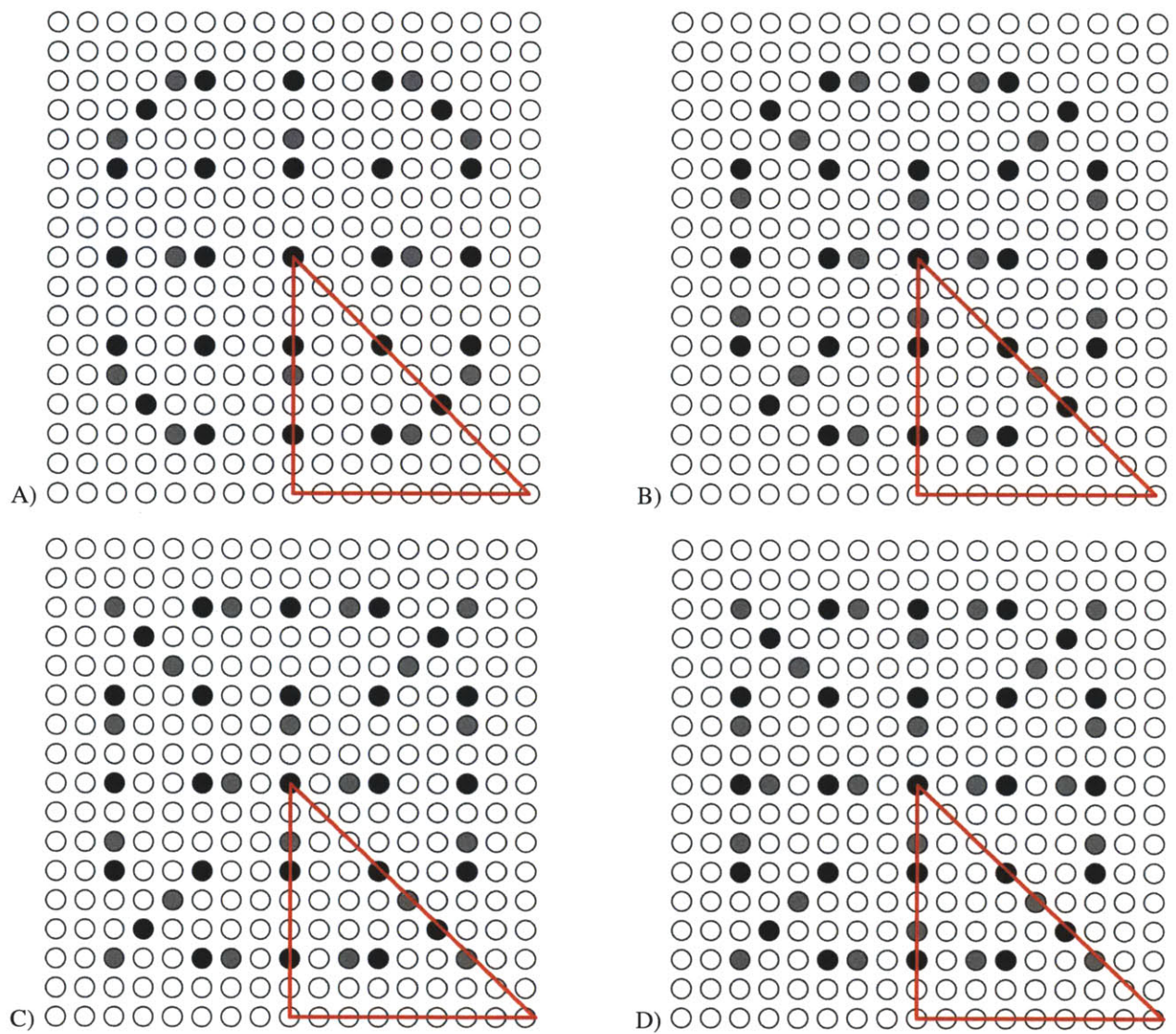


Figure A.2 A) 12-Gd B) 16-Gd C) 20-Gd D) 24-Gd rod layout.

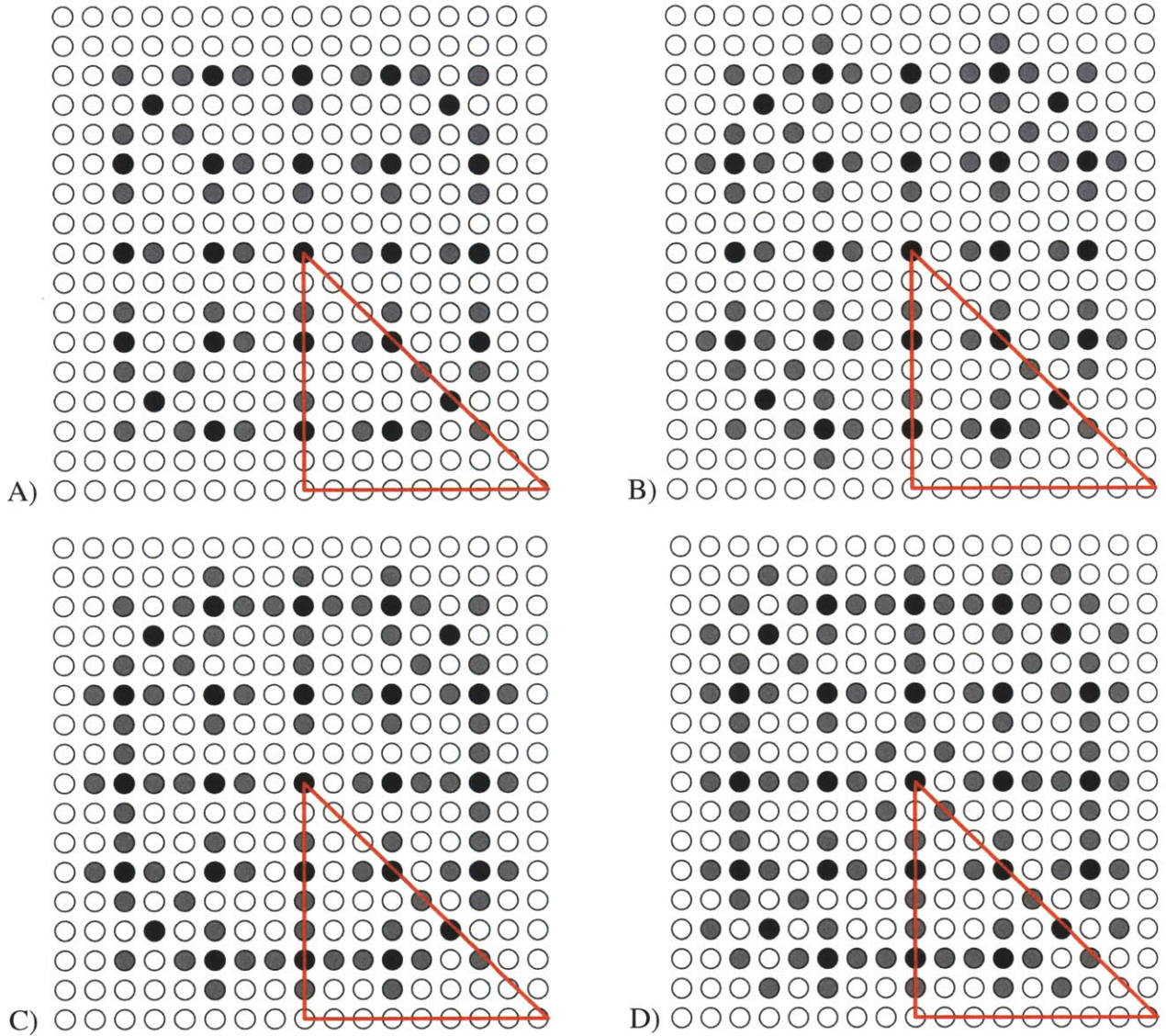


Figure A.3 A) 40-Er B) 56-Er C) 72-Er D) 84-Er rod layout

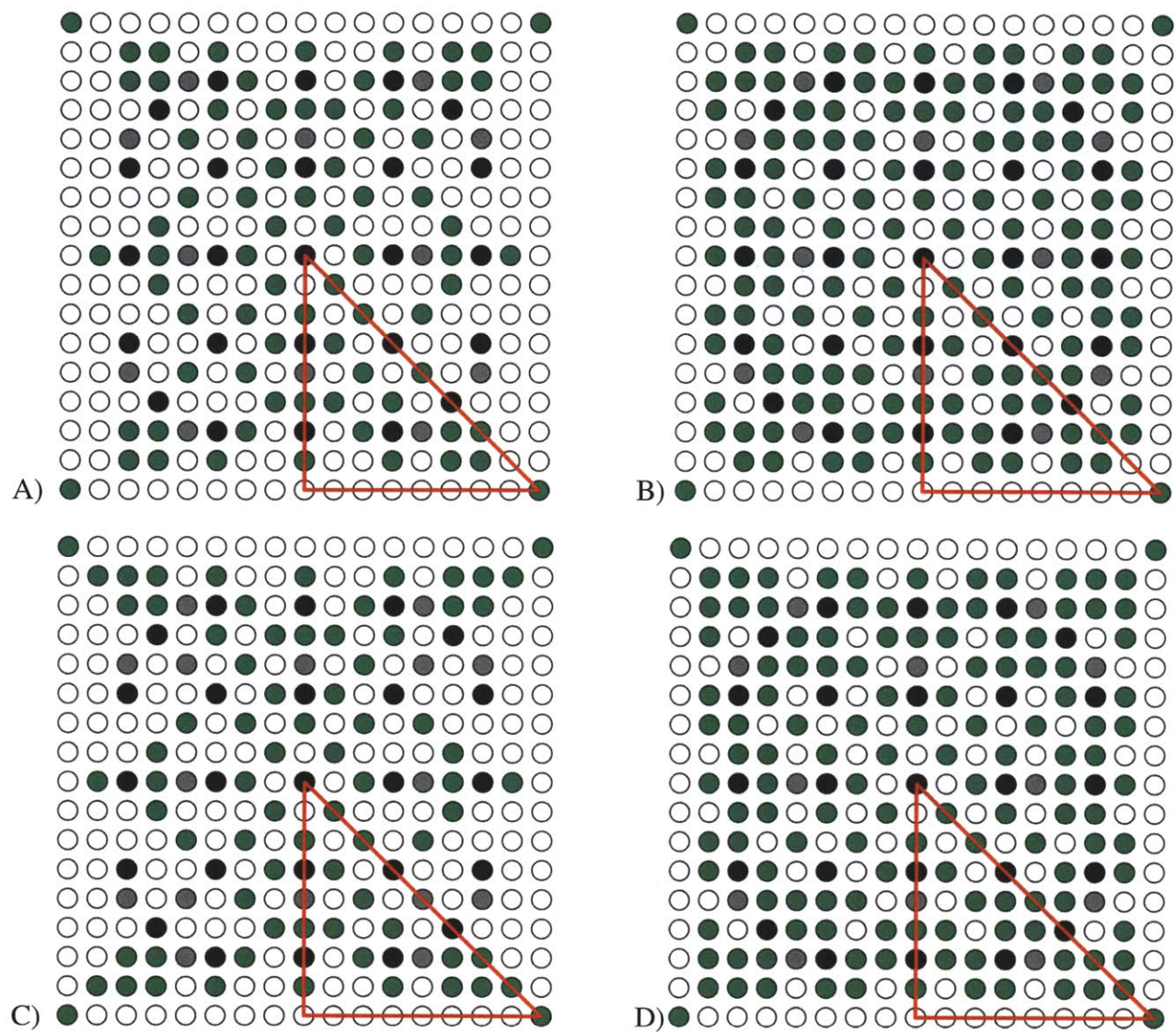


Figure A.4 A) 12-Gd, 104 IFBA B) 12-Gd, 128 IFBA C) 16-Gd, 104 IFBA D) 16-Gd, 128 IFBA rod layouts.

APPENDIX B: COMPUTER-BASED MODELING INPUT FILES & FLOWCHARTS

```

* FUEL SEGMENT: W44I104L

ITL * STANDARD WESTINGHOUSE PWR ASSEMBLY, 17X17 LATTICE

***** STATE POINT PARAMETERS *****
TFU=905 TMO=585 BOR=600 VOI=0.0
SIM 'W44I104L'

***** OPERATING PARAMETERS *****
PRE 155.1296 * CORE PRESSURE, bars
PDE 109.926111 'KWL' * POWER DENSITY, kW/liter

***** MATERIAL COMPOSITIONS *****
FUE 1 10.47/4.4
FUE 2 10.47/4.4
MI1 2.39 1.0E-06/14000=62.0 6000=37.0 8000=1.0 * SiC
SPA 10.81934 0.1800E-4,,8.154/718=84.59 347=15.41
BP3 //5010=0.61811
BP2 //5010=6.03

***** GEOMETRY SPECIFICATION *****
PWR 17 1.26 21.5
PIN 1 0.129 0.410 0.418 0.475/"AIR" "1" "AIR" "MI1"
PIN 2 0.129 0.410 0.4107 0.418 0.475/"AIR" "2" "BP3" "AIR" "MI1"
PIN 5 0.5690 0.6147/'COO' 'MI1' * GUIDE TUBE
PIN 9 0.5690 0.6147/'COO' 'MI1'
PIN 9 0.286 0.339 0.353 0.404 0.418 0.484 0.569 0.612/"MOD" "MI1" "AIR" "BP2"
"AIR" "MI1" "MOD" "MI1"//1 "WAB" "ROD"
PIN 9 0.4331 0.4369 0.4839 0.5690 0.6147/'AIC' 'AIR' 'CRS' 'COO' 'MI1'
//1 'RCC' 'ROD'

LPI 5
  1 2
  2 1 2
  9 2 1 9
  2 1 2 1 2
  1 2 1 2 1 9
  9 1 2 9 2 1 2
  2 1 1 2 1 2 2 1
  1 1 1 1 1 1 1 1 2

***** BASE CASE WITH INSTANTANEOUS BRANCHES *****
DEP -100
S3C 'CLD' 'VOI'
STA
END

```

Figure B.1 Example Input File for CASMO-4E.

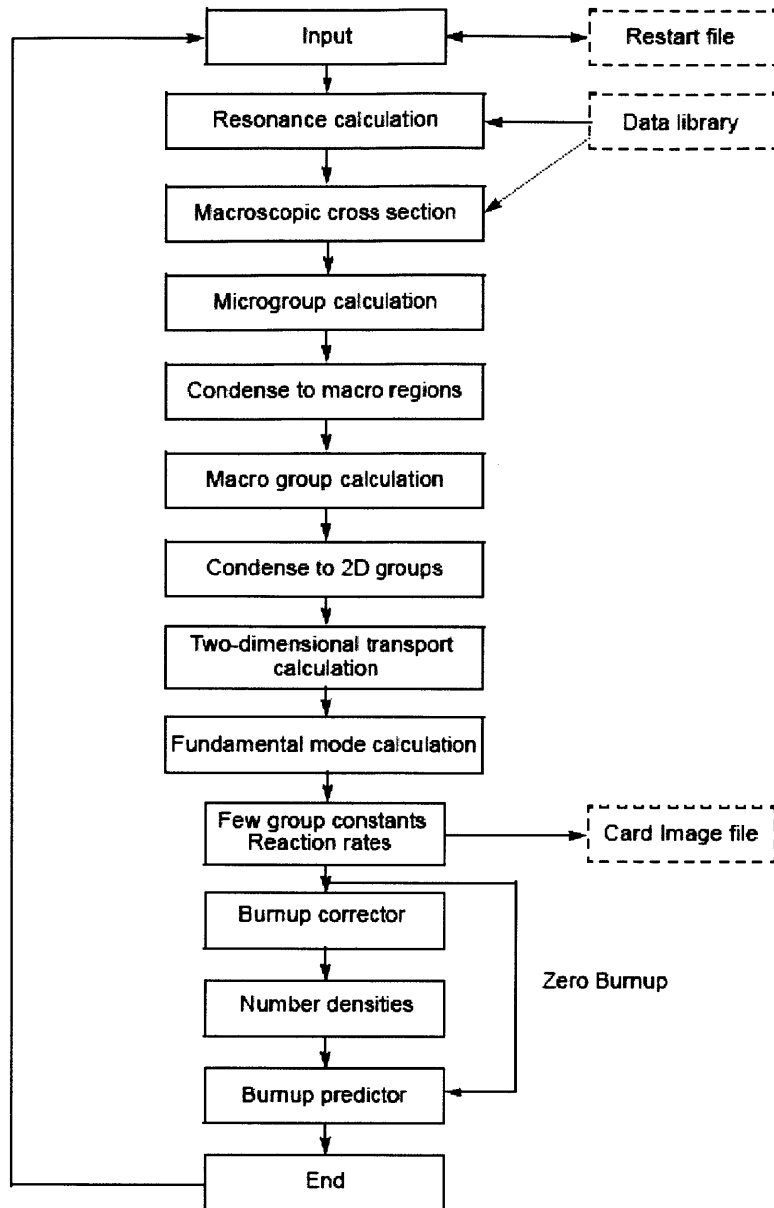


Figure B. 2 CASMO-4E flow diagram.

```

***** BASE CASE WITH INSTANTANEOUS BRANCHES *****
DEP -100
STA
COE ,,0 0.5 1 2 3 4 5 6 7 8 9 10 15 20 22.5 25 27.5 30 32.5 35 37.5 40
+ 42.5 45 47.5 50 52.5 55 57.5 60 62.5 65 67.5 70
TMO 550 585 600 615 TFU 905 1200 1500
TMO 550 585 600 615 BOR 0 1200 1800
TMO 550 585 600 615 ROD 'RCC'
CLD 293 350 450 TFU 293 450 550 TMO 293 350 450 500
SDC 100 100 100 100 100 1691.5 6574.5 8766.0 26298.0 43830.0/'DT'

TTL * LOW FUEL TEMPERATURE HISTORY
TFU=550 TMO=585 BOR=600 VOI=0.0
DEP -100
STA
COE ,,0 0.5 1 2 3 4 5 6 7 8 9 10 15 20 22.5 25 27.5 30 32.5 35 37.5 40
+ 42.5 45 47.5 50 52.5 55 57.5 60 62.5 65 67.5 70
TFU 905
*
TTL * HIGH FUEL TEMPERATURE HISTORY
TFU=1500 TMO=585 BOR=600 VOI=0.0
DEP -100
STA
COE ,,0 0.5 1 2 3 4 5 6 7 8 9 10 15 20 22.5 25 27.5 30 32.5 35 37.5 40
+ 42.5 45 47.5 50 52.5 55 57.5 60 62.5 65 67.5 70
TFU 905
*
TTL * LOW MODERATOR HISTORY
TFU=905 TMO=550 BOR=600 VOI=0.0
DEP -100
STA
COE ,,0 0.5 1 2 3 4 5 6 7 8 9 10 15 20 22.5 25 27.5 30 32.5 35 37.5 40
+ 42.5 45 47.5 50 52.5 55 57.5 60 62.5 65 67.5 70
TMO 585
*
TTL * HIGH MODERATOR HISTORY
TFU=905 TMO=615 BOR=600 VOI=0.0
DEP -100
STA
COE ,,0 0.5 1 2 3 4 5 6 7 8 9 10 15 20 22.5 25 27.5 30 32.5 35 37.5 40
+ 42.5 45 47.5 50 52.5 55 57.5 60 62.5 65 67.5 70
TMO 585
*
TTL * LOW BORON HISTORY DEPLETION
TFU=905 TMO=585 BOR=0.0 VOI=0.0
DEP -100
STA
COE ,,0 0.5 1 2 3 4 5 6 7 8 9 10 15 20 22.5 25 27.5 30 32.5 35 37.5 40
+ 42.5 45 47.5 50 52.5 55 57.5 60 62.5 65 67.5 70
BOR 600
*
TTL * HIGH BORON HISTORY DEPLETION
TFU=905 TMO=585 BOR=1800 VOI=0.0
DEP -100
STA
COE ,,0 0.5 1 2 3 4 5 6 7 8 9 10 15 20 22.5 25 27.5 30 32.5 35 37.5 40
+ 42.5 45 47.5 50 52.5 55 57.5 60 62.5 65 67.5 70
BOR 600

END

```

```

-----
***** BASE CASE WITH INSTANTANEOUS BRANCHES *****
DEP -100
S3C 'CLD' 'VOI'
STA
END

```

Figure B.3 The coding above (in black) shows the previous amount of CASMO coding required by TABLES to generate the same library that is now generated by CMS-LINK with much less CASMO coding (in red).

```

'COM' CMS-LINK INPUT FILE
'COM' by Jacob Dobisesky
'COM' Go Navy

'TTL' 'PWR - SiC 84 Nominal EQUILIBRIUM LIBRARY ' /
'NEW' '/home/jacobd/CMSLink/cms.84nom.lib' / Library Name for SIM3

'COM' MAJOR FLAG DEFAULT = 0 IS HOT LIBRARY
'CAS' '/home/jacobd/IFBA/c4.S18.55I156L_s3c.cax' /
'STA' /
'CAS' '/home/jacobd/IFBA/c4.S18.44I156L_s3c.cax' /
'STA' /
'CAS' '/home/jacobd/IFBA/c4.S18.50I128L_s3c.cax' /
'STA' /
'CAS' '/home/jacobd/IFBA/c4.S18.55I128L_s3c.cax' /
'STA' /
'CAS' '/home/jacobd/Blankets/c4.S18.320.cax' /
'STA' /
'CAS' '/home/jacobd/Blankets/c4.S18.440.cax' /
'STA' /
'CAS' '/home/jacobd/Blankets/c4.S18.500.cax' /
'STA' /
'CAS' '/home/jacobd/Blankets/c4.S18.550.cax' /
'STA' /

'COM' HOT REFLECTOR SEGMENTS
'CAS' '/home/jacobd/Reflectors/c4.SRADREF500.cax' 'SRADREF',, 'RAD' /
'STA' /
'CAS' '/home/jacobd/Reflectors/c4.SBOTREF500.cax' 'SBOTREF',, 'BOT' /
'STA' /
'CAS' '/home/jacobd/Reflectors/c4.STOPREF500.cax' 'STOPREF',, 'TOP' /
'STA' /

'COM' COLD LIBRARY
'COM' MAJOR FLAG = 1
'CAS' '/home/jacobd/IFBA/c4.S18.55I156L_s3c.cax' ,, 1 / *
'STA' /
'CAS' '/home/jacobd/IFBA/c4.S18.44I156L_s3c.cax' ,, 1 / *
'STA' /
'CAS' '/home/jacobd/IFBA/c4.S18.50I128L_s3c.cax' ,, 1 / *
'STA' /
'CAS' '/home/jacobd/IFBA/c4.S18.55I128L_s3c.cax' ,, 1 / *
'STA' /
'CAS' '/home/jacobd/Blankets/c4.S18.320.cax' ,, 1 / *
'STA' /
'CAS' '/home/jacobd/Blankets/c4.S18.440.cax' ,, 1 / *
'STA' /
'CAS' '/home/jacobd/Blankets/c4.S18.500.cax' ,, 1 / *
'STA' /
'CAS' '/home/jacobd/Blankets/c4.S18.550.cax' ,, 1 / *
'STA' /

'COM' COLD REFLECTOR SEGMENTS
'CAS' '/home/jacobd/Reflectors/c4.SRADREF500.cax' 'SRADREF',1, 'RAD' /
'STA' /
'CAS' '/home/jacobd/Reflectors/c4.SBOTREF500.cax' 'SBOTREF',1, 'BOT' /
'STA' /
'CAS' '/home/jacobd/Reflectors/c4.STOPREF500.cax' 'STOPREF',1, 'TOP' /
'STA' /
'END' /

```

Figure B. 4 Example input file for CMS-Link.

```

'COM' JACOB DOBISESKY
'COM' 18 MONTH CYCLE ANALYSIS
'COM' TYPICAL WESTINGHOUSE 4-LOOP PWR WITH
'COM' 84 RELOAD FUEL ASSEMBLIES WITH 3.2 w/o AXIAL BLANKETS
'COM' SIC CLAD FUEL & BLANKET HAS 10% CENTER VOID
'COM' CYCLE 10: EQUILIBRIUM CYCLE CORE

'DIM.PWR' 15/
'DIM.CAL' 24 2 2/ * 24 AXIAL NODES, QUARTER CORE, 2X2 NODES PER ASSY
'DIM.DEP' 'EXP' 'SAM' 'HTMO' 'HBOR' 'HTFU' 'PIN' 'EBP' / * DEPLETION ARGUMENTS

'TIT.CAS' 'CYCLE 10 (EQC) '/

'FUE.NEW' 'TYPE01' 'M101' 16 02/ * FRESH, S55I156L
'FUE.NEW' 'TYPE01' 'M117' 16 03/ * FRESH, S44I156L
'FUE.NEW' 'TYPE01' 'M133' 20 04/ * FRESH, S44I156L
'FUE.NEW' 'TYPE01' 'M153' 16 05/ * FRESH, S50I128L
'FUE.NEW' 'TYPE01' 'M169' 16 06/ * FRESH, S55I128L

'COM' -R- -P- -N- -M- -L- -K- -J- -H- -G- -F- -E- -D- -C- -B- -F-
'FUE.SER' 4/
01 1 L105 L148 L113 M175 L112 L147 L104
02 1 L121 L129 M157 L165 M165 L159 M164 L164 M156 L128 L120
03 1 L122 M171 M181 L140 M149 L181 M135 L180 M148 L139 M180 M170 L119
04 1 L130 M182 L135 M141 L173 M129 K118 M128 L172 M140 L134 M179 L127
05 1 L106 M158 L141 M142 L155 M121 K173 M107 K172 M120 L154 M139 L138 M155 L103
06 1 L149 L166 M150 L174 M122 K135 M113 K102 M112 K134 M119 L171 M147 L163 L146
07 1 L114 M166 L182 M130 K174 M114 K155 M103 K154 M111 K171 M127 L179 M163 L111
08 1 M176 L160 M136 K119 M108 K103 M104 K177 M102 K101 M106 K117 M134 L158 M174
09 1 L115 M167 L183 M131 K175 M115 K156 M101 K153 M110 K170 M126 L178 M162 L110
10 1 L150 L167 M151 L175 M123 K136 M116 K104 M109 K133 M118 L170 M146 L162 L145
11 1 L107 M159 L142 M143 L156 M124 K176 M105 K169 M117 L153 M138 L137 M154 L102
12 1 L131 M183 L136 M144 L176 M132 K120 M125 L169 M137 L133 M178 L126
13 1 L123 M172 M184 L143 M152 L184 M133 L177 M145 L144 M177 M169 L118
14 1 L124 L132 M160 L168 M168 L157 M161 L161 M153 L125 L117
15 1 L108 L151 L116 M173 L109 L152 L101
0 0

'RES' '/home/jacobd/RES/s3.S1884.c9t.res' 20000/

'CRD.GRP' 1
4*0 00 00 00 00 00 00 00 00 4*0
2*0 00 9 00 3 00 2 00 3 00 9 00 2*0
0 00 00 00 6 00 8 00 8 00 7 00 00 00 0
0 9 00 1 00 00 00 5 00 00 00 1 00 9 0
00 00 7 00 4 00 00 00 00 00 4 00 6 00 00
00 3 00 00 00 2 00 4 00 2 00 00 00 3 00
00 00 8 00 00 00 00 00 00 00 00 8 00 00
00 2 00 5 00 4 00 1 00 4 00 5 00 2 00
00 00 8 00 00 00 00 00 00 00 00 8 00 00
00 3 00 00 00 2 00 4 00 2 00 00 00 3 00
00 00 6 00 4 00 00 00 00 00 4 00 7 00 00
0 9 00 1 00 00 00 5 00 00 00 1 00 9 0
0 00 00 00 7 00 8 00 8 00 6 00 00 00 0
2*0 00 9 00 3 00 2 00 3 00 9 00 2*0
4*0 00 00 00 00 00 00 00 4*0/
'CRD.ZON' 1 1 'ARO' 0 0.0 0 365.76/ * NO CONTROL ROD
'CRD.ZON' 2 1 'AIC' 0 0.0 0 7.57 10 365.76/ * AIC CONTROL ROD
'CRD.DAT' 226 1.585/
'CRD.TYP' 1
4*0 1 1 1 1 1 1 1 4*0
2*0 1 02 1 02 1 02 1 02 1 02 1 2*0
0 1 1 1 02 1 02 1 02 1 1 1 0

```



```

0      02  1 02  1  1  1 02  1  1  1 02  1 02      0
1  1 02  1 02  1  1  1  1  1 02  1 02  1  1
1 02  1  1  1 02  1 02  1 02  1  1  1 02  1
1  1 02  1  1  1  1  1  1  1  1  1 02  1  1
1 02  1 02  1 02  1 02  1 02  1 02  1 02  1
1  1 02  1  1  1  1  1  1  1  1  1 02  1  1
1 02  1  1  1 02  1 02  1 02  1  1  1 02  1
1  1 02  1 02  1  1  1  1  1 02  1 02  1  1
0      02  1 02  1  1  1 02  1  1  1 02  1 02      0
0      1  1  1 02  1 02  1 02  1 02  1  1  1      0
2*0      1 02  1 02  1 02  1 02  1 02  1      2*0
4*0      1  1  1  1  1  1  1  1      4*0/
'CRD.SEQ'  1  000 000 000 000 115 226 226 226 226 226/ * CD
'CRD.SEQ'  2  000 000 000 000 115 226 226 226 226 226/ * CC
'CRD.SEQ'  3  000 000 115 226 226 226 226 226 226 226/ * CB
'CRD.SEQ'  4  000 115 226 226 226 226 226 226 226 226/ * CA
'CRD.SEQ'  5  226 226 226 226 226 226 226 226 226 226/ * SE
'CRD.SEQ'  6  226 226 226 226 226 226 226 226 226 226/ * SD
'CRD.SEQ'  7  226 226 226 226 226 226 226 226 226 226/ * SC
'CRD.SEQ'  8  226 226 226 226 226 226 226 226 226 226/ * SB
'CRD.SEQ'  9  226 226 226 226 226 226 226 226 226 226/ * SA
'CRD.SEQ' 10  226 226 226 226 226 226 226 226 226 226/ * NO BANK REGION
'CRD.PAS' 10 6/

'BAT.EDT' 'OFF'/
'PIN.FIL' 'ON' 'PINFILE' 'ADD' '2D' '3D' 'EXE'/
'PIN.EDT' 'ON' 'SUMM' '2PIN' '2EXP' 'AEXE'/
'PIN.ASM' 'K177'/

'ITE.BOR' 1500/
'ITE.SRC' 'SET' 'EOLEXP',,0.001,,, 'KEF' 1.000 0.00001 'MINBOR'/

'DEP.CYC' 'CYCLE10' 0.0 10/
'DEP.STA' 'AVE' 0.0 0.15 0.25 0.5 -0.5 24/
'WRE' '/home/jacobd/RES/s3.S1884.eqct.res' -24/

'STA'/
'END'/

```

Figure B. 5 Example input file for equilibrium cycle of 84-reload core modeled in SIMULATE-3.

APPENDIX C: TRANSITION CYCLE FUEL RELOADING SUMMARIES

These summaries describe the different types of assemblies in all batches during each transition cycle. While a few SiC assemblies exceed the 5 w/o limit, there are enrichment facilities capable of easily enriching fuel to the required 5.5 w/o and with even more advanced computer optimization programs, it may be possible to refuel an 84-reload core with SiC-clad fuel at a lower average enrichment.

Table C.1 Equilibrium core summary for transition cycle analysis.

Burned Fuel #	Fuel Batch ID	Cladding Material	# Assemblies	Enrichment	BP Rod #	IFBA Loading (mg ¹⁰ B/in)
Twice	50I156L	Zr	4	5.0	156	1.57
Twice	43I156L	Zr	4	4.3	156	1.57
Twice	43I156L	Zr	4	4.3	156	1.57
Twice	47I128L	Zr	4	4.7	128	1.57
Twice	50I128L	Zr	9	5.0	128	1.57
Once	50I156L	Zr	16	5.0	156	1.57
Once	43I156L	Zr	16	4.3	156	1.57
Once	43I156L	Zr	20	4.3	156	1.57
Once	47I128L	Zr	16	4.7	128	1.57
Once	50I128L	Zr	16	5.0	128	1.57
Fresh	50I156L	Zr	16	5.0	156	1.57
Fresh	43I156L	Zr	16	4.3	156	1.57
Fresh	43I156L	Zr	20	4.3	156	1.57
Fresh	47I128L	Zr	16	4.7	128	1.57
Fresh	50I128L	Zr	16	5.0	128	1.57

Table C.2 Core summary first loading of SiC-clad fuel for transition cycle analysis.

Reload Cycle #	Fuel Batch ID	Cladding Material	# Assemblies	Enrichment	BP Rod #	IFBA Loading (mg ¹⁰ B/in)
Twice	50I156L	Zr	4	5.0	156	1.57
Twice	43I156L	Zr	4	4.3	156	1.57
Twice	43I156L	Zr	4	4.3	156	1.57
Twice	47I128L	Zr	4	4.7	128	1.57
Twice	50I128L	Zr	9	5.0	128	1.57
Once	50I156L	Zr	16	5.0	156	1.57
Once	43I156L	Zr	16	4.3	156	1.57
Once	43I156L	Zr	20	4.3	156	1.57
Once	47I128L	Zr	16	4.7	128	1.57
Once	50I128L	Zr	16	5.0	128	1.57
Fresh	55I156L	SiC	16	5.5	156	1.57
Fresh	42I156L	SiC	16	4.2	156	1.57
Fresh	42I156L	SiC	20	4.2	156	1.57
Fresh	47I128L	SiC	16	4.7	128	1.57
Fresh	55I128L	SiC	16	5.5	128	1.57

Table C.3 Core summary second loading of SiC-clad fuel for transition cycle analysis.

Reload Cycle #	Fuel Batch ID	Cladding Material	# Assemblies	Enrichment	BP Rod #	IFBA Loading (mg ¹⁰ B/in)
Twice	50I156L	Zr	4	5.0	156	1.57
Twice	43I156L	Zr	4	4.3	156	1.57
Twice	43I156L	Zr	4	4.3	156	1.57
Twice	47I128L	Zr	4	4.7	128	1.57
Twice	50I128L	Zr	9	5.0	128	1.57
Once	55I156L	SiC	16	5.5	156	1.57
Once	42I156L	SiC	16	4.2	156	1.57
Once	42I156L	SiC	20	4.2	156	1.57
Once	47I128L	SiC	16	4.7	128	1.57
Once	55I128L	SiC	16	5.5	128	1.57
Fresh	56I156L	SiC	16	5.6	156	1.57
Fresh	44I156L	SiC	16	4.4	156	1.57
Fresh	44I156L	SiC	20	4.4	156	1.57
Fresh	49I128L	SiC	16	4.9	128	1.57
Fresh	56I128L	SiC	16	5.6	128	1.57

Table C. 4 Core summary final loading of SiC-clad fuel for transition cycle analysis.

Reload Cycle #	Fuel Batch ID	Cladding Material	# Assemblies	Enrichment	BP Rod #	IFBA Loading (mg ¹⁰ B/in)
Twice	55I156L	SiC	4	5.5	156	1.57
Twice	42I156L	SiC	4	4.2	156	1.57
Twice	42I156L	SiC	4	4.2	156	1.57
Twice	47I128L	SiC	4	4.7	128	1.57
Twice	55I128L	SiC	9	5.5	128	1.57
Once	56I156L	SiC	16	5.6	156	1.57
Once	44I156L	SiC	16	4.4	156	1.57
Once	44I156L	SiC	20	4.4	156	1.57
Once	49I128L	SiC	16	4.9	128	1.57
Once	56I128L	SiC	16	5.6	128	1.57
Fresh	57I156L	SiC	16	5.7	156	1.57
Fresh	43I156L	SiC	16	4.3	156	1.57
Fresh	43I156L	SiC	20	4.3	156	1.57
Fresh	49I128L	SiC	16	4.9	128	1.57
Fresh	57I128L	SiC	16	5.7	128	1.57